



Run Run Shaw Library

香港城市大學
City University of Hong Kong

Copyright Warning

Use of this thesis/dissertation/project is for the purpose of private study or scholarly research only. ***Users must comply with the Copyright Ordinance.***

Anyone who consults this thesis/dissertation/project is understood to recognise that its copyright rests with its author and that no part of it may be reproduced without the author's prior written consent.

CITY UNIVERSITY OF HONG KONG
香港城市大學

Interaural Time Difference Processing in
Wistar Rats: Sensitivity and Temporal
Weighting

Wistar 大鼠對雙耳時間差的處理：
靈敏度及時間權重

Submitted to

Department of Biomedical Sciences

生物醫學系

In Partial Fulfillment of the Requirements

for the Degree of Doctor of Philosophy

哲學博士學位

by

LI Kongyan

李孔燕

November 2020

二零二零年十一月

ABSTRACT

Mammals use binaural cues, interaural time differences (ITDs) and interaural level differences (ILDs), to localize sound. Bilateral cochlear implants help people suffering from severe to profound hearing loss in both ears to restore binaural hearing to a certain extent, but not as good as normal hearing listeners. The restored binaural hearing benefits significantly from ILDs. But a lack of ITD sensitivity has been observed in bilateral cochlear implant users, and it hinders their ability to perceive speech in a noisy environment. A novel cochlear implant stimulation strategy may be needed to facilitate ITD sensitivity as well as speech perception. Before a novel strategy can be tested and applied on deaf children in clinics, tests must be done on animals. Hence, a suitable animal model is needed.

Rats are widely used in science, but not commonly seen in binaural hearing research. One concern about using laboratory rats in binaural hearing research was that they were suspected of not to be sensitive to ITDs. Previous studies conducted with rats trained to localize in the free field had concluded that rats are insensitive to the interaural phase of pure tones. However, we suspected that rats may nevertheless be sensitive to envelope ITDs.

Here, we designed and used a behavioural training setup to train rats in a near-field 2-alternative forced choice (2-AFC) sound localization task, presenting them with more natural “pulse-resonance” sounds to test their perception of ecologically more relevant stimuli. A wide range of pulse rates were tested: 50 Hz, 300 Hz, 900 Hz, 1800 Hz, 2400Hz, 4800 Hz. Those click trains were enveloped with rectangular window which provided onset ITD cue or Hanning window which only ongoing ITD was conserved to test the sensitivities to onset and ongoing ITD, respectively. The results supported our suspicions and revealed that rats are highly sensitive to both onset and ongoing envelope ITDs down to a microsecond level. The ITD sensitivity to rectangular windowed click trains was

higher than to the Hanning ones of the same click rate. The sensitivity dropped as the pulse rate increased for both window types, and dramatically declined at 900 Hz for Hanning windowed, and at 1800 Hz for rectangular windowed click trains.

I also performed electrophysiological recordings from inferior colliculus of rats, and observed that the envelope type and click rate, but not training, are the factors that govern the extent to which neuronal responses distinguish left ear leading from right ear leading ITDs. The trends in neural sensitivity as a function of pulse rate and inflection point were consistent with our behavioural results. Our findings confirmed that the rat is a highly suitable model for both psychoacoustic and physiological binaural hearing research.

In order to investigate the importance of onset, ongoing and offset parts of a stimulus carrying ITD information, behavioural “temporal weighting functions” were measured to quantify the weights of each click in an 8-click click train with different ITD values embedded in each click. Rats performed 2-AFC sound localization task while listening to the target stimuli in 20 Hz, 50 Hz, 300 Hz and 900 Hz click rates, respectively. A Probit regression was conducted to generate the coefficients which represent the weight of the corresponding click. The results demonstrated clear onset dominance, with the ITD of the first click in the train dominating the perceptual decisions. Rats weighted the first click increasingly highly as click rate increased. The neural decoding for electrocorticographic signal recorded at 300 Hz and 900 Hz from the auditory cortex also revealed profound precedence effect. Our results are strikingly similar to those previously reported for humans, further illustrating that rats are a highly suitable model for the study of mammalian ITD processing.

Keywords: interaural time difference, ITD sensitivity, temporal weighting, precedence effect, onset dominance, rat, inferior colliculus, primary auditory cortex

CITY UNIVERSITY OF HONG KONG

Qualifying Panel and Examination Panel

Surname:	LI
First Name:	Kongyan
Degree:	PhD
College/Department:	Department of Biomedical Sciences

The Qualifying Panel of the above student is composed of:

Supervisor(s)

Prof. Jan SCHNUPP	Department of Neuroscience City University of Hong Kong
-------------------	--

Qualifying Panel Member(s)

Dr. LAU Chun Yue Geoffrey	Department of Neuroscience City University of Hong Kong
---------------------------	--

Dr. YANG Sungchil	Department of Neuroscience City University of Hong Kong
-------------------	--

This thesis has been examined and approved by the following examiners:

Dr. CHAN Ho Man	Department of Electrical Engineering City University of Hong Kong
-----------------	--

Prof. HE Jufang	Department of Neuroscience City University of Hong Kong
-----------------	--

Prof. Jan SCHNUPP	Department of Neuroscience City University of Hong Kong
-------------------	--

Dr. SUMNER Christian	School of Social Sciences Nottingham Trent University
----------------------	--

DECLARATION

I hereby declare that the thesis summarizes my own research work, which was carried out within the period of September 2016 to April 2020 for the degree of Doctor of Philosophy under the supervision of Prof. Jan W. H. Schnupp, and which has not previously been part of a thesis, dissertation or report submitted to this or any other institution for a degree, diploma or other qualification.

Signature: _____

LI Kongyan

November 2020

DEDICATION

I would like to dedicate this work

To my parents, grandparents, brothers, nephews, nieces

To all of them, I dedicate this work

ACKNOWLEDGMENTS

I am grateful to my learned and talented supervisor Prof. Jan W.H. Schnupp. His intelligence, guidance, kindness and humour guide my way throughout my PhD study, and will continue to influence my further life.

Special thanks go to Dr. Nicole Rosskothén-Kuhl for training me to be passionate and rigorous in research. Many thanks go to my labmates Vani G. Rajendran, Ryszard Aukstulewicz, Chloe H.K. Chan, Ambika P. Mishra, and Qinglin Meng for their generous help in my research work and also to Hyunjung An, Dan Luo and Hijee Kang for their assistance.

I appreciate the valuable advice from the qualifying panel members Dr. Geoffrey C.Y. Lau and Dr. Sungchil Yang.

Thanks owe to the technical advice and support from technical staff of Biomedical Sciences and Laboratory Animal Research Unit, especially Mr. Eric K.W. Shum, Ms. Helen O.L. Mok and Mr. Kelvin Yip.

Thanks to all the instructors in my course study. The courses expand my knowledge and broaden my horizon. Special thanks should go to Prof. Hing Cheung So and Dr. Cheung Fat Chan in Department of Electrical Engineering, and Dr. Antoni Bert Chan in Department of Computer Science, for their kindness and patience in instructing me.

I would like to extend my thanks to my friends for their generous help in course study: Jianfeng Zhou, Martin Garaj, Avirup Singh and Chao Zhao.

Thanks to Martin Garaj again and Gona Choi, the friends indeed always by my side. I am grateful to Eldeeb Mohammed and Jay Greenberg for their spiritual support in tough days. Many thanks to Jihwan Lee, for physical fitness training and daily caring. Thank you Mengling Huang and Sujun Pan, for over 20 years of friendship.

I deeply thank my mother and brothers for loving and supporting me unconditionally. I could not have become who I am today without you. I love you.

Publications list

PAPERS:

1. **Li KY**, Chan CH, Rajendran VG, Meng QL, Rosskothén-Kuhl N, Schnupp JW. Microsecond sensitivity to envelope interaural time differences in rats. *The Journal of the Acoustical Society of America*. 2019 May 2;145(5):EL341-7.
2. Rosskothén-Kuhl N, Buck AN, **Li KY**, Schnupp JW. Microsecond interaural time difference discrimination restored by cochlear implants after neonatal deafness. Under review. Preprint available at BioRxiv. 2019 Jan 1:498105.

Two further manuscripts are in preparation.

CONFERENCE POSTERS:

1. **Li KY**, Chan CH, Mishra AP, Stecker CG, Schnupp JW. Temporal weighting functions for binaural cues in rats. Poster presented at: Neuroscience 2019. Society for Neuroscience; 2019 Oct 19-23; Chicago, IL.
2. **Li KY**, Chan CH, Chan, Rosskothén-Kuhl N, Schnupp JW. Sensitivity to interaural time differences in rats. Poster presented at: Neuroplasticity of Sensory Systems. Gordon Research Conference; 2018 Jun 3-8; Hong Kong, China.
3. Buck A, Rosskothén-Kuhl N, Khurana L, Mayer S, **Li KY**, Schnupp JW. Onset weighting of temporal spatial cues with cochlear implant stimulation in early on-

set deafness. Poster presented at: ARO 2020. Association for Research in Otolaryngology; 2020 Jan 25-29; San José, CA.

Table of Contents

ABSTRACT.....	i
Qualifying Panel and Examination Panel.....	iii
DECLARATION.....	iv
DEDICATION.....	v
ACKNOWLEDGMENTS.....	vi
Publications list.....	vii
List of Figures.....	xii
List of Tables.....	xiv
List of Abbreviations.....	xv
1 Chapter 1 General introduction.....	1
1.1 Binaural hearing.....	3
1.1.1 Binaural cues.....	3
1.1.2 The importance of binaural hearing.....	6
1.1.3 The pathway of sound localization.....	7
1.1.4 Precedence effect.....	11
1.1.5 Temporal weighting functions.....	12
1.2 Cochlear implants.....	14
1.2.1 Prevalence of hearing loss.....	14
1.2.2 Etiology of hearing loss.....	14
1.2.3 Treatments of hearing loss.....	15
1.2.4 Bilateral cochlear implantation.....	16
1.2.5 Why focus on ITD.....	17
1.3 Is rat a suitable animal model to study binaural hearing?.....	19
1.3.1 Auditory characteristics of rats.....	20
1.3.2 The controversy over ITD sensitivity in rats.....	21
1.4 Basic of signal detection theory.....	23
1.4.1 Sensitivity index.....	26
1.4.2 The area under the ROC curve.....	26
1.4.3 Psychometric function.....	27
1.5 Field potential.....	28
1.5.1 Local field potential.....	31
1.5.2 Electrographicography.....	32
1.5.3 Neural activity quantification.....	32
2 Chapter 2 Microsecond sensitivity to envelope interaural time differences in rats.....	34
2.1 Introduction.....	34
2.2 Materials and Methods.....	35
2.2.1 Subjects.....	35
2.2.2 Stimuli.....	36
2.2.3 Training.....	39
2.2.4 Psychometric analysis.....	40
2.3 Results and discussion.....	42

3 Chapter 3 Dependence of Interaural Time Difference Tuning in the Rat Inferior Colliculus on Rate and Envelope of Pulsatile Stimuli.....	47
3.1 Introduction.....	47
3.2 Materials and methods.....	49
3.2.1 Animals.....	49
3.2.2 Behavioral training (for the trained cohort).....	49
3.2.3 Extracellular recording.....	50
3.2.3.1 Stimuli.....	50
3.2.3.2 Surgical Procedure.....	51
3.2.3.3 Electrophysiological Recording.....	52
3.2.4 Analysis of electrophysiological data.....	53
3.2.4.1 Data preprocessing.....	53
3.2.4.2 Mutual Information calculation.....	53
3.2.4.3 Calculation of neural d' based on ROC analysis of ITD tuning curves.....	54
3.2.5 Statistical analysis.....	56
3.2.5.1 Mixed effects ANOVA.....	56
3.3 Results.....	57
3.3.1 Approximately half of rat IC multi-units show significant tuning to ITD.....	57
3.3.2 Neural d' depends on pulse rate and envelope, but not on training....	60
3.4 Discussion.....	63
3.4.1 Principal findings.....	63
3.4.2 Late exposure cannot alter the sensitivity to ITDs in IC.....	63
3.4.3 The effect of window type and click rates match the behavioral results.....	64
3.4.4 Stimuli envelop plays an important role in neural response to ITD cue.....	65
3.4.5 What is the best stimulation rate?.....	65
3.5 Conclusion.....	66
4 Chapter 4 Temporal weighting function for interaural time differences in rats.	68
4.1 Introduction.....	68
4.2 Materials and Methods.....	70
4.2.1 Animals.....	70
4.2.2 Behavioral study.....	72
4.2.2.1 Behavioral training setup.....	72
4.2.2.2 Behavioral training task.....	72
4.2.2.3 Acoustic stimuli.....	73
4.2.2.4 Behavioral data analysis.....	76
4.2.3 Electrophysiological experiment.....	77
4.2.3.1 ECoG recording apparatus.....	77
4.2.3.2 ECoG recording procedure.....	78
4.2.3.3 Acoustic stimuli.....	79
4.2.3.4 ECoG data analysis.....	80
4.3 Results.....	85
4.3.1 Behavioral task showed profound onset dominance.....	85
4.3.2 Channel-wise regression shows weak precedence effect in ECoG signals from the auditory cortex.....	91

4.3.3 Multivariate decoding shows strong precedence effect in ECoG signals from the auditory cortex.....	94
4.4 Discussion.....	97
4.4.1 Principal findings.....	97
4.4.2 Possible mechanism of precedence effect.....	98
4.4.3 Neural decoding as a correlate of the precedence effect in the auditory cortex of rats.....	101
4.4.4 Precedence effect is encoded in the auditory cortex of rats as in other mammals.....	104
4.5 Conclusion.....	105
5 Chapter 5 Conclusions and Future Perspectives.....	106
5.1 Conclusions.....	106
5.2 Future perspective.....	107
References.....	108

List of Figures

Figure 1.1.1: Diagram of the spatial coordinate system.....	4
Figure 1.1.2: Binaural cues for sound localization.....	5
Figure 1.1.3: Threshold interaural time differences as a function of frequency for four listeners measured by Brughera et al. (2013).....	6
Figure 1.1.4: A cross-section of the side of the head, showing structures of the outer, middle, and inner ear.....	8
Figure 1.1.5: The mammalian ascending auditory pathway.....	9
Figure 1.4.1: Distributions of strength for Noise and Signal.....	25
Figure 1.4.2: Receiver operating characteristics (ROCs) for two normal distributions with the same variance.....	27
Figure 1.5.1: Field potential recording modalities.....	30
Figure 2.2.1: Rat binaural psychoacoustics near-field setup.....	37
Figure 2.3.1: Psychometric curves for rats localizing rectangular window click trains by ITD.....	43
Figure 2.3.2: Psychometric curves for rats localizing Hanning window click trains by ITD.....	44
Figure 2.3.3: Summary of ITD sensitivity across click rates and window types.....	45
Figure 3.3.1: Distribution of mutual information (MI) values between the 17 ITD values and neural responses across the recorded neural population for the 300 Hz rectangular window stimulus condition.....	57
Figure 3.3.2: Calculation of neural d' and a comparison with MI for example multiunits.....	59
Figure 3.3.3: Comparison of MI and $ d' $ metrics.....	60
Figure 3.3.4: Comparing neural $ d' $ and behavioural d' as a function of stimulus pulse rate and envelope type.....	62
Figure 4.2.1: Acoustic stimuli examples for honesty trial and probe trial.....	74
Figure 4.2.2: High-resolution, flexible electrode array of 61 electrodes.....	78
Figure 4.3.1: Temporal weighting functions for interaural time differences at different click rates in rats.....	89

Figure 4.3.2: Temporal weighting functions for ITDs at different click rates for each individual rat.....	90
Figure 4.3.3: Examples of the weightings on each click at 61 recorded sites.....	93
Figure 4.3.4: Boxplots for the absolute wight with p value < 0.05 of four ECoG recorded rats at 300 Hz and 900 Hz click rates.....	94
Figure 4.3.5: Neural decoding based on average RMS activity and active fluctuations.....	96

List of Tables

Table 3.3.1: The fixed effects coefficients (95% CIs) returned by the mixed effects ANOVA.....	61
Table 4.3.1: A summary of the data collected in the final “honesty + probe” testing stage.....	87

List of Abbreviations

ABRs.....	35
auditory brainstem responses.....	35
AMPA.....	31
α -amino-3-hydroxy-5-methyl-4-isoxazolepropionic acid.....	31
AMUA.....	32
analog multi-unit activity.....	32
AUC.....	13
area under the curve.....	13
CI.....	15
Cochlear Implant.....	15
CN.....	7
cochlear nucleus.....	7
DNLL.....	22
dorsal nucleus of the lateral lemniscus.....	22
ECoG.....	28
electrocorticography.....	28
EEG.....	28
electroencephalography.....	28
Fs.....	53
sampling rate.....	53
HL.....	16
hearing level.....	16
IC.....	7
inferior colliculus.....	7
ICc.....	9
central nucleus of the inferior colliculus.....	9
ICIs.....	13
inter-click intervals.....	13
ILDs.....	3
interaural level differences.....	3
IPI.....	18
inter-pulse interval.....	18
ISD.....	12
inter-stimulus delay.....	12
ITDenv.....	17
envelope ITD.....	17
ITDfs.....	17
fine structure ITD.....	17
LFP.....	28
local field potentials.....	28
MEG.....	28
magnetoencephalography.....	28
MI.....	35

mutual information.....	53
MUA.....	
multi-unit activity.....	33
NLL.....	
nuclei of the lateral lemniscus.....	7
NMDA.....	
N-Methyl-D-aspartic acid.....	31
OLS.....	
ordinary least squares.....	82
PE.....	
precedence effect.....	11
pps.....	
pulse per second.....	18
ROC.....	
receiver operating characteristic.....	2
SDT.....	
signal detection theory.....	23
SNR.....	
signal-to-noise.....	83
SOC.....	
superior olivary complex.....	7
SPL.....	
sound pressure level.....	21
SSHL.....	
Sudden sensorineural hearing loss.....	15
Stereo-EEG.....	
stereotactic electroencephalography.....	28
TWF.....	
Temporal weighting function.....	12

1 Chapter 1 General introduction

We have two ears to hear sounds. This ability allow us to listen to a conversation, appreciate a piece of music, enjoy the sound of waves, and avoid a dangerous situation, etc. We take it as granted. But, as many as 0.7% of the population suffer from profound to severe hearing loss (Turton and Smith, 2012), and their world is in silence. They become deafened due to many reasons, be it congenital deafness, or side effects of ototoxic drugs, or diseases or accidents. Sign language may help them communicate with each other if they are raised in a signing culture and they can see. But communication with the vast majority of normally hearing individuals who do not know any sign language is severely limited. As technology developed, cochlear implantation opened up a path to auditory experience for many of them. With cochlear implantation, they can hear sounds, participate in conversations and live a richer social life. Cochlear implantation provides hearing restoration to a certain extent, not yet as perfect as normal hearing, even though some of them are bilaterally implanted. The stimulation strategies of such prostheses need improvement, and a suitable animal model is required to help meet this purpose. This leads to the aims of our current research: to verify if rat is a suitable model in binaural hearing research. The lack of interaural time differences (ITDs) encoded in clinic cochlear implant is the major reason why cochlear implant users have difficulty in hearing in complex environment. But, there is controversy about the rats' ability to localize sound. Electrophysiological record-

ing showed ITD sensitivity (Kelly et al., 1991; Kidd and Kelly, 1996), while a behaviour study claimed that the rats can not use interaural phase differences to localize sound (Wesolek et al., 2010). I wanted to clarify whether rats can use ITDs to localize sound in a different experimental condition, using more ecologically relevant sound stimuli. And we were also interested in whether rat binaural processing exhibits similar precedence effects as are seen in humans. I examined this using “temporal weighting” methods in rats.

In this general introduction chapter, I mainly focus on five sections of relevant background material. Section 1 - Binaural hearing: explains what is binaural cues, the importance of binaural hearing, how we can hear sound in respect of binaural cues, and the concepts of the precedence effect and temporal weighting functions. Section 2 - Cochlear implants: introduces the prevalence, etiology and treatments of hearing loss, bilateral cochlear implant, and why ITD needs to be encoded properly to enhance hearing in noise for bilateral cochlear implants. Section 3 - Is the rat a suitable animal model to study binaural hearing?: Discusses the hearing characteristic and the controversy on ITD sensitivity in rats. Section 4 - Basics of signal detection theory: introduces the concepts of three methods to illustrate the sensitivity to a signal --- sensitivity index d' , the area under the receiver operating characteristic (ROC) curve and the psychometric function. Section 5 - Field potentials: talking about local field potentials, electrocorticography, and the quantification of neural activity.

1.1 Binaural hearing

1.1.1 Binaural cues

To pinpoint a sound, we need the azimuth and elevation angle (**Figure 1.1.1**) (Middlebrooks et al., 1989), and distance information. ITDs and interaural level differences (ILDs) are the binaural cues for localizing sound in the horizontal plane, and their contribution to spatial hearing is hugely important (Schnupp et al., 2012). When a sound originates away from the median sagittal plane hits our ears, it will result in an ITD due to the difference of distance of the sound source to the two ears. It will also create an ILD due to the directional filtering properties of the external ears and the “head shadow effect” for short wavelength (high frequency) sound (**Figure 1.1.2**). ITD has traditionally been thought to be particularly important for space coding of low frequency sounds, while ILDs are more effective for high frequency sound. This is known as the “duplex theory” (Rayleigh, 1907), and the low/high frequency boundary is firstly believed to be in a region near 1300 Hz (Klumpp and Eady, 1956; Zwislocki and Feldman, 1956), but later revised to be closer to 1400 Hz (Mills, 1958; Brughera et al., 2013; Hartmann and Macaulay, 2014)(**Figure 1.1.3**). The current convention usually sets the boundary at 1500 Hz, below which ITD is dominant, and above which ILD is dominant. Note, however, that the effectiveness of ITDs and ILDs can vary from listener to listener, may change with training and will depend on features such as amplitude modulation. Thus, although humans have essentially no sensitivity to the ongoing interaural phase difference of pure tones above 1500 Hz, humans have been known for a long time to be sensitive to envelope ITDs in amplitude modulated high frequency sounds (Henning, 1974). Thus, there can be

important exceptions to the “classic rule” that ITDs only operate at frequencies below 1500 Hz, and in a world where complex sounds with rapidly fluctuating envelopes are pervasive, these exceptions may be more common than sounds which obey the rule.

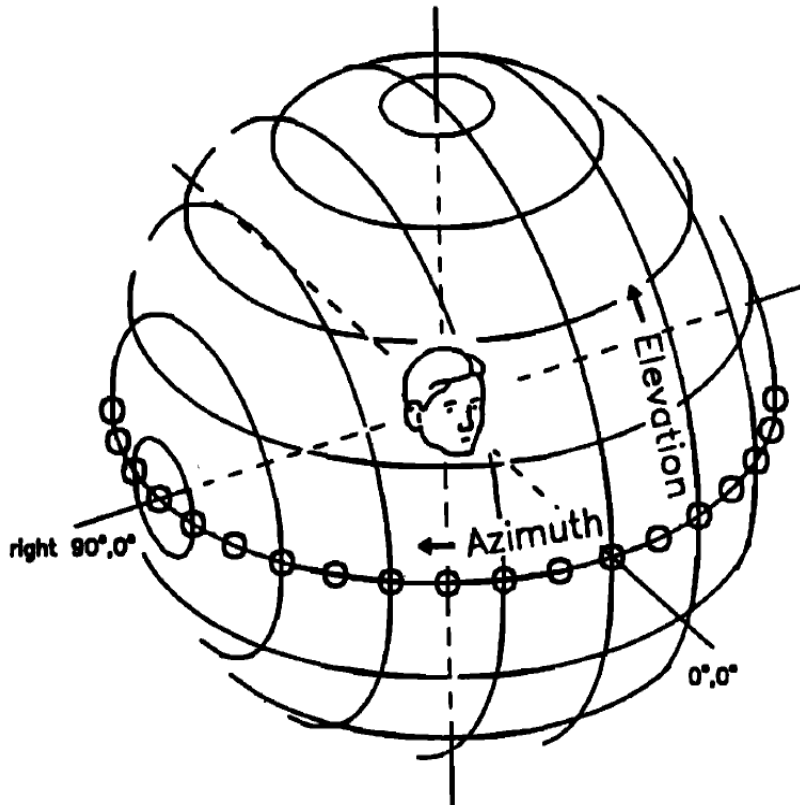


Figure 1.1.1: Diagram of the spatial coordinate system.

The locations of sound sources are represented on a unit sphere as if looking in toward the subject from a location 30° above the horizontal plane and 30° to the subject's right. Locations are given by the angles measured at the center of the subject's interaural axis: Horizontal locations are given by *azimuth*, the angle to the right (+) or left (-) of the vertical midline plane, and vertical locations are given by *elevation*, the angle above (+) or below (-) the horizontal plane. Isoazimuth and isoelevation lines are shown in 20° increments. The loudspeakers, represented here by small circles, were separated in azimuth by 10° . Reprinted with permission from Middlebrooks, J., Makous, J., and Green, D. (1989). Directional sensitivity of sound-pressure levels in the human ear canal. *The Journal of the Acoustical Society of America* 86, 89-108. Copyright 1989, Acoustical Society of America. (Middlebrooks et al., 1989).

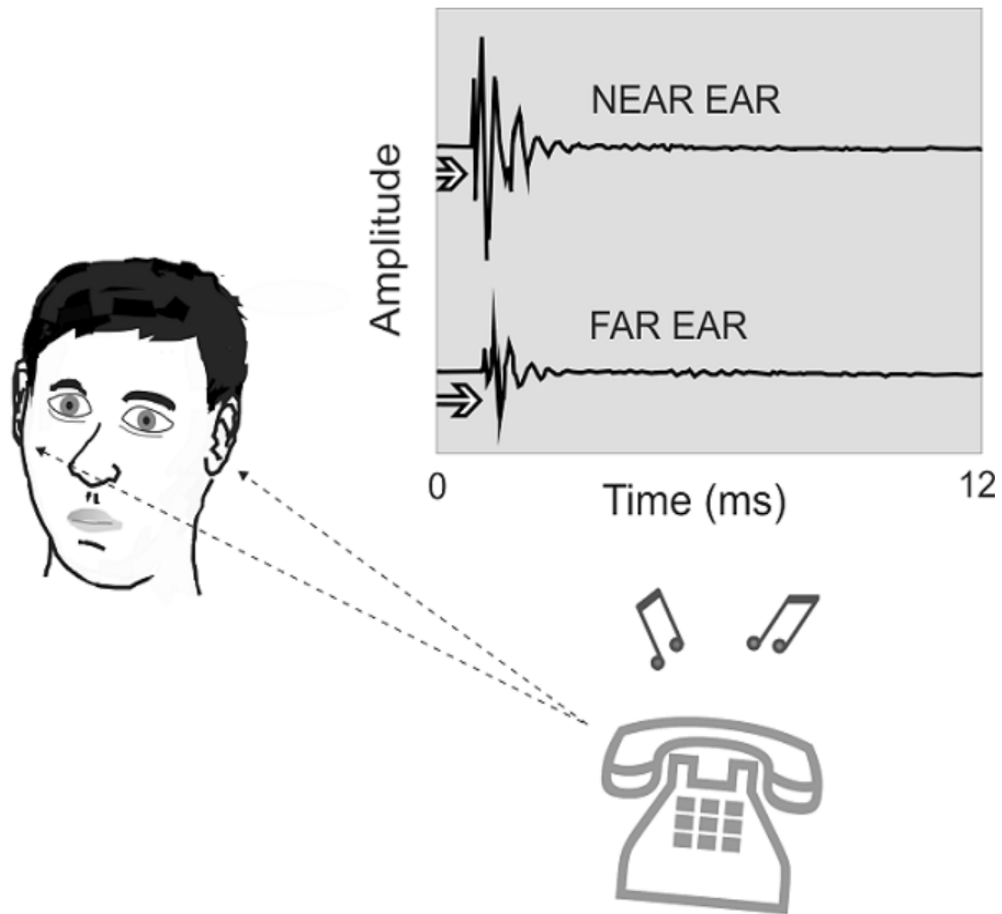


Figure 1.1.2: Binaural cues for sound localization.

Sounds originating from one side of the head will arrive first at the ear closer to the source, giving rise to an interaural difference in time of arrival. In addition, the directional filtering properties of the external ears and the shadowing effect of the head produce an interaural difference in sound pressure levels. These cues are illustrated by the waveform of the sound, which is both delayed and reduced in amplitude at the listener's far ear. Reprinted with permission from *Auditory Neuroscience: Making Sense of Sound*, by Jan Schnupp, Israel Nelken, and Andrew King, published by The MIT Press. (Schnupp et al., 2012).

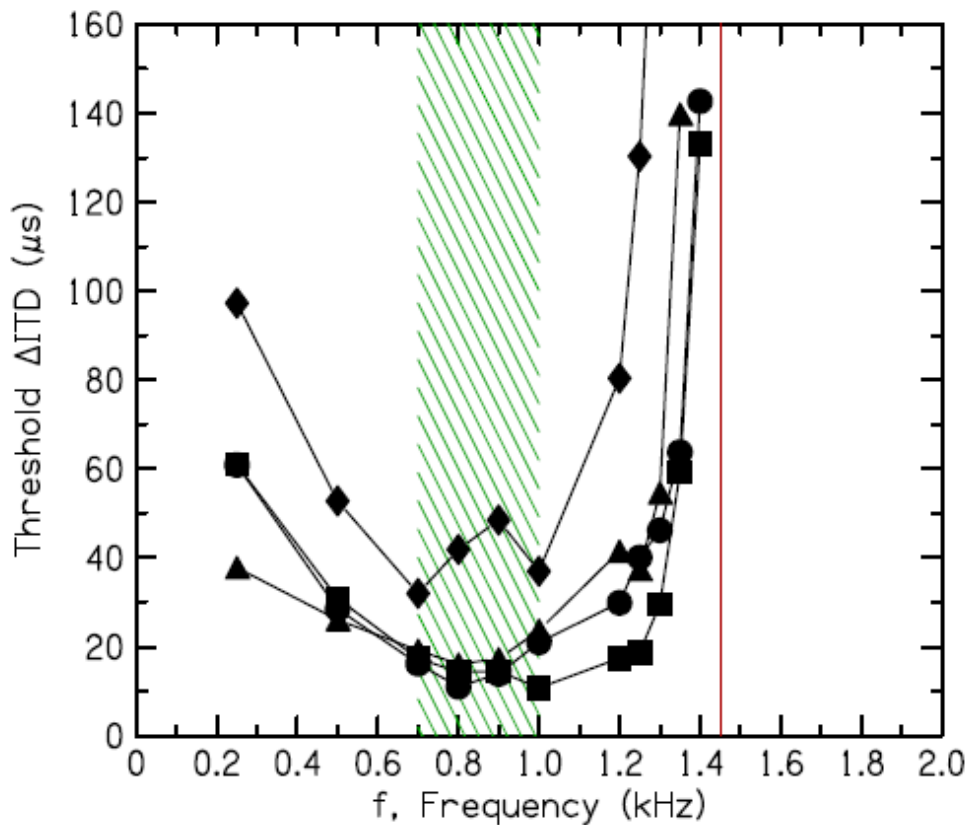


Figure 1.1.3: Threshold interaural time differences as a function of frequency for four listeners measured by Brughera et al. (2013).

The shaded rectangle shows the frequency region of greatest sensitivity. The vertical solid line indicates the upper limit at 1450 Hz. Reprint from Hartmann, W., and Macaulay, E. (2014). Anatomical limits on interaural time differences: an ecological perspective. *Frontiers in Neuroscience* 8, 34. (Hartmann and Macaulay, 2014).

1.1.2 The importance of binaural hearing

A fundamental aspect of binaural hearing is sound spatial localization. For animals, accurate detection of sound sources is a survival skill that helps them avoid an approaching predator or find a potential mate; for humans, it is more related to extracting target sounds from a noisy background. Binaural hearing can improve the performance of speech intelligibility in noise. Binaural unmasking

and attention-driven spatial release from masking are the two major mechanisms that contribute to this improvement and ITD is the dominant cue for both mechanisms (Laback et al., 2015).

1.1.3 The pathway of sound localization

How can we hear a sound? Sound which is emitted from the surface of vibrating objects propagates through the air, reaches our outer ear canal and pushes against the tympanic membrane (eardrum). The pressure on the tympanic membrane triggers the movement of auditory ossicles, which acts as an impedance bridge linking the air-filled ear canal and the fluid-filled cochlea, and facilitates the transmission of the tiny sound vibrations on to the snail-shaped cochlea. The movement of the hair cells on the organ of Corti, which sits on the basilar membrane, opens ion channels and allows changes in membrane voltage gradients that turn the mechanical vibration into electrical signals. These in turn activate synapses which will trigger the excitation of auditory (VIII cranial nerve) fibers (**Figure 1.1.4**) (Schnupp et al., 2012).

The signal transmits through the anterior ventral cochlear nucleus (CN) to the superior olivary complex (SOC) on both sides of the brain. The information then projects onto the contralateral nuclei of the lateral lemniscus (NLL) and inferior colliculus (IC). Meanwhile, the NLL and IC receive direct, major projections via the dorsal and intermediate acoustic striae from the contralateral CN. On the contralateral hemisphere, NLL provide additional input to the IC. Therefore, every nuclear group within the auditory pathways can innervate the IC. The acoustic

cues processed by IC are then further projected to the next synaptic levels in the thalamocortical system (**Figure 1.1.5**) (Grothe et al., 2010).

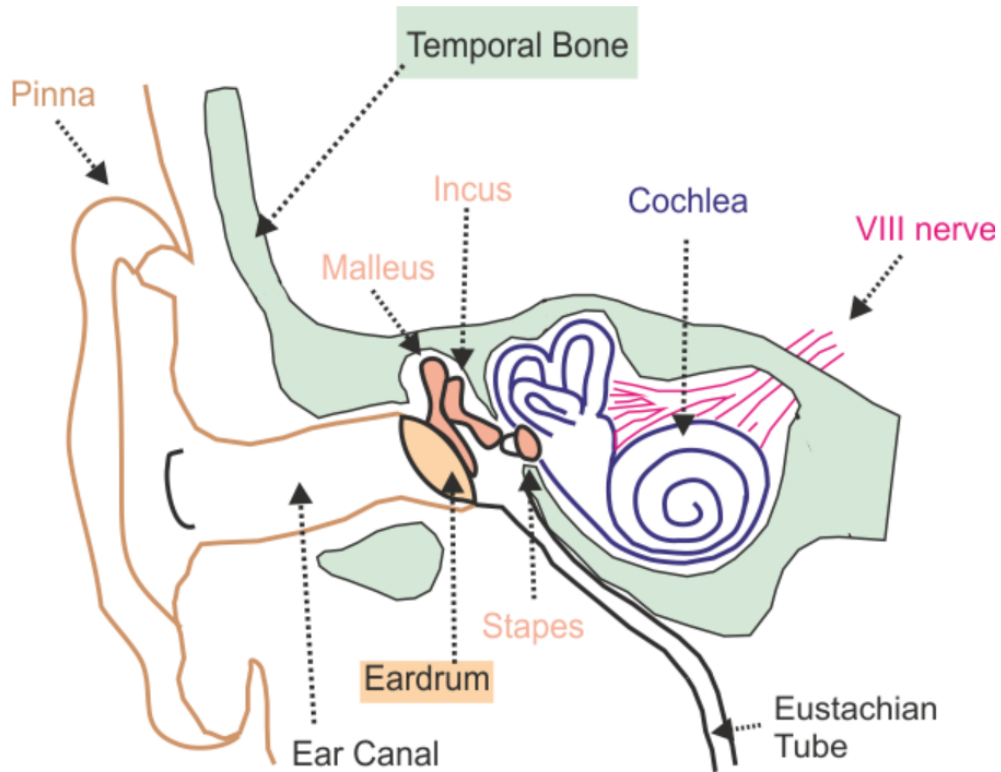


Figure 1.1.4: A cross-section of the side of the head, showing structures of the outer, middle, and inner ear.

Reprinted with permission from Auditory Neuroscience: Making Sense of Sound, by Jan Schnupp, Israel Nelken, and Andrew King, published by The MIT Press. (Schnupp et al., 2012).

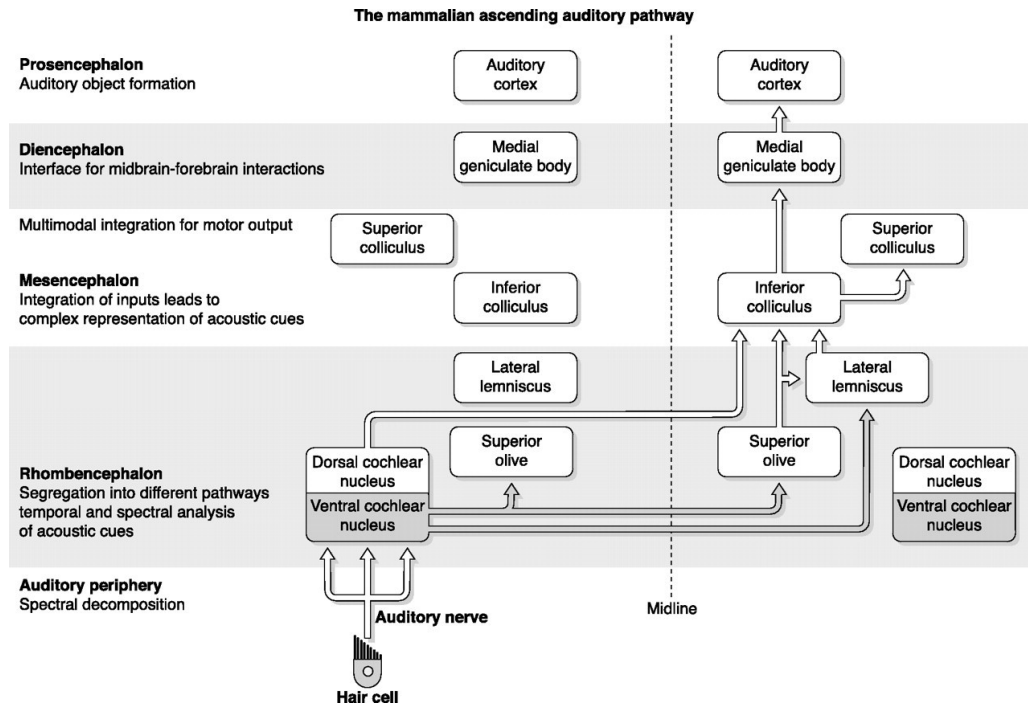


Figure 1.1.5: The mammalian ascending auditory pathway.

Simplified circuit diagram of ascending pathways involved in sound localization. Reprinted with permission from Grothe, B., Pecka, M., and McAlpine, D. (2010). Mechanisms of sound localization in mammals. *Physiological Reviews* 90, 983-1012. (Grothe et al., 2010).

In the ascending auditory pathway of mammals, the SOC is the first major junction for binaural information in the central auditory system and the first site to encode ITDs and ILDs (Goldberg and Brown, 1969). A larger size of the animal's medial superior olive (MSO) facilitates the performance in localization of middle and low frequency tone pips (Masterton et al., 1975), which indicates that the size of MSO is correspondent to ITD sensitivity.

Although subdivisions of the SOC are predominantly involved in the research of ITD and ILD, abundant ITD and ILD sensitive neurons are also found in the central nucleus of the inferior colliculus (ICc) (Moore, 1991). In the ICc, the neuronal best frequency of frequency-band laminae are increased along the

dorsolateral to ventromedial axis (Schreiner and Langner, 1988; Kelly et al., 1991; Joris et al., 2004).

ICc is a mandatory auditory relay. Neural signals from all lower auditory nuclei pass directly or indirectly through the IC (Beyerl, 1978; Druga and Syka, 1984) before projecting on to higher order auditory cortex. The IC in turn is a major target of descending projections from the auditory cortex, with the densest projections to the dorsal cortex of the IC (Andersen et al., 1980; Faye-Lund, 1985), but projections to the ICc were also found (Saldaña et al., 1996).

The cortical fields that are functionally specified in mammals are at least in part determined by the types of sensory input they receive (Ehret, 1997). As in the auditory cortex, the input from thalamic nuclei of the medial geniculate complex and other thalamic and extrathalamic nuclei is the determinant (Winer, 1992; Ehret and Romand, 1997).

The structure of the auditory cortex in mammals is usually tonotopically organized (Ehret, 1997). In the primary auditory cortex (AI) of rats, the isofrequency areas are orthogonal to the rostro-caudal axis (Sally and Kelly, 1988) and the frequency representation is in an ascending order from caudal to rostral (Sally and Kelly, 1988; Masri et al., 2018).

The location of AI in human is along the Heschl's gyrus (HG), running from the superior temporal gyrus (STG) into the lateral sulcus (LS) (Brewer and Barton, 2016). In humans, the tonotopic organization is mirrored: centered on HG with low frequency representation which is surrounded by gradually increasing

frequency bands represented in the form of an approximately circular shape (Brewer and Barton, 2016).

At least in cats, AI appears to be essential for sound localization (Jenkins and Masterton, 1982; Jenkins and Merzenich, 1984). In the AC of human, sound laterality is integrately coded, but the information of binaural cues are retained independently (Edmonds and Krumbholz, 2013).

1.1.4 Precedence effect

In a reverberant environment (that is, anywhere where we may encounter hard surfaces that can reflect sounds), reflections of the original sound overlap with the direct sound, but the spatial cues of the reflected sounds do encode the location of the reflecting surface, not the original sound source, creating a potential confound. The “precedence effect”(PE) is a term first used by Wallach et al. (1949) to describe the fact that the brain appears to rely almost exclusively on the earliest wavefront when judging the spatial direction of sounds. A simplification of this natural situation is a direct sound (the lead) and a single “reflection” (the lag) delivered in an anechoic room: two equally distant loudspeakers deliver identical sounds, but the onset of the sound from one speaker is leading to the other. The delay of lead and lag stimuli determines how we perceive the sound. If the delay is within 0 to 1 ms, “summing localization” happens, and the lead and lag sound are perceptually fused and both contribute to the perceived direction of the fused image. When there is no temporal overlap between lead and lag signal, a location that is the average of the two directions will be perceived. When the

lead and lag signal overlap in time, a location that is a more complex average of the two signals will be perceived, which depends on the relative amplitudes and phases of the summed wave forms. If the delay is more than 1 ms, the “echo threshold” determines whether one fused auditory event is perceived or whether two distinct sounds are heard. Fusion typically occurs when the delay is short, ranging from 1 ms to the echo threshold (5 ms or more, depending on the room acoustic and stimulus waveform). Note that the echo threshold here is not the detectability threshold of the lead-lag sound, but the perceived separation into two distinct auditory images. The image location in the short delay lead-lag stimulus is dominated by the leading part, which is known as “law of the first wavefront” or “localization dominance”. The fact that the lagging part is less discriminable is known as “lag-discrimination suppression” (Litovsky et al., 1999). The lag-discrimination suppression thresholds were estimated to be at 5-10 ms (Yang and Grantham, 1997).

Listeners are relatively accurate in leading sound localization or discrimination between locations. In case of lagging sound localization, only when the stimulus has longer inter-stimulus delay (ISD) can lead to promising accuracy (Litovsky et al., 1999). The lagging sound localization is impaired at ISDs $\lesssim 10$ ms in human (Mickey and Middlebrooks, 2005)

1.1.5 Temporal weighting functions

Temporal weighting function (TWF) is a term used to describe how much the auditory system relies on a portion (onset, ongoing, offset) of an acoustic stimu-

lus to localize sound. In acoustic experiments, click trains are commonly used to explore the weight on each click in a train in a sound localization task. Different approaches can be used to express the weightings. For example, if a multi-linear regression is applied, those weightings are the returned coefficients of each click in the click train (Stecker and Hafter, 2002); If a ROC analysis is conducted separately for each click, those weightings are the area under the curve (AUC) for the specific click (Brown and Stecker, 2010). In sound lateralization tasks which produce binary left or right responses a Probit regression is more appropriate to fit the discrete binary data than multi-linear regression.

G. Christopher Stecker has done ample work on TWFs in human listeners. A summary of his main findings follows.

First, smaller inter-click intervals (ICIs) (higher click rate) will generate stronger PE. In normal hearing human subjects, apparent onset dominance was shown at high rates for ITD and ILD at 1.25 ms and 2.5 ms ICI, but not at 5 ms or 10 ms ICI (Brown and Stecker, 2010). In sound localization tasks, subjects also showed high onset weight at 2 ms ICI though flatter weighting at 5- 10 ms ICI in the Gabor click trains with binaural cues was found. “Up weighting” of the last click was also seen in the stimuli with ILD information (Stecker et al., 2013). Second, aperiodicity will deteriorate the PE. Onset weight dominated for periodic and reduced dramatically for aperiodic noise-burst trains. For the periodic amplitude-modulated noise-burst trains, there was a stronger weight on the earliest and least intense bursts of the increasing envelope slope (Stecker, 2018). Third, “temporal jitter” will reduce the PE. The “temporal jitter” implemented into the brief Gabor click trains would reduce the onset weighting at 1.25 ms and 2.5 ms ICI

and enhance the post-onset weight at 2.5 ms ICI for binaural cues (Brown and Stecker, 2011).

1.2 Cochlear implants

1.2.1 Prevalence of hearing loss

There are around 466 million people suffered from disabling hearing loss globally (hearing threshold of the better hearing ear greater than 40 dB in adults and greater than 30 dB in children) and 34 million of them are children. Over 1 million people aged from 12 to 35 years are exposed to loud sounds in recreational settings, which put them at higher risk of hearing loss. For the population over 65 years old, approximately 1/3 are affected by disabling hearing loss. By 2050, the estimated population of disabling hearing loss will be over 900 million. The world wide annual overall cost for unaddressed hearing loss is US\$ 750 billion (WHO, 2020). Hearing loss has negative effect on individuals' social competence (Hoffman et al., 2014), education, income, and employment status (Emmett and Francis, 2015).

1.2.2 Etiology of hearing loss

There are congenital and non congenital causes for hearing loss. Congenital hearing loss is presented at birth, and causes by a series of risk factors. In lower income communities, environmental and prenatal factors are the prevalent causes. Another common risk factor for hearing loss is congenital infections, particularly

cytomegalovirus infection. In developed countries, genetic causes is the dominant cause for hearing loss. Mutations can affect any aspect of the hearing system, for example, inner ear homeostasis and mechano-electrical transduction (Korver et al., 2017). Sudden sensorineural hearing loss (SSHL) usually happens at the age of 50 to 60, the causes for which includes idiopathic, infectious disease, otologic disease, trauma, vascular or hematologic, neoplastic, and other causes. Among those etiologies for SSHL, idiopathic accounts for 71.0% (Chau et al., 2010).

1.2.3 Treatments of hearing loss

No medicine has been approved by the Food and Drug Administration to treat hearing loss (Müller and Barr-Gillespie, 2015). People with hearing loss depend on medical devices, such as hearing aids, assistive listening devices, cochlear implants, implantable middle ear hearing devices, bone anchored hearing aids, and personal sound amplification products to improve their hearing (U.S. Food & Drug Administration, 2020).

The Cochlear Implant (CI) is an effective approach to treat profound hearing loss. This neuroprosthesis introduces electrical stimulation to the ear and successfully helps to perceive a sensation of sound. In 1961, the two pilot single-channel electrode CIs were implanted inside the cochlea by the American otologist William House and the neurosurgeon John Doyle. In 1978, the first commercialized multi-electrode CI under the name of Cochlear/Nucleus was implanted by the Australian otologist Graeme Clark (Mudry and Mills, 2013).

Scientists spent decades to develop and polish the CI, from single-channel to multi-channel electrode, from unilateral to bilateral implantation, exerting all their effort to make CI users experience sound perception as close as possible to normal hearing individuals. A majority of binaurally hearing impaired population only receive unilateral cochlear implantation, and the lack of binaural cues leads to poor sound localization and speech perception in noise (Brown and Balkany, 2007). Aside from the economic burden, leaving a chance to receive a better designed CI later in life is another important reason for them to only accept unilateral CI. As the CI technology becomes more sophisticated, more and more deaf people are receiving bilateral CIs to improve their hearing ability (Laszig et al., 2004; Eapen et al., 2009; Bennett and Litovsky, 2020).

1.2.4 Bilateral cochlear implantation

Bilateral CIs provide binaural hearing to severe to profound hearing loss patients, and improve their ability to perceive speech in noisy background and localize sound (Tyler et al., 2003; Schoen et al., 2005; Brown and Balkany, 2007; Lovett et al., 2010; Choi et al., 2017). Severe to profound deafness refers to the ability to hear sound, without acoustic hearing aids bilaterally, only at levels equal to or greater than 80 dB HL (hearing level) at 2 or more of the following pure-tone frequencies: 500 Hz, 1000 Hz, 2000 Hz, 3000 Hz and 4000 Hz (NICE, 2019). For severely hearing impaired patients, the timing of when they receive their cochlear implantation affects the outcome of spoken language perception. Implantation completed before 24 months of age results in a better catch-up with

hearing peers (Nicholas and Geers, 2007). Simultaneous bilateral cochlear implantation is a recommended operation to treat severe to profound deafness for children or blind adults (or adults have to rely more on auditory stimuli due to other disabilities), in preference to other sequential bilateral cochlear implantation (NICE, 2019).

1.2.5 Why focus on ITD

The advantage of fitting CIs in both ears is that it can provide binaural cues to improve sound localization (Grantham et al., 2007; Grieco-Calub and Litovsky, 2012) and speech intelligibility in noise compared to unilateral CI (Litovsky et al., 2009; Dunn et al., 2010). However, those improvements primarily rely on ILDs (van Hoesel, 2004; Seeber and Fastl, 2008). Although measurable sensitivity to ILDs and ITDs were found by using a novel method to measure the unsynchronized CI sound processors, the result suggested that the bilateral CI users may not combine ILDs and ITDs in sound lateralization, because the slope of the lateralization function follows that of ILDs when ILDs and ITDs co-vary (Kan and Litovsky, 2018).

The original design for the implant system was conceived with monaural use in mind and was not considering any binaural synchronization. The stimulation strategy of commercial processor can only encode envelope ITD (ITD_{env}) but not fine structure ITD (ITD_{fs}). A bank of band-pass filters are applied and the envelope of the signal at the output of each band is sampled (the sample rate is also known as update rate) in the clinically prevalent sound-processing strategies for

these pulsatile non-simultaneous cochlear implants (van Hoesel and Tyler, 2003). The issue is that the CI system cannot represent features of sounds that happen on time scales faster than the update rate. CI engineers sometimes think of the CI pulses as “sampling” the sound envelopes, which would set a sort of “Nyquist limit” at half the update rate. However, the updates usually occur only about once every ms, much too slow to encode time with enough precision to allow ITD detection. The switch-on delay between the two processors in bilateral cochlear implant settings would cause a fixed ITD_{fs} within a range of 0 μ s to inter-pulse interval (IPI). Also, the time bases deviate in different IPI due to the existence of manufacturing tolerances. Hence, the pulse rates are hardly considered as exactly equal at both ears even they are being stimulated at the same rate (Thakkar et al., 2018). Because of those technical barriers, it is impossible to have the electrodes in both ears fire synchronously in bilateral cochlear implant users by the time of writing. Another issue raised from the stimulation strategy is that the commonly used clinical processors of CIs are at ~ 1000 pulse per second (pps) for each electrodes to obtain a good speech perception. However, the best sensitivity to ITDs is when the pulse rate is at $\sim 100 - 300$ pps (Thakkar et al., 2018). Researchers found a potential solution for this problem: mixed stimulation rates. Stimulate only one pair of the electrode arrays with low-rate yielded a comparable ITD sensitivity with stimulating all electrode arrays with low-rate. Low-rate stimulation at the basal or middle region provided the best ITD sensitivity in bilateral cochlear implantees (Thakkar et al., 2018).

For implantees, the hearing experience and the uneven number of active neurons in the two ears will lead to neural asymmetries between the ears, and the high-rate pulsatile stimulation and the envelop-extraction process will cause the reduction of binaural sensitivity. The asymmetrical placement of electrodes may affect the excitation range on the cochlear spiral ganglion frequency map (Stakhovskaya et al., 2007). However, evidence showed that when the stimulation placement between ears was carefully matched, the placement of stimulation along the cochlea (apical, mid and basal) did not change the ITD sensitivity in bilateral cochlear implant users (van Hoesel et al., 2009).

The collective effect of all these factors is that currently used cochlear implant technology does not deliver time differences between ears effectively and consistently. Although there are methods to improve ITD sensitivity in laboratory practice, none has gone into industry application yet. More research has to be done and more evidence has to be obtained to realize a better cochlear implant stimulation strategy for clinical practice. A suitable animal model is needed for this purpose.

1.3 Is rat a suitable animal model to study binaural hearing?

Most species of mammals use binaural cues to localize sound, but it has been reported that some species only use one cue. For example, domestic pig, horse and domestic cattle only use ITD cue. Greater spear-nosed bat, big brown bat, African pygmy, hedgehog, short-tailed fruit bat, spiny mouse, desert hedge-

hog, grasshopper mouse, and house mouse only use ILD cue (Heffner and Heffner, 2003). Therefore, to study the sound localization cues in general, a species using both ILD and ITD cues with good acuity is an optimal choice.

Rats are economic, easy to breed and handle, and widely used in many life science fields. To establish a rat model for binaural hearing research brings many potential benefits, as it would allow us to combine multi-level approaches such as behavior, electrophysiology, and molecular studies. The rat is already a state-of-the-art model for investigating the hearing impaired central auditory system with CI stimulation (Rosskothén-Kuhl and Illing, 2010; Rauch et al., 2016). A rat model of bilateral CI in binaural cues studies can provide us an opportunity to explore the underlying mechanism of how bilateral CI stimuli affects the auditory system and investigate novel CI stimulation strategies before clinical use.

These aspects motivated the studies described in this thesis. We wanted to verify whether rat is a suitable model to study binaural hearing, thus it can be further used in cochlear implanted condition and to develop optimal stimulation strategy in order to improve the hearing restoration. To do so, we had to demonstrate that rats process similar auditory processing as humans do.

1.3.1 Auditory characteristics of rats

Auditory systems are different between species because of various living environments they are adapted to. The tympanic ears of mammals evolved independently with amphibians or sauropsids. Hence, the findings regarding hearing

mechanism based on birds or frogs cannot easily be analogized to humans (Grothe et al., 2010). The laboratory albino animals are different from their wild type ancestors not only in the appearance but also in organic functions (Creel, 1980). The lack of melanin may cause visual deficits (Prusky et al., 2002). Carefully selecting a suitable type (wild type or albino, which strain) of animal for research is of considerable importance. Albinism reportedly does not affect the auditory sensitivity in rats. Studies have shown that the albinism has no effect on the cochlear degeneration in the aged rat cochlea (Keithley et al., 1992). But, there are differences at their auditory sensitivity extremes. Rats are known for their ultrasonic vocalizations and sensitivity to high frequency sounds. The hearing range at 60 dB SPL (sound pressure level) is from 530 Hz to 68 kHz for hooded rats, while is from 400 Hz to 76 kHz (estimated) for albino rats (Heffner et al., 1994). At 70 dB SPL, the auditory hearing range of the albino rat extends from 250 Hz to 80 kHz with the greatest sensitivity to tones at 8 kHz and 38 kHz (Kelly and Masterton, 1977). As the human hearing range is from 31 Hz to 17.6 kHz at 60 dB SPL (Jackson et al., 1999), the overlapped hearing range between albino rat and human is about 5 octave (400 Hz – 17.6 kHz) at 60 dB SPL. In the hearing range respect, rat is suitable for preclinical hearing research.

1.3.2 The controversy over ITD sensitivity in rats

As early as in the 1970s, behavioral studies have shown that rats could use both ITD and ILD cues for tone bursts localization, with specially utilized ITD cue for frequencies below 5 kHz and ILD above about 6 kHz, and were able to lateralize the sound source when the stimulus was leading by 80 μ s (phase-shift

equivalent) at one ear at 3 and 4 kHz but not at 5 and 7 kHz (Flammino and Clopton, 1975a). An electrophysiological study from Kelly and colleagues discovered that neurons of the IC of rats are highly sensitive to ITDs over the range of -1.0 to +1.0 ms, by processing time differences between clicks delivered to the two ears (Kidd and Kelly, 1996) and the neurons of dorsal nucleus of the lateral lemniscus (DNLL) of rats showed sensitivity to ILD and ITD to both dichotic tone and clicks stimuli (Kelly et al., 1998). Acoustically, the maximum envelope-based ITDs that female Sprague Dawley rats would experience given their head size was reported to be $127 \pm 14 \mu\text{s}$, and the maximum low-frequency ongoing ITDs was $158 \pm 8 \mu\text{s}$ (Koka et al., 2008). Heffner reported that wild Norway rat can use both ITD and ILD cues to localize broadband noise (Heffner and Heffner, 2003).

However, another paper from the Heffner's lab (Wesolek et al., 2010) later claimed that rat, may not use ITDs to localize sounds. In their study, sound was delivered via two loudspeakers located 30° apart from the midline. This free field sound localization test was the basis of their conclusion that rat lacked the ability to use binaural time cues to localize sound. They claimed that the illusion which rat could use ITD for sound localization in low frequency was due to overtones which made it possible for the rats to localize using transient binaural intensity-difference cue. We cast doubt on this result and proposed to verify the rat's sensitivities to ITD with improved method.

In studies of sound localization, free field sound stimuli is widely used (Brugge et al., 1994; Faller and Merimaa, 2004); but for rats, firstly, the size of

the head is much smaller and secondly, they do not tend to stay still. Although close-field sound stimuli was also used to study the sound localization of ferret (Keating et al., 2013), this method requires craniotomy and anesthesia. Taking animal welfare into account, we modified the placement of the sound source to introduce a near-field sound stimulus other than using a commonly used free-field one to better control the experiment condition. Here, we established a new training setup to mimic near-field environment for sound presentation to test the sensitivities of ITD of normal hearing rats.

1.4 Basic of signal detection theory

To verify whether rat is a suitable animal model for binaural research, behavioral and electrophysiological approaches will be used. Here I give a brief introduction into the basics of signal detection theory (SDT), which underpins the analytic methods used to analyze the data I collected.

In SDT it is recognized that, in the real world, signals always come with background noise. The noise may sometimes be strong enough to be mistaken for a signal. Imagine that you are talking with your friend in a cafe with background music (BGM) playing. If you want to listen to your friend, then your friend's speech is a signal, and the BGM is a noise. But, if you want to enjoy the BGM, your friend's speech is a noise while the BGM is a signal in such a case (your friend will be a little bit upset though). In our nervous system, a continuous spontaneous activity randomly varies over time, and this background noise is also embedded in neural signals.

One simple assumption often made in SDT is that the Signal and Noise follow a Gaussian distribution with the same variance. In a yes-no paradigm, the observers have to decide whether the signal or noise generate their sensations to make a binary response base on a certain criterion. When an observer is trying to distinguish signal from noise, the response of a trial will fall into one of the four outcome categories (hits, misses, false alarms, correct rejections), as shown in **Figure 1.4.1**. Errors occurs because of the overlap of Signal and Noise distribution. The accuracy or sensitivity can be measured inversely by the degree of overlap. Reduce the overlap is the only way to improve sensitivity (Stevens, 2002).

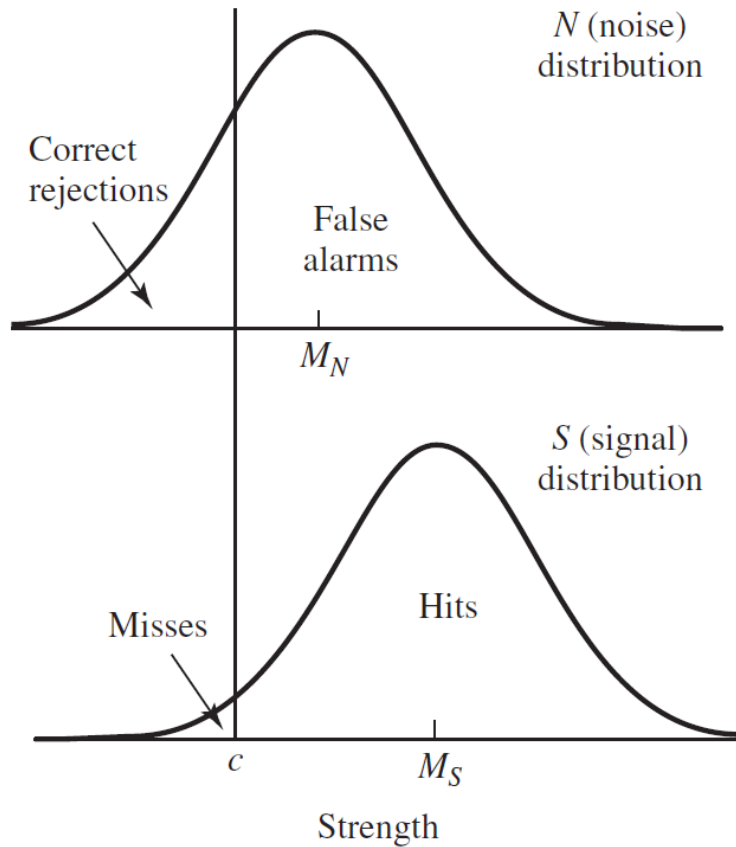


Figure 1.4.1: Distributions of strength for Noise and Signal.

NOTE: The upper curve is the distribution due to Noise trials; values above the criterion c lead to false alarms, and those below to correct rejections. The lower curve is the distribution due to Signal trials; values above the criterion lead to hits, those below to misses. The means of the distributions are M_N and M_S , and the variances are equal. Reprinted with permission from Stevens' Handbook of Experimental Psychology, Volume 4: Methodology in Experimental Psychology, 3rd edition, by Hal Pashler (Editor-in-Chief), John T. Wixted (Editor), published by Wiley. (Stevens, 2002).

There are several methods to evaluate the sensitivity to the received signal. The sensitivity index d' can be estimated from the proportions of the hits and false-alarm trials. There are non-parametric measures of sensitivity as well, such as the area under the ROC curve. The slopes of a psychometric function also indicates the response sensitivity.

1.4.1 Sensitivity index

The observer's true sensitivity is reflected by the difference between the means of the Signal and Noise distributions, and is unaffected by the criterion location. Letting $z(p)$ denote the z-score of a corresponding proportion p , we have $z(H) = M_S - c$ and $z(F) = M_N - c$. Then the sensitivity index $d' = M_S - M_N = z(H) - z(F)$, where H and F is Hit rate and False-alarm rate, respectively. This definition expresses accuracy as the difference between the z-score transformation of hit rate and false alarm rate (Stevens, 2002).

1.4.2 The area under the ROC curve

As the criterion c decreases (moves from right to left in **Figure 1.4.1**), both $z(H)$ and $z(F)$ increase. The relation between $z(H)$ and $z(F)$ can be demonstrated in a ROC curve (**Figure 1.4.2 (a)**). From $d' = z(H) - z(F)$, we have $z(H) = d' + z(F)$, which is a straight line with unit slope and intercept d' , as shown in **Figure 1.4.2 (b)**.

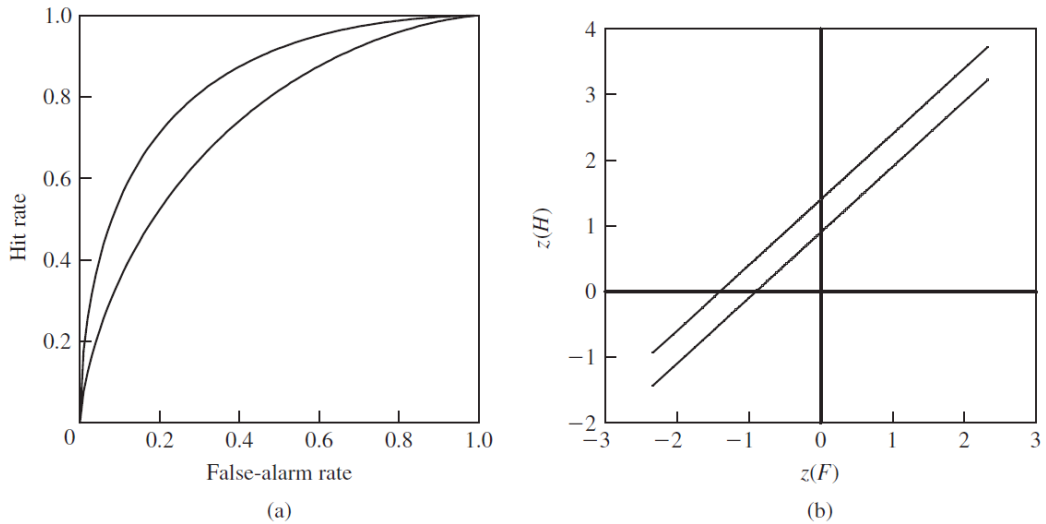


Figure 1.4.2: Receiver operating characteristics (ROCs) for two normal distributions with the same variance.

(a) Probability coordinates. (b) z coordinates. NOTE: In both panels, the two curves are for $d' = 0.9$ (lower curve) and 1.4 (higher curve). Reprinted with permission from Stevens' Handbook of Experimental Psychology, Volume 4: Methodology in Experimental Psychology, 3rd edition, by Hal Pashler (Editor-in-Chief), John T. Wixted (Editor), published by Wiley. (Stevens, 2002)

1.4.3 Psychometric function

Psychophysics is a discipline that studies the correlation of physical stimuli and subjective responses. Psychometric function is a function that addresses the probability of response as a function of the stimulus strength to interpret the psychophysical data.

One century ago, Boring proved that the *phi*-function of gamma $\Phi(\gamma)$ is valid as the psychometric function, which the sigmoid curve is symmetrical about the 50%-line and asymptotic to the 100% and 0% lines (Boring, 1917). Practically, the subjects sometimes tend to ignore the stimulus even the levels are far beyond the threshold, i.e. to have lapses or rate of false negative errors. Similarly, the

subjects may give a yes response when the stimulus levels are below the threshold, the probability of these actions is named the guessing rate or the rate of false positive errors (Treutwein, 1995). The concepts of lapsing rate and guessing rate will be applied later to the analysis of behavior data from rats performing 2-AFC tasks.

1.5 Field potential

Neuronal activity induces transmembrane currents that can be detected in the extracellular medium. This extracellular signal majorly comes from the synaptic transmembrane current, while other sources also contribute substantially to shape the extracellular field, such as Na^+ and Ca^{2+} spikes, ionic fluxes via voltage-gated channels and ligand-gated channels, and intrinsic membrane oscillations. The electric currents superimpose at a given location and generate an electric potential, V_e (a scalar in Volts), against a reference potential (Buzsáki et al., 2012). Field potentials may reflect the activity of adjacent or remote neurons (Herreras, 2016).

Field potentials are conventionally categorized based on the recorded site, such as in brain local field potentials (LFP), epidural or subdural electrocorticography (ECoG), scalp electroencephalography (EEG), intracranial stereotactic electroencephalography (stereo-EEG), and magnetoencephalography (MEG; **Figure 1.5.1**) (Pesaran et al., 2018). The first two of these are particularly relevant to our purposes, as we will encounter intra-cranial LFP and ECoG recordings from the auditory midbrain and cortex in response to binaural stimulation in

later chapters. All field potential recordings have fine temporal precision in the range of millisecond and are applicable in humans and nonhuman animals as well. The techniques distinguished mostly on the spatial resolution, coverage, and invasive level (Pesaran et al., 2018).

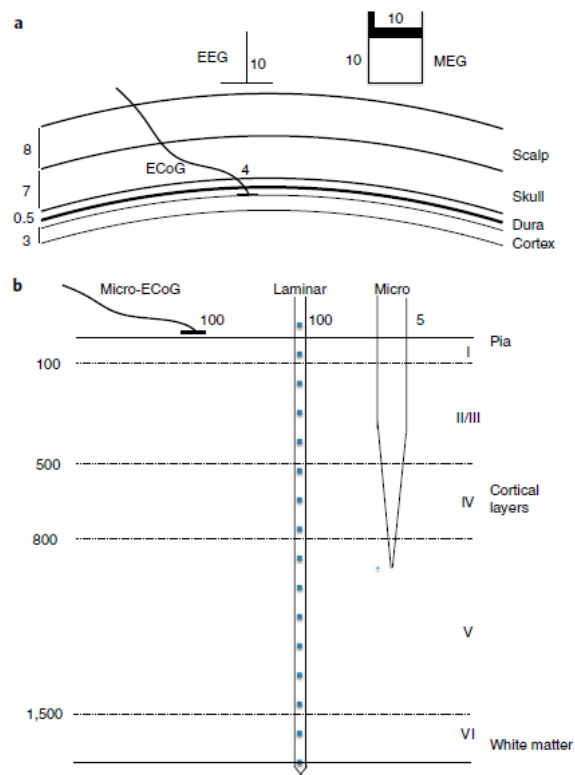


Figure 1.5.1: Field potential recording modalities.

a, EEG and MEG signals are measured noninvasively. EEG involves electrodes ~ 10 mm in size placed at the scalp across the head. MEG is measured using sensitive sensors (superconducting quantum interference devices, or SQUIDS) placed just outside the head (**Hämäläinen et al., 1993**). ECoG is measured invasively and involves placing electrodes either epidurally, on the dura that protects the brain, or subdurally, directly on the pia at the surface of the brain. ECoG can be performed in humans in the relatively rare case of epilepsy surgery and is otherwise mainly used in animal models. ECoG electrodes are smaller than EEG electrodes and range in size from 1 to several millimeters in size (Chao, 2010). All dimensions are in millimeters. **b**, Invasive recordings can also be made at finer spatial scales. Micro-ECoG involves $20\text{--}200\ \mu\text{m}$ contacts placed on the pia (Khodagholy et al., 2014; Insanally et al., 2016). Coverage can extend to many square centimeters at sites across the brain. LFP is the most invasive procedure and involves inserting electrodes into the brain. As a result, LFP recordings are made with even smaller recording contacts than ECoG, extending to microelectrodes and thin-film electrodes that can also record the activity of individual neurons. All dimensions are in micrometers. Reprinted by permission from [Springer Nature]: [Nature] [Nature Neuroscience] [Investigating Large-scale Brain Dynamics Using Field Potential Recordings: Analysis and Interpretation, Bijan Pesaran, Martin Vinck, Gaute T. Einevoll, Anton Sirota, Pascal Fries, Markus Siegel, Wilson Truccolo, Charles E. Schroeder & Ramesh Srinivasan], [2018]. (Pesaran et al., 2018)

1.5.1 Local field potential

The electrophysiological signal recorded using an extracellular microelectrode is called local field potential. The electrical fluctuations generated by synaptic activity of the whole population of neurons closed to the tip of the electrode accumulate and form the overall recorded potential (Takamori et al., 2009). The amount of information carried in the LFP corresponding to the neuronal activity at the source location inversely related to the distance between the recording site and the source (Buzsáki et al., 2012).

The synaptic activity is the largest contributor to the LFP. The synaptic AMPA (α -amino-3-hydroxy-5-methyl-4-isoxazolepropionic acid) and NMDA (N-Methyl-D-aspartic acid) receptor bind with neurotransmitters and mediate Na^+ and Ca^{2+} excitatory currents flowing into the synapse, respectively. The influxes generate a local extracellular sink. To maintain electroneutrality within a time constant, an inverse direction ionic flux is needed to balance the extracellular sink. This flux from the intracellular to the extracellular medium is known as passive current or return current.

The distance r from the source current(s) (net local outward currents) and the location of the sink current(s) (net local inward currents) determine the formation of a dipole or an n -pole. The contribution of monopole or dipole to V_e is dependent on the distance r , for monopole scales as $1/r$, while for dipole scales as $1/r^2$. This rapid decay of the influence is because of the dipole have two opposing charges cancelling out each other to first order (Buzsáki et al., 2012). When the source of local field potential is weak, susceptibility to volume conduction effects will increase over the distance (Kajikawa and Schroeder, 2015).

1.5.2 Electrocorticography

Compared to intraparenchymal LFP recordings, ECoG can be recorded without penetrating the electrodes into the brain tissue. In comparison to non-invasive recording methods, ECoG has higher signal to noise ratio (Ball et al., 2009), higher spatial resolution (Freeman et al., 2000), more resistant to noise, and more prone to long lasting recording. ECoG attracts increasing interest in Brain-Computer-Interface research field because of its detailed reflection of brain activity and its robust and chronic implantability (Schalk and Leuthardt, 2011).

Oscillations in the ECoG is one type of intrinsic brain activity that primarily reflect cortical synaptic potentials (Groppe et al., 2013). Some of the oscillation rhythms are robustly reflect the character of particular brain states, functions and regions. Based on this, the oscillations are conventionally classified into delta [1–4 Hz], theta [4– 8 Hz], alpha/mu [8–13 Hz], beta [13–30 Hz], gamma [30–80 Hz], and high gamma [80–150 Hz] (Canolty et al., 2006; Crone et al., 2011), the boundaries may vary slightly from study to study.

1.5.3 Neural activity quantification

We used a measurement based on analog multi-unit activity (AMUA) to quantify the neural activity from extracellular recording. This method quantifies neural activity by measuring the voltage signal power in the frequency band covered by extracellular recorded action potentials. In particular, to extract the

recorded voltage in a frequency range accounted for spikes, a band-pass filter between 300 and 6000 Hz was applied, and the absolute value of the band-passed data was taken, followed by applying a low-pass filter below 6000 Hz to avoid aliasing, then signal downsampling was conducted (Schnupp et al., 2015).

Comparing to other multi-unit activity (MUA) measurements that rely on thresholding and event count, this AMUA approach does not require any prior free parameters, and can obtain substantially clear signal in comparison with thresholding. In thresholding method, errors may occur in the following conditions: false negative happens when the electrical noise occasionally intervenes with MUA spikes and drags their amplitudes lower than the threshold; while false positive occurs when noise events sum up to surpass the threshold. Undercounting takes place when several MUA spikes collide in time and only a single threshold is counted (Schnupp et al., 2015).

2 Chapter 2 Microsecond sensitivity to envelope interaural time differences in rats

The text and figures of this chapter have been adapted from an article I have been able to publish on my thesis work, and were reprinted with permission from [Li, K., Chan, C., Rajendran, V., Meng, Q., Rosskothén-Kuhl, N., and Schnupp, J. (2019). Microsecond sensitivity to envelope interaural time differences in rats. *The Journal of the Acoustical Society of America* 145, EL341-EL347]. Copyright [2019], Acoustic Society of America. (Li et al., 2019).

2.1 Introduction

Binaural cues are important for sound localization. The two primary binaural cues are differences in sound level and arrival time between two ears, known as interaural level differences (ILDs), and interaural time differences (ITDs), respectively. The species most commonly used in binaural hearing research, including gerbils (Lingner et al., 2012; Tolnai et al., 2017), ferrets (Keating et al., 2013), cats (Brugge et al., 2001), and guinea pigs (Greene et al., 2018), all show sensitivity to both ILDs and ITDs.

Rats are relatively rarely used in studies of binaural hearing due to a reputation for relatively poor sound localization abilities (Heffner and Heffner, 1985; Kavanagh and Kelly, 1986) and controversy around the extent to which they can

use ITDs to localize sound. While neurophysiological evidence for ITD sensitivity in rats has been documented in the literature (Kidd and Kelly, 1996), a recent behavioral study by Wesolek et al. (2010) used low frequency (0.5 to 2 kHz) pure tone free-field stimuli to conclude that rats were unable to use ITDs to localize sound. However, the restricted choice of stimuli did not allow the authors to fully explore the rats' sensitivity to envelope ITDs, which feature prominently in many natural sounds, and which can in principle provide both transient and ongoing ITD information over the entire frequency range (Bernstein, 2001).

Here we evaluated the rat's ability to use ITDs to localize pulse-resonance sounds, an important class of broadband sounds that also comprises communication calls used by humans and many other animal species (Patterson, 2015). These stimuli provided both transient onset and ongoing envelope ITD information across a wide frequency range. By comparing responses to pulse trains with either sharp onset rectangular windows or with very gradual Hanning windows, we were able to assess the rats' sensitivity to onset and ongoing envelope ITDs at different pulse rates.

2.2 Materials and Methods

2.2.1 Subjects

Five female Wistar rats (220–260 g, two months old at the beginning of training) were used in this study. The rats' hearing thresholds were confirmed to be in the normal range by recording auditory brainstem responses (ABRs) under anesthesia [ketamine (80 mg/kg) and xylazine (12 mg/kg)], and their tympanic mem-

branes and outer ear canals were inspected to confirm the absence of obstruction or outer or middle ear disease. All experimental procedures were approved by the Committee on the Use and Care of Animals at City University of Hong Kong, and under license by the Department of Health of Hong Kong [Ref. No. (16–86) in DH/HA&P/8/2/5 Pt.5].

2.2.2 Stimuli

Stimuli consisted of single sample pulse (delta function “click”) trains of 200 ms duration generated at a sample rate of 44 100 Hz and pulse rates of 50, 300, 900, 1800, or 4800 Hz. Click trains were presented at an average binaural acoustic level of 80–85 dB sound pressure level. To investigate the contributions of onset and ongoing ITD cues, click trains were enveloped with either rectangular or Hanning windows of 200 ms duration [Figure 2.2.1(C)]. To produce ITDs of $\pm 175 \mu\text{s}$ [$\sim 130\%$ of the rat’s physiological range of $\pm 130 \mu\text{s}$ (Koka et al., 2008)], identical stimulus pulse trains were presented to each ear, with the stimulus in one ear delayed relative to the other by an appropriate number of samples (22.7 μs steps). Negative ITD values are when the stimulus in the left ear leads relative to that in the right.

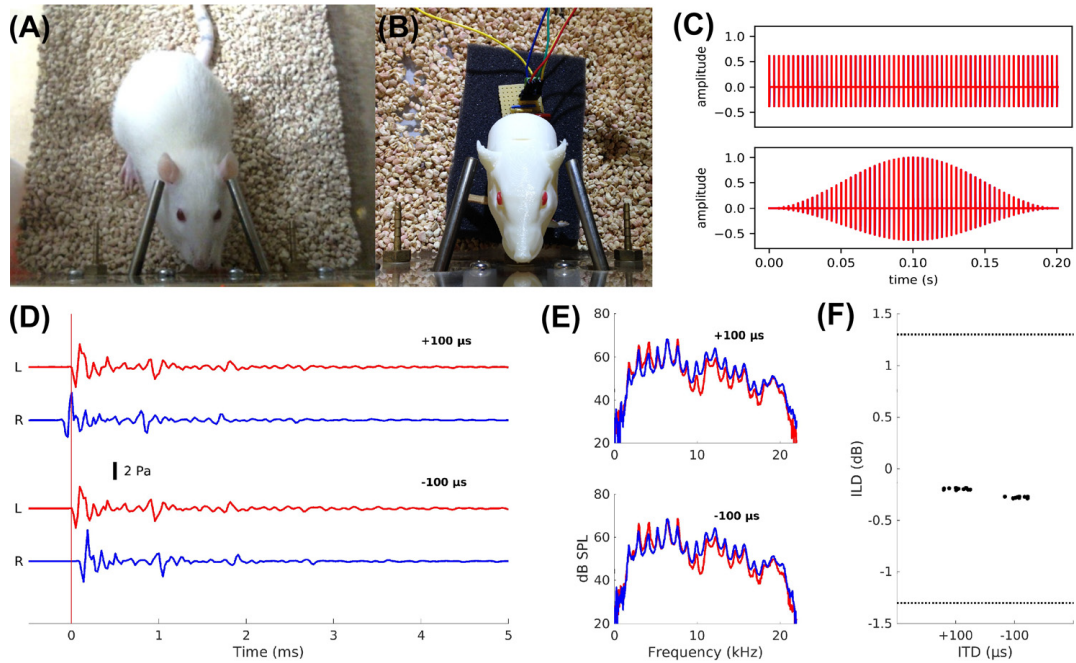


Figure 2.2.1: Rat binaural psychoacoustics near-field setup.

(A) Rat during a testing session, initiating a trial by making contact with the central “start” spout. Steel tube phones are positioned close to each ear. (B) 3D printed rat acoustic manikin with miniature microphones in each ear canal used for calibrating and validating the setup. (C) Example waveforms of 300 Hz rectangular window (top) and Hanning window (bottom) pulse trains used. (D) Waveforms of a single binaural pulse as recorded from the microphones inside each ear canal of the acoustic manikin (L: left ear, R: right ear) for $\pm 100 \mu\text{s}$ ITD (top and bottom pair of traces, respectively). The pulse train stimuli shown in (C) are made from sequences of pulses like the one shown. Cross correlation functions of the recorded signals confirmed what is also apparent by inspection of the waveforms, namely, that the ITDs of the acoustically recorded signals corresponded precisely to the electric interaural delays. (E) Frequency spectra of the sound waveforms in (D) for $\pm 100 \mu\text{s}$ ITD. (F) Acoustic ILDs (y axes) measured from microphones placed in the ear canals of the acoustic manikin for $\pm 100 \mu\text{s}$ ITD. ILDs were computed as the difference in root mean square (RMS) power of the signals in (D). Waveforms were recorded for ten pulses at each ITD. Each dot therefore represents one trial. A small random x axis scatter was added for visualization. Dotted lines indicate average broadband ILD thresholds of ferrets (Keating et al., 2013) for comparison. Behavioral rat ILD thresholds have not been reported in the literature, but are estimated to be around 2.8–4 dB (Greene et al., 2018).

Signals were generated on a Raspberry Pi 3 computer and sent through a USB sound card (StarTech.com, Ontario Canada, part No. ICUSBAUDIOMH)

running at 16 bit, and amplifier (Adafruit stereo 3.7W class D audio amplifier, part No. 987) to miniature high fidelity headphone drivers (GQ-30783-000, Knowles, Itasca, Illinois, US), which were mounted to hollow stainless steel tubes for sound delivery. The pulses resonated in the tubes to produce pulse-resonant sounds resembling single-formant artificial vowels, with a fundamental frequency corresponding to the click rate. These tube phones were held in place by custom 3D printed ball-in-socket joints and were positioned such that, when the rat started a trial by licking a center start spout, the tips of the tubes were located right next to each ear, allowing for near-field stimulation [**Figure 2.2.1(A)**]. Note that this mode of sound delivery is similar to that produced by “open” headphones, such as those commonly used in previous studies on binaural hearing in humans and animals, e.g., Keating et al. (2013).

The acoustic setup was validated using a custom, 3D printed acoustical manikin rat head with miniature microphones in each ear canal [**Figure 2.2.1(C)**]. Waveforms for a single binaural pulse recorded at each ear are shown in **Figure 2.2.1(D)**, and their frequency spectra are shown in **Figure 2.2.1(E)**. As might be expected, **Figure 2.2.1(E)** reveals interaural spectral differences at some frequencies due to manufacturing tolerances, but these do not result in systematically varying ILDs, and **Figure 2.2.1(F)** confirms that any residual ILDs were negligible and did not covary with ITD conditions. The crosstalk between the ears over the full 500 Hz to 20 kHz signal range was -20 dB. This setup therefore provided robust and naturalistic ITDs but no useable ILD cues to the animals.

2.2.3 Training

Rats were trained to perform a two-alternative forced choice sound lateralization task using established methods (Itskov et al., 2012; Keating et al., 2013). Rats were put on a schedule of 5 days of testing, during which drinking water was a positive reinforcer, followed by two days off with *ad lib* water. Drinking bottles were removed ~16 h prior to the next testing period. Rats performed two sessions per day, each lasting 30 min, corresponding to ~200 trials and ~15 ml of water consumed.

One of the walls of a perspex cage was fitted with three brass water spouts, mounted ~7 cm from the floor and separated by ~6 cm (**Figure 2.2.1(A)**). Contact with the spouts was detected by touch detectors (Adafruit industries, USA, part No. 1362). Initiating a trial at the center spout triggered the release of one small drop of water through a solenoid valve on a fraction (1/7) of trials, followed by presentation of the sound stimulus. Correct lateralization of the stimulus by licking the left or right response spouts triggered four small drops of water as positive reinforcement. Incorrect responses triggered no water delivery, a negative feedback sound, and a 15–30 s timeout during which no new trial could be initiated. After an incorrect trial, the same stimulus was repeated as a “correction trial” to prevent animals from developing idiosyncratic biases favoring one side (Keating et al., 2013). Correction trials were excluded from analysis. Rats were initially trained to lateralize 300 Hz trains containing both ILDs of ± 6 dB and ITDs of ± 175 μ s. Once they performed at $\geq 80\%$ correct, ILD cues were removed, and variable ITDs were gradually introduced. Training to a high level of perfor-

mance with variable ITD-only stimuli took between 14 and 20 days (28–40 sessions).

2.2.4 Psychometric analysis

When sensory signals are large relative to noise, the task is easy and performance will be consistent, but when sensory signals are close to threshold, performance will be near chance. This relationship is captured by the sigmoidal cumulative Gaussian function Φ (Schnupp et al., 2005) (see also section 1.4.3) which we fitted to our data to quantify ITD sensitivity,

$$p_R = \Phi(ITD \cdot \alpha) \quad (2.2.1)$$

where p_R denotes the probability of choosing the right (R) spout, ITD denotes the interaural time difference (positive if the right ear leads, in ms), and α is the ITD sensitivity parameter with units of 1/ms that captures the change in the proportion of R responses a given change in ITD would induce.

This model was extended to account for possible additive lapses of attention and idiosyncratic biases towards one ear or one spout. The γ term denotes the lapse rate and it compresses the range of the psychometric sigmoid to $[\gamma/2, 1 - \gamma/2]$, which is equivalent to scaling by $1 - \gamma$ and shifting by $\gamma/2$. An ear bias exists if chance (50%) performance occurs at an ITD value some small value β away from zero. The parameter δ captures the increased probability of choosing the R spout due to an idiosyncratic preference. The extended model is

$$P_R = \Phi(ITD \cdot \alpha + \beta) (1 - \gamma) + \frac{\gamma}{2} + \delta \quad (2.2.2)$$

and maximum likelihood estimates for the parameters α , β , γ , and δ were derived from the data using gradient descent [scipy.optimize minimize()] (Jones et al., 2001)].

For stimuli that the animals could only lateralize with difficulty or not at all (i.e., ITD sensitivity α is close to zero) the parameters of the sigmoid model become poorly constrained by the data. Therefore, two alternative models were additionally fitted: a null model that assumes that $\alpha = 0$ and the rate of R responses is simply a constant,

$$p_R = 0.5 + \delta \quad (2.2.3)$$

and a linear model that assumes $\alpha > 0$ but does not fit a sigmoid because the proportion of R responses does not asymptote over the tested range of ITDs,

$$p_R = ITD \cdot \alpha + \delta \quad (2.2.4)$$

A χ^2 deviance test was used to choose the best model from **Equations** (2.2.2), (2.2.3), and (2.2.4) for each condition, and ITD sensitivity was in all cases defined as the slope of the modeled psychometric function around zero. ITD sensitivity was either zero if the null model gave the best fit, α for the linear model, or

$$slope = \varphi(0) \cdot \alpha \cdot (1 - \gamma) \quad (2.2.5)$$

for the sigmoidal model. **Equation** (2.2.5) is obtained by differentiating Eq. (2.2.2) and setting $ITD = 0$, and $\varphi(0)$ is the Gaussian normal probability density at zero (~ 0.3989). The ITD sensitivity metric is interpretable as the increase in the proportion of R spout choices for each μs increase in ITD.

D-prime values were estimated using the standard formula $d' = z(\text{hit rate}) - z(\text{false alarm rate})$, where the hit rate is the proportion of “right” responses for a

given positive ITD and the false alarm rate is the proportion of “right” responses for the corresponding negative ITD.

2.3 Results and discussion

Figures 2.3.1 and 2.3.2 show the psychometric curves obtained for each rat (rows of panels) at each click rate (columns of panels) using rectangular or Hanning window click trains, respectively. There is considerable variability between individual rats: Rats #2 and #4 are examples of particularly good and poor performers, respectively. There are also clear, systematic effects of pulse rate and envelope. ITD sensitivity declined rapidly as pulse rates exceeded a few hundred Hz. Similar sharp declines in ITD sensitivity with pulse (Laback et al., 2007; van Hoesel et al., 2009; Chung et al., 2016) or AM (Joris and Yin, 1995; Bernstein, 2001) rates above 500 Hz have been reported in previous physiological and behavioral studies on humans and other species.

Figure 2.3.3 summarizes the ITD sensitivities across conditions. In addition to illustrating inter-subject variability and the overall decline in ITD sensitivity with increasing pulse rate, **Figure 2.3.3** also shows that ITD discrimination was consistently better for rectangular than for Hanning windowed stimuli. For rectangular windows, the mean sensitivity remained significantly above zero at all click rates, but for Hanning windows it declined to zero for four out of five rats at 900 Hz, and for all rats above 900 Hz. (Note that the model selection described in

Sec. 2.2.4 only assigns non-zero ITD sensitivities to psychometrics where a χ^2 deviance test rejects the zero slope null model at $p < 0.05$.)

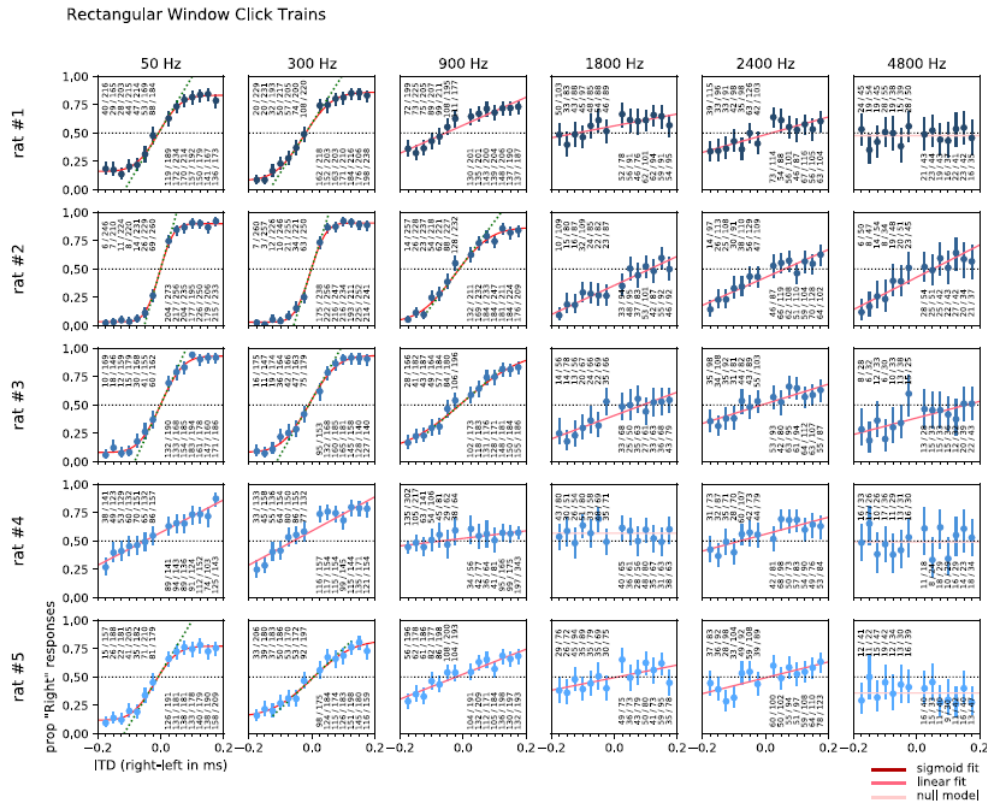


Figure 2.3.1: Psychometric curves for rats localizing rectangular window click trains by ITD.

Rows: individual rats. Columns: stimulus click rates. X-axes: stimulus ITD. Y-axes: proportion of responses to the right (R) spout. Negative ITDs mean the stimulus in left ear is leading. Dots indicate the observed proportion of R responses at each ITD tested. The fractions in small print show raw number of R responses / total number of trials at the corresponding ITD value. Error bars: 95% Wilson confidence intervals for the underlying probability of choosing the R spout. Solid lines: fitted psychometric models, as described in Sec. 2.2.4. Sigmoid fits are shown with dark lines, linear fits in a lighter shade, null model fits in a very light shade. Dotted diagonals: slopes of the fitted psychometric at ITD = 0.

Hanning Window Click Trains

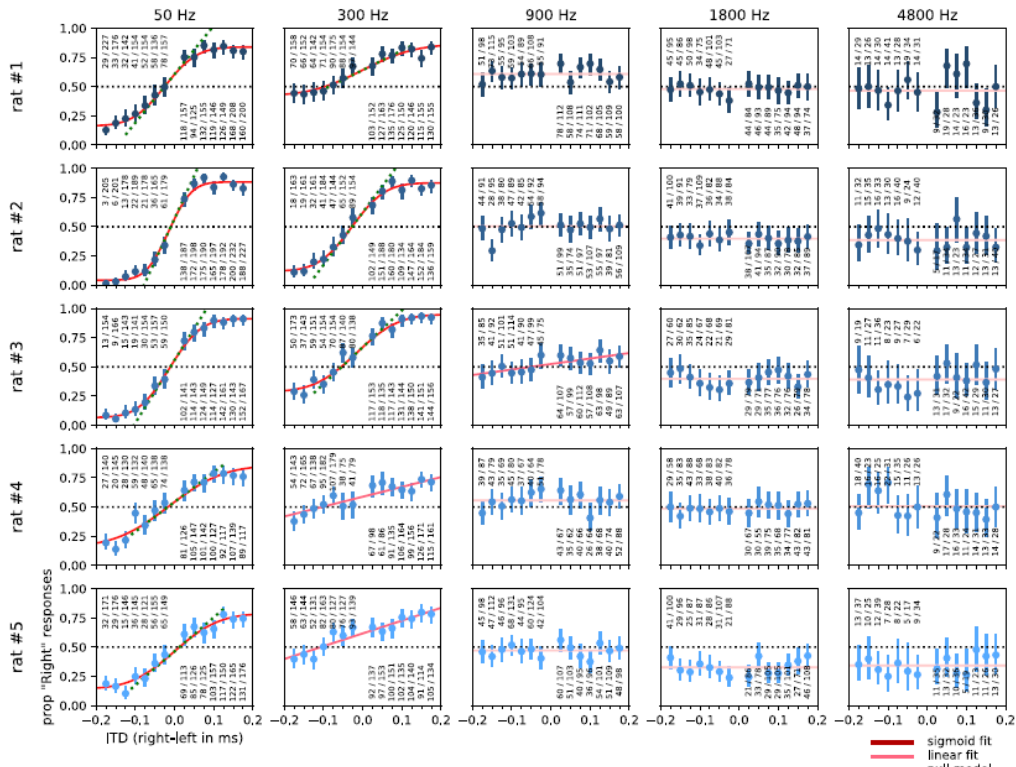


Figure 2.3.2: Psychometric curves for rats localizing Hanning window click trains by ITD.

Plotted as in Figure 2.3.1.

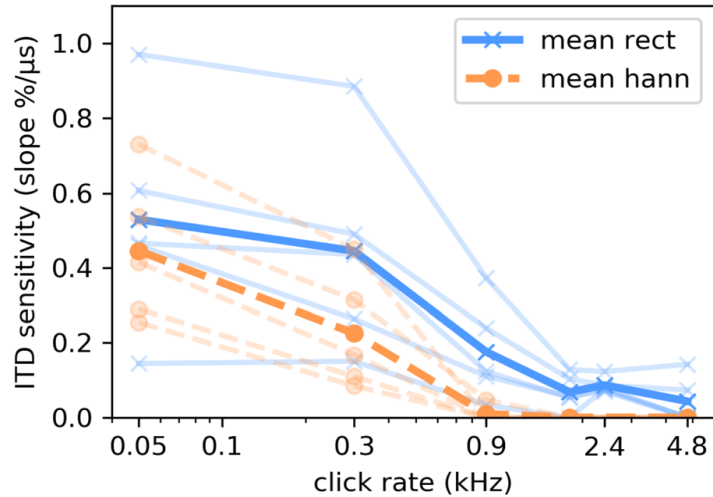


Figure 2.3.3: Summary of ITD sensitivity across click rates and window types.

Faded lines show the ITD sensitivity of individual rats for rectangular (continuous lines) and Hanning (broken lines) windows. Dark lines show mean performance across animals.

A repeated measures analysis of variance confirmed that ITD sensitivity exhibited a strong and highly significant dependence on click rate ($F = 19.12$, $df = 4$, $p < 10^{-5}$, $\eta^2_{\text{partial}} = 0.93$) as well as on click-rate by window type interactions ($F = 7.414$, $df = 4$, $p = 0.0014$, $\eta^2_{\text{partial}} = 0.74$). Thus, consistent with previous work in other species (Stecker and Hafter, 2002), rectangular windowed stimuli produced onset ITD cues that facilitated localization across all click rates tested, whereas Hanning windowed stimuli, with their very gentle on- and offset slopes, generated only ongoing ITD cues. Arguably, our 50 Hz pulse rate condition, which is near the “fusion boundary rate” where human listeners no longer perceive click trains as individual clicks but instead as a continuous complex tone, might be considered as “consisting of nothing but onsets” irrespective of the window. However, the same cannot be said for our Hanning windowed 300 Hz click trains, which all our rats were able to localize with fairly high sensitivity, demonstrating

that rats are able to use ongoing envelope ITDs. Sensitivity to ongoing ITDs has also recently been demonstrated in gerbils (Tolnai et al., 2018).

With 50 Hz rectangular click trains, our rats had a median 75% correct threshold of 65 μ s ITD and a mean of 77 μ s. Median and mean ITD thresholds corresponding to $d' = 1$ were 46 and 56 μ s, respectively. Our best performing rat (#2) exhibited 75% correct thresholds as low as \sim 29 μ s (compare **Figure 2.3.1**) and $d' = 1$ thresholds as low as 21 μ s. These values are similar to the \sim 10–60 μ s range of 75% correct ITD discrimination thresholds reported for normal hearing human subjects tested with noise bursts (Klumpp and Eady, 1956) and pure tones (Zwislocki and Feldman, 1956), or the \sim 40 μ s ITD thresholds reported for normal hearing ferrets tested with noise bursts (Keating et al., 2013). These values also compare well to behavioral measures and theoretical estimates of ITD thresholds for other small mammals; these are reported to be \sim 30 μ s for cats (Wakeford and Robinson, 1974), \sim 23–45 μ s for guinea pigs (Greene et al., 2018), \sim 50–60 μ s for rabbits (Ebert et al., 2008), \sim 55 μ s for chinchilla (Koka et al., 2011), and 12–96 μ s for Mongolian gerbils (Tolnai et al., 2017).

In conclusion, even though free field localization experiments with low frequency tones have led to the suggestion that rats may be unable to use ITDs to localize sounds (Wesolek et al., 2010), we have shown that Wistar rats tested with pulse-resonance sounds clearly can lateralize both onset and ongoing envelope ITDs with a sensitivity and a reliance on onsets that are broadly similar to that seen in humans and other mammalian species.

3 Chapter 3 Dependence of Interaural Time Difference Tuning in the Rat Inferior Colliculus on Rate and Envelope of Pulsatile Stimuli

3.1 Introduction

Cochlear implant (CI) users face an enormous challenge when trying to localize sound. The inability of CI users to use interaural time difference (ITD) cues in particular is thought to be due to the lack of normal hearing experience during a critical period in development (Seidl and Grothe, 2005; Hancock et al., 2010; Kan and Litovsky, 2015). However, emerging evidence challenges this theory. Specifically, neonatally deafened rats fitted with CIs that are synchronized between the two ears such that they provide meaningful ITD information could localize sound with ITD thresholds that were indistinguishable from normal hearing animals (Rosskothén-Kuhl et al., 2019), in contrast to prelingually deaf human CI users, who typically show ITD thresholds too large to measure (Litovsky et al., 2010). These findings raise the possibility that maladaptive plasticity, rather than a missed critical period, may render human CI users unable to use ITD cues to localize sound.

If this is the case, the parameters that govern the development of and tuning to the ITDs of pulsatile stimuli in the mammalian brain are worth revisiting, given that all CIs in current clinical use encode sounds as electrical stimulus pulse trains. Two parameters of particular relevance are pulse rate and envelope

shape, both of which influence the detectability of ITDs of individual pulses. CI processors typically deliver pulses at around 900 Hz at each electrode, but the range of technically feasible pulse rates that allow good speech perception appears to be quite wide (Battmer et al., 2010; Shannon et al., 2011).

A recent study (carried out by myself and presented in the previous chapter) demonstrated that normal hearing rats could localize click trains based on envelope ITD, but that performance would decline for high pulse rates (≥ 900 Hz) and for Hanning windowed stimuli (Li et al., 2019). Here, we performed extracellular multi-unit recordings in the central nucleus of the inferior colliculus of normal hearing rats, with the aim of quantifying neural tuning to envelope ITD, and its dependence on pulse rate, envelope shape, and prior training on a sound localization task. A range of pulse rates (50, 300, 900, 1800, 4800 Hz) with Hanning or rectangular envelopes were tested on two cohorts of animals, one that was naive and one that had been trained on a sound localization task using these stimuli. We found that the multi-units' ability to discriminate left from right – based on a neural sensitivity d' metric derived from their ITD tuning curves – declined with increasing pulse rate, was overall lower for Hanning windowed stimuli, and was not affected by training on a sound localization task.

3.2 Materials and methods

3.2.1 Animals

Eleven female Wistar rats were used in this study: Six rats aged 8 weeks without any prior behavioral training formed the “naive” cohort, while five rats aged 76 to 86 weeks which had previously been trained in sound lateralization formed the “trained” cohort. Rats were housed with 2 or 3 animals in one cage and on *ad-lib* feed. All procedures were assessed and approved by the animal care and use committees of City University of Hong Kong, and under license by the Department of Health of Hong Kong (Ref No.: (18-9) in DH/SHS/8/2/5 Pt.3).

3.2.2 Behavioral training (for the trained cohort)

The 5 trained animals had previously been subjects of the Li et al. (2019) study to determine the psychoacoustic ITD sensitivity to click trains in rats, and the methods and results of their behavioral training are described in further detail there. Briefly, rats were trained 5 days per week, using drinking water as positive reinforcer in an instrumental conditioning task. Rats were trained to perform a two-alternative forced choice task to lateralize pulse trains delivered in the near field that had either a left-leading or right-leading ITD. In a custom behavioral cage with three spouts, the animals initiated trials by licking the center spout, and indicated whether they heard click train stimuli as coming from the left or right by licking the corresponding response spouts. Correct responses (on the side of the “leading ear”) resulted in the deliver a few drops of drinking water, incorrect responses triggered a “timeout” period of 15-30 s during which no new trials

could be initiated and a negative feedback sound was played. Rats performed 2 training sessions per day, with each session last about 30 min, resulting in ~200 trials per day. Stimuli were 200 ms broadband click trains enveloped with either a rectangular or Hanning window. Pulse rates were 50, 300, 900, 1800, or 4800 Hz, and sounds were presented at a sample rate of 44,100 Hz and an average binaural acoustic level of approximately 80-85 dB SPL. The ITD values tested spanned the physiological range of the rat, ranging from -175 μ s (negative refers to left ear leading) to +175 μ s (right ear leading) in 22.7 μ s steps. ITDs varied randomly from trial to trial and in each session a subset of the aforementioned click rates and window types were tested.

3.2.3 Extracellular recording

3.2.3.1 Stimuli

In the physiological experiments described here, 100 ms click trains enveloped with a rectangular or Hanning window were delivered to the ear canals of the anesthetized animals as described below. Pulse rates were again 50 Hz, 300 Hz, 900 Hz, 1800 Hz and 4800 Hz, and stimuli were delivered at an average binaural level of 80-85 dB SPL and at a sampling rate of 48828.125 Hz. The stimulus to one ear was offset from that in the other by an integer number of samples, to generate ITDs varying between -164 μ s (left ear leading) and +164 μ s (right ear leading) in 20.5 μ s steps.

3.2.3.2 Surgical Procedure

Rats were anesthetized by intraperitoneal injection of ketamine (80mg/kg, 10%, Alfasan International B.V., Holland) and xylazine (12 mg/kg, 2%, Alfasan International B.V., Holland). The integrity of the rats' tympanic membranes and outer ear canals were checked visually, and acoustic brainstem responses (ABRs) were recorded to confirm that the animals had normal hearing thresholds. Rats' eyes were rinsed with 0.9% Sodium Chloride (Normal Saline, B.Braun Medical Industries Sdn. Bhd, Malaysia) and eye gel was applied (Lubrithal, Dechra Veterinary Products A/S Mekuvej 9 DK-7171 Uldum) to prevent drying.

Following ABR recording, the analgesic Carprofen (5 mg/kg, 50 mg/mL, Norbrook Laboratories Australia Pty Ltd, UK) was subcutaneously injected. A deep cut in the midline of the skull was made to expose the skull. Lignocaine (0.3 mL, 20 mg/mL, Troy Laboratories Pty Ltd, Australia) was applied to the surface of the skull for additional local anesthetics. A craniotomy was made over the right occipito-parietal cortex, along the sagittal suture, extending roughly 3 mm rostral and 1 mm caudal to lambda and 4 mm lateral from midline. The toe pinch reflex was checked periodically to monitor the depth of anesthesia, and a one-third dose of the initial anesthesia induction dose was injected intraperitoneally if needed. Intraperitoneal injections of atropine sulphate (0.13 mg/kg, 0.65 mg/mL, Troy Laboratories Pty Ltd, Australia) were given if the rat's heart rate was noticeably slow. During the experiment, anesthesia was maintained by continuous i.p. infusion of a 0.9% sodium chloride solution of ketamine (17.8 mg/kg/h, 10%, Alfasan International B.V., Holland) and xylazine (2.7 mg/kg/h, 2%, Alfasan International B.V., Holland) through a syringe pump running at a rate of 3.1 ml/h.

3.2.3.3 Electrophysiological Recording

Stimuli were generated by an RZ6 multi-I/O processor (Tucker-Davis Technologies, USA) and delivered over a pair of custom-made speakers (GQ-30783-000, Knowles) connected to the openings of stainless steel hollow ear bars that were placed inside the ear canals of the rat and also served to fix the rat into a stereotaxic frame (RWD Life Sciences, China). These speakers were calibrated using a G.R.A.S 46DP-1 microphone. Neural signals were captured through the PZ5 neurodigitizer (Tucker-Davis Technologies, USA) at a 24414.0625 Hz sample rate and processed via RZ2 bioamp processor (Tucker-Davis Technologies, USA).

Extracellular multi-unit activity was recorded using a 32-channel single shaft electrode (E32-50-S1-L6, ATLAS Neuroengineering, Belgium) inserted vertically into the rats' right inferior colliculus (IC) to a depth of approximately 5.0 mm below the surface of the occipital cortex, using a micromanipulator (RWD Life Sciences, China). A white noise burst search stimulus was presented, and a robust, short latency (3-5 ms) responses to the sounds were taken as an indication that recordings sites were likely inside the central nucleus of the IC. At the beginning of every penetration, single click stimuli at various sound levels were presented to the left (contralateral to the recording side) ear to estimate neural response thresholds, and then the test stimuli were presented. At the end of the experiment, animals were overdosed with pentobarbital sodium (1~2 mL, 20%, Alfasan International B.V., Holland).

3.2.4 Analysis of electrophysiological data

3.2.4.1 Data preprocessing

Voltage traces from each recording site were acquired at a sampling rate (F_s) of 24414.0625 Hz. Analog multi-unit activity (AMUA) was calculated following the procedure used in (Schnupp et al., 2015). First, traces were bandpass filtered between 300 Hz and 6000 Hz using a 3rd order Butterworth filter. The absolute value was then taken, and then a low pass 3rd order Butterworth filter was applied below 6000 Hz. In this study, traces were additionally downsampled by a factor of 20 using the Matlab function ‘decimate.m,’ which filters the data with an 8th order Chebyshev Type I low pass filter with a cutoff frequency of $0.8 * (F_s/2) / R$, where F_s is the original sampling rate (24414.0625 Hz) and R is the resampling factor (20). The resulting AMUA traces used for subsequent analysis were thus at a sampling rate of 1220.7 Hz.

Stimuli were 100 ms in duration and were followed by at least 400 ms of silence before the next stimulus was delivered. Baseline-corrected neural responses to each stimulus were calculated by subtracting baseline activity (average AMUA in a 150 ms window, 155-305 ms post stimulus onset) from the stimulus-driven activity (average AMUA in a 50 ms window, 5-55 ms post stimulus onset) in each trial. Baseline-corrected neural responses were used in all subsequent analyses.

3.2.4.2 Mutual Information calculation

To determine which recorded units were significantly tuned to ITD, and to quantify the strength of tuning, we computed the mutual information (MI) be-

tween the 17 tested ITD values and the neural response. Since we would expect MI values to be lower for the more behaviorally challenging stimulus conditions (Hanning as opposed to rectangular envelopes or higher click rates), a relatively “easy” condition was chosen for the initial MI analysis (rectangular window, 300 Hz click rate). MI values were calculated using the adaptive direct (AD) method described in (Nelken et al., 2005) using 5 initial discretization levels for the neural response values. Raw MI values were bias corrected by subtracting the average MI value obtained after scrambling which ITD condition each trial belonged to 100 times. Units were considered to have significant MI for ITD if they satisfied two conditions: that their raw MI was larger than their bias estimate for 100 of the 100 iterations ($p < 0.01$), and that the raw MI was at least twice as large as the bias MI.

3.2.4.3 Calculation of neural d' based on ROC analysis of ITD tuning curves

The rationale behind the receiver operating curve (ROC) analysis was to estimate each recorded multi-unit’s “ability to discriminate left from right” in the sense of whether the delivered stimuli had a positive (right-leading) or negative (left-leading) ITD. The resulting metric is a d' value that can be compared to d' values obtained behaviorally. The method used here is inspired by the method described in Shackleton et al. (2003) to quantify the neural sensitivity to a stimulus parameter.

First, for a given envelope and click rate, trial-by-trial neural responses for all negative ITD stimulus presentations (8 negative ITD values \times 30 repeats = 240 values) and all positive ITD stimulus presentations (8 positive ITD values \times 30 repeats = 240 values) were assembled (see **Figure 3.3.2 B**). An ROC curve was constructed in the usual manner, considering the full range of possible decision criteria above which the neural response would indicate that the stimulus had a negative (left-ear leading) ITD. (Neurons in the IC of small mammals predominantly show “contralateral” spatial tuning, so that stronger responses are expected for negative ITDs.) The “hit rate” was defined as the proportion of trials with neural responses above the decision criterion that actually came from a negative ITD stimulus, and the “false alarm” rate was the proportion of trials with neural responses above the decision criterion that actually came from a positive ITD stimulus. The ROC curve (**Figure 3.3.2 C**) plots the hit rate as a function of the false alarm rate as the decision criterion is moved across the full range of the combined data from positive and negative ITD trials. The area under the ROC curve (AUC), which would ideally range between 0.5 (chance) and 1 (perfect performance), corresponds to the probability of correct responses in a 2-alternative forced choice task which an optimal observer would be able to achieve. It is also directly related to d' (**Equation 3.2.1**). To compute d' from the AUC, multiplying the square root of 2 by the inverse of the standard normal cumulative distribution function Z (the function ‘norminv.m’ in Matlab) evaluated at the probability value ($Z(p)$, $p \in [0,1]$) specified by the AUC.

$$d' = \sqrt{2} Z(AUC) \quad (3.2.1)$$

The resulting d' values are interpretable as a multi-unit's ability to localize stimuli as coming from the left or right. Negative d' values indicate units that are tuned ipsilaterally. Larger absolute values of d' indicate higher sensitivity.

3.2.5 Statistical analysis

MATLAB (MathWorks, USA) was used to conduct statistical analysis.

3.2.5.1 Mixed effects ANOVA

It is well known that IC neurons located in close anatomical proximity tend to have similar tuning to acoustic stimuli, and consequently multi-unit responses recorded from adjacent recording sites along a single multi-electrode penetration are likely to be correlated, and cannot be treated as statistically independent samples. To determine whether the stimulus conditions tested (click rate, envelope, training) had main effects or interaction effects on d' , a mixed effects analysis of variance analysis (ANOVA) was used, which used penetration number as a random effect to compensate for the lack of statistical independence between channels recorded from the same penetration. The mixed effects ANOVA was run on absolute values of d' which were transformed by taking the cube root in order for the transformed values to be approximately normally distributed, given that ANOVA assumes normally distributed data. The mixed effects ANOVA model comprised the following terms: an intercept (1), all main effects (3, pulse rate, envelope and training), 2-way (3), and 3-way (1) interaction effects for a total of 8 parameters or explanatory variables.

3.3 Results

3.3.1 Approximately half of rat IC multi-units show significant tuning to ITD

Just over half of the recorded multiunits (668 out of 1280, ~52%) were significantly tuned to the tested range of ITDs, as evidenced by bias corrected MI values significantly above zero (**Figure 3.3.1**; $p < 0.01$, permutation test). Some example tuning curves are shown in **Figure 3.3.2 A**. The examples shown in **Figure 3.3.2 A** were selected to illustrate the range of response patterns observed.

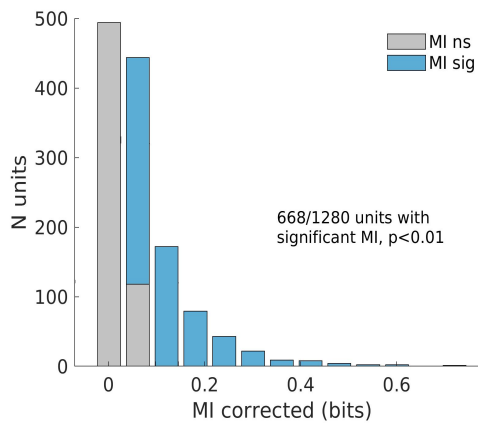


Figure 3.3.1: Distribution of mutual information (MI) values between the 17 ITD values and neural responses across the recorded neural population for the 300 Hz rectangular window stimulus condition.

Approximately 52% of recorded multi-units show significant MI for the range of ITD values tested. MI ns: non significant MI; MI sig: significant MI ($p < 0.01$, permutation test).

To explore the ability of these neurons to distinguish whether a sound comes from the left or the right, a neural d' sensitivity index was computed using a receiver operating characteristic (ROC) analysis (see Methods). Briefly, a multiunit's trial-by-trial responses for all negative ITD trials of a given condition were pooled together, and the same was done for all positive ITD trials. A small over-

lap between -ITD and +ITD response distributions (**Figure 3.3.2 B**) would indicate that a multiunit is highly sensitive to whether sound comes from the left or right. This is captured by the ROC curves shown in **Figure 3.3.2 C**, which plot hit rates against false alarm rates for a decision threshold that is moved across the range of the data in **Figure 3.3.2 B**. A d' value can be calculated from the area under the ROC curve (see methods), and multiunit responses with large MI values often also have large d' values (e.g. top row of **Figure 3.3.2**). However, this need not necessarily be the case, for example if tuning curves were symmetric about 0 ITD, which could result in a large MI but a low d' (**Figure 3.3.2**, second row). This is because the computed neural d' values capture an upper bound on the ability to use the strength of a multiunit's response to distinguish negative from positive ITDs, while the MI quantifies an "entropy reduction" in the uncertainty about which of any of the 17 possible ITD values was presented at a given trial. Note that a d' of 1 indicates that an ideal observer should be able to use the multiunit's responses to lateralize ITDs with ~75% accuracy. (This follows from **Equation 3.2.1**, noting that the cumulative normal distribution value of $1/\sqrt{2}$ equals 0.76). Similarly, a d' of 2.24 (**Figure 3.3.2 C**, top panel) corresponds to nearly 95% accuracy, and a d' of 0.81 (**Figure 3.3.2 C**, third row) corresponds to roughly 71% accuracy.

Only a very small minority of multiunits with significant MI (N=20, ~3% of total) had negative d' values due to ipsilateral tuning. An example is shown in **Figure 3.3.2**, 5th row. In the following analyses absolute values of d' were used, given that a large magnitude of d' indicates good discriminability of left from

right ITDs irrespective of whether tuning happens to be contralateral or ipsilateral.

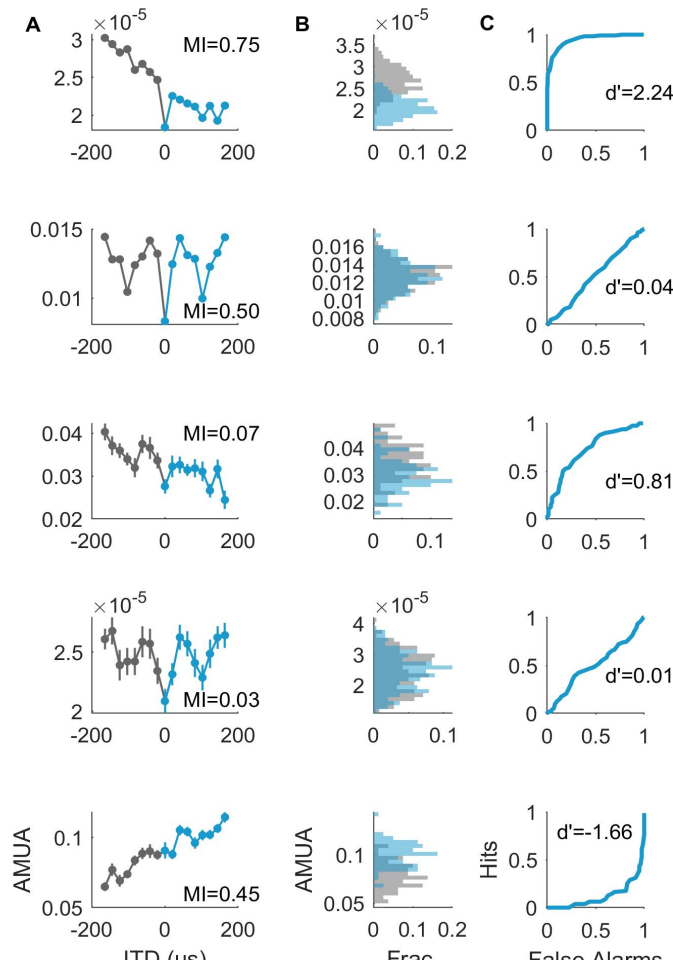


Figure 3.3.2: Calculation of neural d-prime and a comparison with MI for example multiunits.

1st row – high MI, high d’; 2nd row – high MI, low d’; 3rd row – low MI, high d’; 4th row – low MI, low d’; 5th row – negative d’ due to ipsilateral tuning. **A**, Tuning curves showing mean +/- sem of neural responses as a function of stimulus ITD. **B**, Histograms pooling trial-by-trial neural responses for all positive (blue) or negative (gray) ITD conditions. **C**, ROC curve based on splitting the AMUA range in **B** into 50 linearly spaced ‘criterion’ points. Hits were defined as the proportion of negative ITD responses larger than a given criterion value, and false alarms were defined as the proportion of positive ITD responses larger than the given criterion value. Note the correspondence between the degree of overlap in panel **B** and the resulting d’ value.

The relationship between $|d'|$ and MI across pulse rates is explored in **Figure 3.3.3**. At every pulse rate we see multiunits with significant MI (black dots), and the spread of the data along the MI (x-axis) is broadly comparable at different pulse rates. In contrast, the distribution of $|d'|$ values, which captures discriminability of left from right ITDs, has its maximal extent for 300 Hz pulse trains and shows a clear decline with increasing pulse rate. This implies that ITD tuning curves become flatter and/or more symmetric tuning curves for the higher pulse rates (see also **Figure 3.3.4**).

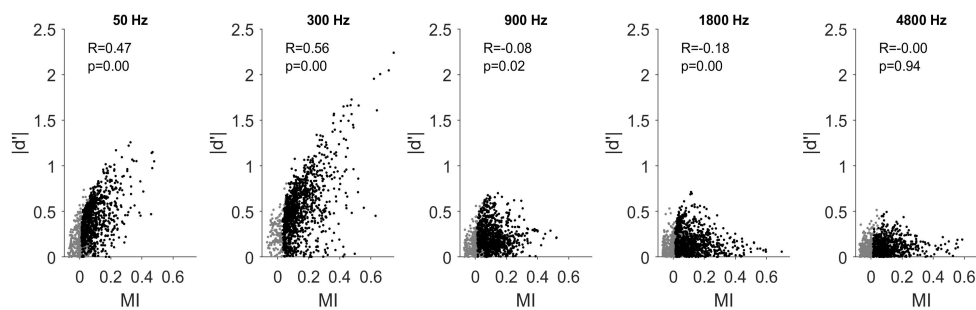


Figure 3.3.3: Comparison of MI and $|d'|$ metrics.

Each panel shows all multiunits with significant MI (based on the 300 Hz rectangular window condition) at a given pulse rate. Gray dots show data from multiunits with MI values that failed to reach statistical significance.

3.3.2 Neural d' depends on pulse rate and envelope, but not on training

We sought to explore the effects of three variables on ITD tuning in the IC: pulse rate, envelope, and training, on neural d' values in order to assess whether the neural d' values exhibited trends that may explain the parameter sensitivity

observed in our previous behavioral study (Li et al., 2019) or whether neural sensitivity in IC improved with training. A mixed effects ANOVA was applied to transformed neural d' values (see *Methods*) to test for main effects, 2-way interactions, and 3-way interactions among these factors. Penetration number was treated as a random effect since multi-units from the same penetration cannot be assumed to be independent samples. **Table 3.3.1** shows the statistical results of the mixed effects ANOVA. Significant main effects were found for pulse rate and envelope, but not for training. No significant interaction effects were found.

Table 3.3.1: The fixed effects coefficients (95% CIs) returned by the mixed effects ANOVA

Name	Estimate	Lower	Upper	p Value
Intercept	1.1771	0.8652	1.4890	1.5448e-13
Pulse Rate	-0.1124	-0.1519	-0.0729	2.553e-08***
Training	-0.1116	-0.2832	0.0599	0.2021
Envelope	-0.1757	-0.2783	-0.0730	0.0008***
Pulse Rate \times Training	0.0146	-0.0078	0.0370	0.2002
Pulse Rate \times Envelope	0.0169	-0.0133	0.0471	0.2720
Training \times Envelope	0.0462	-0.0113	0.1037	0.1150
Pulse Rate \times Training \times Envelope	-0.0023	-0.0190	0.0144	0.7895

Note: ***: $p < 0.001$. DF = 6582.

Figure 3.3.4 shows population neural $|d'|$ values across the different pulse rates and envelope shapes, pooled across training conditions. Population $|d'|$ is highest for 300 Hz and declines to near zero at high click rates. Neural $|d'|$ values are also consistently larger for rectangular window stimuli than for Hanning window stimuli. Notably, at low pulse rates, a number of multiunits show $|d'|$ values well above 1, indicating that these multiunits could theoretically distinguish left

and right ITDs with well over 75% accuracy. At 300 Hz, some multiunits show a $|d'|$ larger than 2, and the median $|d'|$ of the entire neural population is around 0.5, corresponding to a median accuracy in discriminating left and right of ~64% for individual multiunits. At 900 and 1800 Hz, there is a substantial drop in the IC's ability to distinguish left ITDs from right, with a slight advantage for rectangular windowed stimuli. At 4800 Hz, the IC appears equally poor in distinguishing left from right for both Hanning and rectangular windowed stimuli, and even the largest outliers in the population have a $|d'|$ only around 0.5.

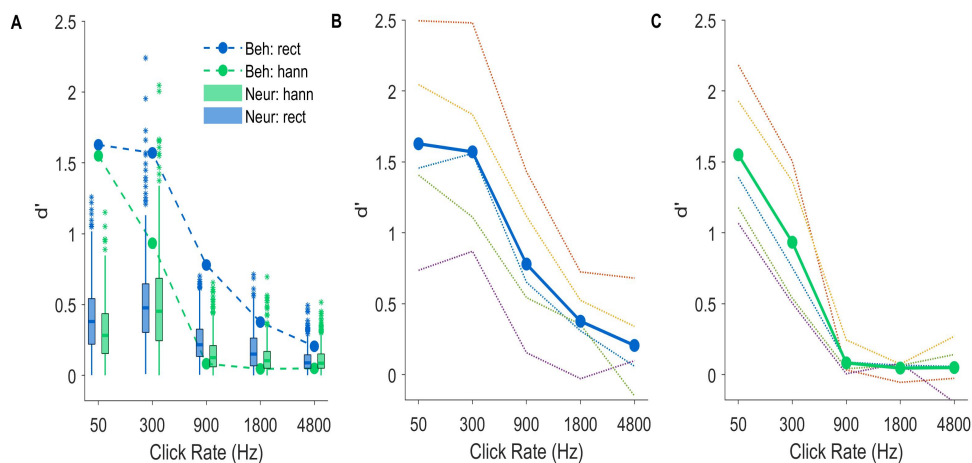


Figure 3.3.4: Comparing neural $|d'|$ and behavioural d' as a function of stimulus pulse rate and envelope type.

A) The boxplots show the distributions of neural $|d'|$ values, pooled across the naive and trained cohorts. There is a decline in $|d'|$ with increasing pulse rate, and $|d'|$ is generally higher for rectangular windowed stimuli. Dotted lines show behavioural d' values computed from data in Li et al. (2019) for comparison. **B)** Behavioural d' for rectangular window stimuli for individual rats (light dotted lines) and the mean across animals (bold blue line). **C)** Same as panel B, but for Hanning window stimuli.

3.4 Discussion

3.4.1 Principal findings

Although a number of researchers placed their interest in testing various properties concerning ITDs in the IC of rats (Flammino and Clopton, 1975b; Møller and Rees, 1986; Irvine et al., 1995), our attempt was the first to investigate the effects of click rates, envelope type of pulsatile stimuli, and prior training on the left/right discrimination acuity of ITD tuning in the rat IC. Our results demonstrated that the left/right discriminability of the neurons in the rat's IC was affected by click rates and window types, but not by training. Higher click rates correspond to lower discriminability, and the discriminability is higher for rectangular windowed stimuli than for Hanning windowed at the same click rate.

3.4.2 Late exposure cannot alter the sensitivity to ITDs in IC

Similar result of no training effect was obtained in a study in the ICc of deafen cats, which revealed that a critical amount of electric stimulation was a dependent factor but the relevant behavioral training was an independent factor in the temporal plasticity (Vollmer et al., 2017). The lack of a training effect may be due to the late exposure to the target stimuli. Rats exposed to a particular pattern of sound in the first 4 months of life evoked more spikes from units in the IC stimulated by that pattern than the other pattern. However, the mother rats showed no similar effects (Clopton and Winfield, 1976). The best frequencies of the single unit responses had strong clustering around the frequency of tone that

the rat had been exposed during postnatal 3 weeks (Poon and Chen, 1992). In human, azimuthal sound localization is relatively mature at the age of five (Litovsky, 1997; Sanes and Woolley, 2011). The critical period of hearing development of rat is from postnatal 9 days to 22 days (Chen and Yuan, 2015). In our investigation, rats in the Trained group started being trained at the age of 2 month, already past the critical period. Rats may be hard to form an experience-dependent effect in the IC in such a late exposure.

3.4.3 The effect of window type and click rates match the behavioral results

We enveloped the click train stimuli with rectangle or Hanning window, to generate a stimulus with sharp onset and another with gentle ramp on and off gating to test the neurons' response to onset and ongoing ITD cues, respectively. The ITD induced neuronal response was more discriminable in rectangle than Hanning window stimuli at the same click rate, and had a reverse relationship with click rates. The results from the electrophysiological experiment here replicated some of the results from the behavioral experiment (Li et al., 2019) (see chapter 2) in which we observed higher sensitivity to ITD for rectangle rather than Hanning window stimuli at any given click rate, and where ITD sensitivity decreased as the click rate increased beyond 300 Hz.

3.4.4 Stimuli envelop plays an important role in neural response to ITD cue

Consistent higher sensitivities to ITDs in rectangular window than in Hanning window at the same click rate indicated that the envelope type of a stimulus could determine the neural spike activity, which was consistent with a previous finding that “the role of neuron-specific excitatory and inhibitory inputs in creating ITD sensitivity (or the lack of it) depending on the specific shape of the stimulus envelope ” (Dietz et al., 2016), and was also in line with the results obtained in a research base on “raised-sine” stimuli that “graded increases in the exponent led to graded decreases in envelope-based threshold ITDs” (Bernstein and Trahiotis, 2009), and again agree with the observation that “increased attack steepness and increased pause duration prior to the attack resulted in the lowest JND” (Klein-Hennig et al., 2011).

3.4.5 What is the best stimulation rate?

The parameters investigated here were chosen for their relevance to binaural hearing in CI users. Two factors likely to limit the ability of human CI users to discriminate ITDs of binaural inputs are the poor synchronization of CI pulses to stimulus fine structure, and the fact that the pulse rate of CI processors are often quite high, at 900 Hz or greater. Despite the poor synchronization between the two ears under everyday listening conditions, some post-lingually deaf bilateral CI users do show good envelope ITD sensitivity ($\sim 100 \mu\text{s}$) at a pulse rates at 100 Hz and sometimes up to 300 Hz (van Hoesel and Tyler, 2003; van Hoesel, 2007; Laback et al., 2007). However, sensitivity to rate discrimination or temporal in-

formation in both bilateral and unilateral CIs generally deteriorates dramatically at pulse repetition rates faster than about 300 pps (Shannon, 1983; Townshend et al., 1987; van Hoesel, 2008; van Hoesel et al., 2009; Venter and Hanekom, 2014). Our finding that neural sensitivity to ITD also declines sharply for acoustic pulse trains as pulse rates are increased beyond 300 Hz is consistent with these observations.

In rectangular and Hanning window stimuli, the highest d' values were found at 300 Hz, not at 50 Hz nor at 900 Hz, suggesting that the rats are mostly sensitive to ITDs at 300 Hz among the tested click rates. Although the steps of the click rates we tested here were too sparse to say which click rate is the best stimulation rate, definitely would not be 900 Hz. Since 900 Hz is one popular stimulus pulse rate in cochlear implant prosthesis for human, researchers should consider to set the stimulus rate lower to gain better ITD sensitivity, e.g. at 300 Hz.

3.5 Conclusion

We have found that the sensitivity of IC neurons to ITDs of pulsatile stimuli is governed by click rates and envelope type. Click rates below 900 Hz are generally better at evoking high ITD sensitivity, as to stimuli with sharp onsets (rectangular window) compared to sounds with gentle onset ramps (Hanning window). Analyzing the neural response data with an ROC approach thus revealed similar dependencies on pulse rate and envelope as we had previously documented in behavioral experiments (Li et al., 2019). Furthermore, behavioral ITD lateralization training did not significantly affect the ITD sensitivity in the IC neurons of rats.

Thus, rat is behaviorally, suggesting that appropriately measured and analyzed-electrophysiological data from naive animals could be useful in determining limits of likely behavioral performance.

4 Chapter 4 Temporal weighting function for interaural time differences in rats

4.1 Introduction

Binaural cues are essential in sound localization in the horizontal plane. The combined detection of the sound arrival time difference (interaural time differences, ITDs) and intensity differences (interaural level differences, ILDs) between two ears helps us spot where the sound comes from (Schnupp et al., 2012). Unfortunately, this is not the case in patients with severe to profound hearing loss, even for those who are fitted with cochlear implants in both ears. The lack of synchronization of electric signal generated by these two prosthesis leads to a fundamental clinical issue that ITD cue is poorly utilized in bilateral cochlear implant users. This creates difficulties in sound localization in complex sound environments for cochlear implant users. To solve this problem, some studies were done in manipulating the stimuli strategy to enhance the ITD sensitivity. There is evidence showing that introducing temporal jitter can enhance the sensitivity to ITDs at high pulse rates in bilateral cochlear implantees (Laback and Majdak, 2008) and normal hearing listeners (Goupell et al., 2009). More technical improvement methods for cochlear implantation are in needed, and animal models would be useful for developing and testing new technology. Are rats suitable for this purpose? Our recent paper (Li et al., 2019) demonstrated that Wistar rats have similar sensitivity to that of humans and other mammalian species in both onset and ongoing envelope ITDs when tested in a sound lateralization task with

pulse-resonance sounds. This suggests that rats may be a fine candidate for pre-clinical studies of binaural hearing, to test various hypotheses before applying them in human, or in invasive studies which are hard to conduct in human. But is merely showing ITD thresholds of a few 10s of microseconds good enough? Ideally a good model for human binaural hearing would perform similarly to the human auditory system in several important aspects, not merely show comparable sensitivity in basic sound lateralization tests. We therefore decided to explore if rats have similar precedence effect in binaural hearing to human. Precedence effect refers to the phenomenon that the auditory system appears to base its perception of sound source direction largely or entirely on the binaural cues experienced during the first few ms of a sound wave, presumably in order to minimize the effects of confounding cue values that occur when reverberant sounds reflected from surfaces in the environment interfere with the direct sound, which would alter the binaural cues. More detailed information about the precedence effect can be found in Litovsky's review (Litovsky et al., 1999).

Although the precedence effect in rats has been studied 40 years ago (Hoeffding and Harrison, 1979), they only used single click pairs delivered in the free-field and presented the results in percentage of correct response as a function to different echo delay times or echo intensity reductions, or to echoes having both a delay and an intensity reduction, but did not quantitatively measure how much did the rats emphasize the leading stimulus. One quite elegant way to study the precedence effect quantitatively was introduced by Stecker and colleagues with the measurement of so-called temporal weighting functions (TWFs), and we decided to study TWF psychoacoustics in rats. Click trains are commonly used

to measure TWF in psychoacoustic research. Each click in the train carries its own target information (leading to left or right), but the clicks in the train are delivered at a rate that is too high for each click to be perceived independently and with its own source location. The subjects are then asked to judge the perceived location of the whole click train. Methods such as multiple regression analysis can then be used to calculate the relative influence of each click in the train on the perceived source direction. The set of regression coefficients that quantifies the “weight” attached to each click in the final perceptual decision is the TWF. Stecker and his colleagues established this approach in a series of studies on TWF for binaural cues in normal hearing human subjects in a variety of conditions (Brown and Stecker, 2010; Brown and Stecker, 2011; Stecker et al., 2013; Stecker, 2014). The aim of my project was, in a first instance, to take inspiration from Stecker’s work, and, firstly, to measure ITD TWFs in the rat behaviorally and evaluate whether they show similar strong onset dominance as has been reported for humans. The work described here is the first attempt to measure TWFs in a non-human species. If that first part was successful, I set myself the further goal to start the search for neural correlates of ITD TWFs in neural responses recorded from the auditory system.

4.2 Materials and Methods

4.2.1 Animals

Four 8-week-old female Wistar rats weighted from 216 g to 242 g were used. Rats were housed in 2 cages with 2 rats in each. They had water restrain on the day before and during the days of behavioral task performance, otherwise had free access to water. Food was provided *ad lib* at anytime.

All experimental protocols were assessed and approved by the Experimental Animals Research Ethics Subcommittee at the City University of Hong Kong, and performed under license by the Department of Health of Hong Kong [Ref. No.: (18-9) in DH/SHS/8/2/5 Pt.3].

All animals were used in two separate phases of the current study: a behavioural phase (see 4.2.2) and a subsequent electrophysiological experiment (see 4.2.3).

Prior to each of the behavioral and electrophysiological experiments, acoustic brainstem responses (ABRs) recordings, Preyer's reflex and other physical examination were performed to ensure the ears, especially the tympanic membrane, and hearing of the rats had no abnormalities. For this, rats were anesthetized by intraperitoneal injection of ketamine (80mg/kg, 10%, Alfasan International B.V., Holland) and xylazine (12 mg/kg, 2%, Alfasan International B.V., Holland). Eye gel (Lubrithal, Dechra Veterinary Product A/S Mekuvej 9 DK-7171 Uldum) was applied to prevent the eyes from drying. The outer ear canals and tympanic membranes were inspected under microscope (RWD Life Sciences, China). The rats were then fit to a stereotactic instrument with a pair of hollow ear bars in a sound attenuating chamber to record ABRs (auditory brainstem responses) in order to

verify their hearing threshold. In the case of an ECoG recording, the surgical area was shaved before fitting to the stereotactic instrument.

4.2.2 Behavioral study

4.2.2.1 Behavioral training setup

The behavioral setup was identical to that described previously in sections 2.2.2 and the training method was the same as in 2.2.3. In brief, the behavioral training box was situated in a sound attenuating box and the front wall of the training box was mounted with three brass water spouts. Two hollow tubes were connected to a pair of mini headphone drivers (GQ-30783-000, Knowles, Itasca, Illinois, US) to deliver sound that played via a USB sound card (StarTech.com, Ontario Canada, part No. ICUSBAUDIOMH) and amplified by an audio amplifier (Adafruit stereo 3.7W class D audio amplifier, part No. 987) into the behavioral training box as close to the rats' ears as possible.

4.2.2.2 Behavioral training task

In the behavioral experiment, rats performed a two-alternative forced-choice (2-AFC) near-field lateralization task. Rats initialized each trial by licking on the middle water spout and receiving one drop of water in a random subset of 1/7 trials. This was followed by a delivery of the binaural stimulus. Behavioral training and testing were thus essentially identical to Li et al. (2019), except that a different set of stimuli was designed and used to enable the quantification of TWFs.

The rats first received binaural stimuli with both ILD and ITD cues at 300 Hz (left-ear leading: -6 dB, -0.136 ms, 300 Hz; right-ear leading: +6 dB, +0.136 ms, 300 Hz]. We required that the rats lateralized at least 80% correct in at least 2 sessions to enter the next ITD-only training stage (left-ear leading: 0 dB, -0.135 ms, 300 Hz; right-ear leading: 0 dB, +0.136 ms, 300 Hz). After the rats finished the task correctly over 80% twice, they were presented with a series of ITD stimuli (± 0.1587 ms, ± 0.136 ms, ± 0.0907 ms, ± 0.068 ms, ± 0.0454 ms, ± 0.0227 ms) at 300 Hz randomly within one session. At this stage, since some ITD values were close to or lower than their ITD threshold, we set the criterion that the rats had to reach 75% correct rate at least twice to enter the following TWF training stage. If that criterion was not met, the animal would receive further training sessions which included both ILD and ITD cues, and during which timeouts and reward quantities were adjusted as necessary to achieve reliably high performance.

4.2.2.3 Acoustic stimuli

The stimuli in the TWF stage contained 8 click pairs in a train (**Figure 4.2.1**). Click pairs were presented at four separate rates of 20, 50, 300 and 900 Hz. The experiments included randomly interleaved “honesty trials” and “probe trials”. In honesty trials, click trains had a fixed ITD offset of ± 0.083 ms, plus an additional jitter drawn at random from a range of ± 0.042 ms, in steps of $10.4 \mu\text{s}$ afforded by the 96 kHz Hi-Fi USB Audio sound card. Therefore, in honesty trials all ITDs pointed in the same direction (indicated by the fixed offset), and most ITD values should be reasonably large compared to the ITD thresholds reported in Li et al. (2019). Since honesty trials were unambiguous, we expected them to be relatively

easy to lateralize. Responses to honesty trials were only rewarded if the animal responded on the appropriate side. We required that the rats lateralized at least 80% of honesty trials correctly in at least two sessions before they could receive probe trials. All four of the rats that reached the “ITD only” lateralization training criteria described above were also able to meet the 80% correct TWF honesty trial criterion after minimal training, as might be expected given that to casual human observers, TWF stimuli with jittered ITDs and stimuli with fixed ITD sound indistinguishable.

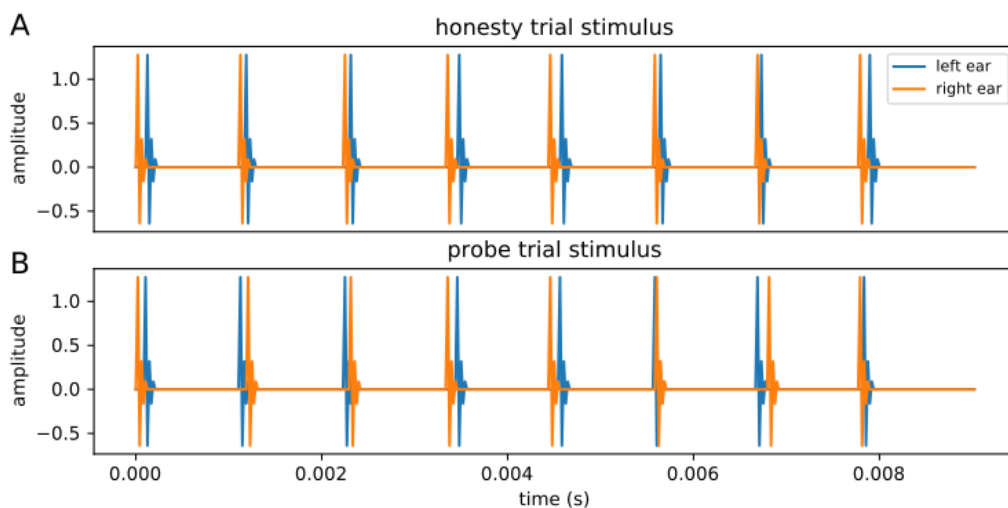


Figure 4.2.1: Acoustic stimuli examples for honesty trial and probe trial

A: honesty trial stimulus at 900 Hz with 0.042 ms jitter and +0.083 ms offset (+: right ear leading, -: left ear leading). The time differences between the two clicks in each click pair were in the range of +0.042 ms to +0.125 ms, which means every click pair leading to the right ear. There is no ambiguity and the rat will only be rewarded for responding “right”. **B:** probe trial stimulus at 900 Hz with 0.125 ms jitter and 0 ms offset. The time differences between the two clicks in each click pair were randomly assigned in the range of -0.125 ms to $+0.125$ ms. Since there was no objective “correct” response to a probe trial, rats could get rewards by licking either water spout. In the experiments, “honesty trials”, and “probe trials” were randomly interleaved in the ratio of 2:1.

In the final training sessions used for TWF calculation, honesty and probe trials were randomly interleaved in the ratio of 2:1. In probe trials, the ITD offset was fixed at zero and the jitter was in the range of ± 0.125 ms. Probe trials would therefore in most cases contain clicks with both left-leading and right-leading ITDs, and consequently there was no *a priori* correct answer to how probe trials should be lateralized. Therefore, the rats' responses could depend on how each of the clicks was weighted. The rats' responses to probe trials were always treated as "correct" and rewarded irrespective of which side they responded. Probe trials were randomly interspersed among honesty trials to keep the animals "honest" in reporting the perceived stimulus lateralization side, rather than choosing response spouts randomly without attending to the sounds.

A correct response would lead to the release of 3 small drops of water as a reward, and a wrong response would trigger a "timeout sound" at 90 dB for 15 s. A new trial could only be initiated after the timeout. If the rat made a wrong response, the following trial would be a "correction trial", in which the last stimulus was repeated. "Correction trials" were used to reduce the tendency of animals to develop responses biases towards one side, but they were excluded from the calculation of the correct response score for the honesty trials.

4.2.2.4 Behavioral data analysis

TWFs were computed from the responses to the probe trials only (separately for each of the four click rates: 20, 50, 300 and 900 Hz), by performing a Probit regression of the ITD values for each of the 8 click pairs in the train against the animals' "left" or "right" responses. A Python library [statsmodels.discrete.discrete_model.Probit] provided by  statsmodels was imported to fit the discrete binary data using maximum likelihood. A constant was added to the exog (independent variable) to include the intercept in the regression results. In Probit regression, the dependent variable can only take two values (in our case here, the response is Left or Right, denoted as 0 or 1 respectively), and the purpose of the model is to estimate the probability of a given observation being assigned into one of the dependent values. The Probit regression model is in the form of

$$Y = \Phi(X^T \beta) \quad (4.2.1)$$

where X^T is the vector of regressors (here: ITD values of each click and the added constant), parameters β are the coefficients (estimated by maximum likelihood), Φ is the cumulative Gaussian normal distribution, and Y is the predicted probability that the animal will respond on the right.

For each rat, we fitted a Probit regression separately for each condition (click rate). The returned coefficients are the weights of the corresponding clicks in a click train, and thus represent the animal's TWF.

4.2.3 Electrophysiological experiment

4.2.3.1 ECoG recording apparatus

In the electrophysiological experiment, the same four rats which performed the psychoacoustic testing were used. Acoustic stimuli were generated by RZ6 multi-I/O processor (Tucker-Davis Technologies, USA) and presented via a pair of custom-made speakers (AS02204MR-N50-R, PUI Audio, Inc.) fitted to the openings of the hollow stainless steel ear bars, which fixed the rat into a stereo-tactic instrument (RWD Life Sciences, China). The speakers were calibrated with a GRAS 46DP-1 microphone (GRAS Sound & Vibration A/S), and their transfer functions were compensated with an inverse filter to be flat over the range of 600 Hz to 20 kHz to $\sim \pm 3$ dB.

Neural activity was recorded using a 61-channel electrocorticographic (ECoG) array (Woods et al., 2015). The flexible (~ 30 μm thin) ECoG array consisted of contacted (can be placed on the surface of cortex) electrodes (203 μm diameter) arranged on an 8×8 square grid with 406 μm spacing between neighboring electrodes, covering an area of 10.6 mm^2 . Three additional electrodes in array corners served as reference electrodes (**Figure 4.2.2**).

The neural signal was captured through PZ5 neurodigitizer (Tucker-Davis Technologies, USA), and processed with RZ2 bioamp processor (Tucker-Davis Technologies, USA). Customized Python routine were used to generate stimuli and save the recorded signals.

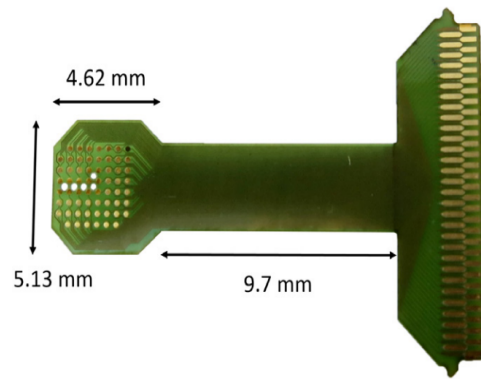


Figure 4.2.2: High-resolution, flexible electrode array of 61 electrodes.

The diameter of electrode contacts are $203\ \mu\text{m}$, and the distance between contacts is $406\ \mu\text{m}$. The upper right intentionally unexposed dark electrode of the array was to test the encapsulation material. Five holes in the diameter of $305\ \mu\text{m}$ cut by laser are to fit with penetrating electrodes. A high density ($200\ \mu\text{m}$ pitch) zero-insertion force (ZIF) connector with 61-pin is used to connect the array to external recording systems. © [2015] IEEE (Woods et al., 2015).

4.2.3.2 ECoG recording procedure

ECoG was recorded from the auditory cortex (AC). At first, rats were anesthetized as described in the ABR recording procedure in 2.1. The sedation state of the rats was continuously monitored by checking the toe pinch reaction. One third of the initial anesthesia dose was injected intraperitoneally if reaction was noticed before craniotomy. Prior to ECoG recording, ABRs were tested again to make sure the ear bars were still in good position, followed by intraperitoneal injection of urethane (20%, 1mL). If a toe pinch reaction was observed during the ECoG recording, an additional 1 mL of urethane was injected. The total amount of injected urethane was less than 7.5 mL/kg.

After ABR recording, butorphanol (10 mg/mL, 0.2mL/kg every 1-2 h, Richter Pharma AG, 4600 Wels, Austria) was subcutaneously injected as a

painkiller during the surgery. A deep cut in the midline of the skull was made and the surgical field was exposed. Local anesthetic Lignocaine (0.3 mL, 20 mg/mL, Troy Laboratories Pty Ltd, Australia) was applied on top of the surgical area. Craniotomy was performed over the right, left, or both temporal cortices. From a point 2.5 mm posterior to Bregma, a line was drawn perpendicular to the sagittal suture to the temporal ridge, and the cross point of this line and the ridge was marked. The craniotomy area was extended 5.0 mm posterior and 4.0 mm ventral to this cross point, to allow the placement of an ECoG electrode array on the auditory cortex. A hole was drawn on the opposite side anterior to Bregma to fix a screw which was connected to the grounding of the recording array.

After placing the ECoG electrode array on the AC, acoustic stimuli were presented to the rat. ECoG neural signals were recorded at 6 kHz sample rate. At the end of the recording experiments, the rats were killed with an overdose of Pentobarbital (1~2 mL, 20%, Alfasan International B.V., Holland).

4.2.3.3 Acoustic stimuli

In ECoG experiments, acoustic stimuli were optimized for estimating TWFs based on neural activity. Looking for neurophysiological correlates of TWFs is altogether more difficult than measuring TWFs behaviorally, because neurons in the auditory pathway do not give binary “left” or “right” responses, but instead have ITD tuning curves which can differ greatly from one neuron to the next, and which link ITD values to neural firing rates in a manner that can be non-monotonic and that is not known a priori. Measuring neural TWFs can therefore easily de-

generate into an underconstrained problem, where one seeks to understand the mapping of a relatively large number of continuous valued stimulus parameters (the ITDs of each click in the train) onto a very noisy continuous valued output variable (the neural firing rate) through an unknown set of tuning curves. In an attempt to make the problem more tractable, we reduced the complexity of the stimuli used here compared to the ones in the behavioral experiment, reducing the number of clicks in the train from 8 to 4, and constraining each click so that it could take only one of two possible ITD values, either -0.16384 ms or $+0.16384$ ms. These ITD values are close to the reported limits of the normal ecological ITD range for rats (Koka et al., 2008). By constraining each stimulus click train to have only four clicks and each click constrained to take one of only two possible ITDs (“far left” or “far right”), we reduced the set of all possible stimulus click trains to only 16, and we presented each of these 16 possible stimuli 40 times, in pseudorandom order, recording 640 responses at each recording site. The tested click rates were 300 Hz (with duration of 13.496 ms) and 900 Hz (with duration of 4.608 ms).

4.2.3.4 ECoG data analysis

4.2.3.4.1 Univariate analysis: channel-wise regression

Our analysis of the responses recorded with these stimuli was further based on the assumption that most ITD sensitive neurons in the central auditory pathway would be tuned so as to have a “preference” for ITDs pointing to the contralateral side, a minority might have an ipsilateral preference, but very few

should have tuning curves that are symmetric at either end of the ecological range of ITDs (Benson and Teas, 1976; Woldorff et al., 1999; Yao et al., 2013). Under these assumptions neural response amplitudes of contralaterally tuned units should consistently increase when contralateral leading ITDs are presented, irrespective of whether these contralateral ITDs occur at the first, second or n-th click, and for ipsilaterally tuned units, response amplitudes should consistently decrease when contralateral ITDs are presented. Under these simplifying assumptions we can attempt to fit TWFs to the neural data using a simple multiple linear regression which regresses response amplitude against the signs of the four ITDs in each stimulus.

The analysis of ECoG voltage data was further based on standard methods for quantifying evoked response amplitudes from LFPs as follows. First, per channel, the signal was bandpassed using a 4th order band-pass filter from 30 Hz to 300 Hz (`scipy.signal.butter`, `scipy.signal.filtfilt`). The bandpassed signal was downsampled by a factor of 4 to a sample rate of 1500 Hz (`scipy.signal.decimate`). The decimated multichannel data were then denoised using the “denoising by spatial filtering” methods developed by de Cheveigné and Simon (2008). The cleaned data were “re-referenced” by subtracting the median across all channels (Liu et al., 2015). Neural responses were then quantified by epoching the cleaned, re-referenced signals into data segments ranging from 1 ms to 30 ms post stimulus onset (Rutkowski et al., 2003), baseline correcting each epoch by subtracting its mean, and computing the RMS amplitude for each response epoch. Outlier epochs with RMS amplitudes greater than three standard deviations above the median RMS amplitude were excluded from further analysis.

The distribution of RMS response amplitudes obtained in this manner was highly positively skewed. To make it more suitable for linear regression analysis to obtain TWF values, we therefore log-transformed the RMS values. Furthermore, we wanted to compute temporal weighting coefficients which were insensitive to site-to-site or animal-to animal variability in the range of observed voltage values, which may result from variable electrode impedances or electrode placements but which do not reflect differences in the stimulus-driven differences in responses. We therefore z-scored the log(RMS) values prior to regression analysis.

The transformed data were then subjected to an ordinary least squares (OLS) regression (`statsmodels.api.OLS`, (Seabold and Perktold, 2010)) with constant added (**Equation 4.2.2**). The form of the regression model is

$$y = X\beta + \epsilon \quad (4.2.2)$$

where y is the z-scored, log transformed LFP amplitude observed in each trial, X is a vector of the regressors (the ITDs of the 4 clicks in ms and the added constant to provide the intercept), β is the vector of regression coefficients (the TWF weights in units of standard deviations of log RMS LFP amplitudes per ms of ITD), and ϵ is an error term which, as usual for normal linear regression, is assumed to follow a Gaussian distribution. In addition to computing the regression weights β , the software returned p values indicating how likely it is that the corresponding β is significantly different from zero.

4.2.3.4.2 **Multivariate analysis: population-based decoding**

In addition to the mass-univariate (i.e., channel-by-channel) analyses described above, data were also subject to a multivariate analysis based on the response of the entire population of recorded neurons (i.e., pooling information from multiple channels). The main aim of this analysis was to decode the ITD of each click pair on a trial-by-trial basis from the pattern of neural activity measured by multiple ECoG channels.

To this end, we first selected channels that showed a robust evoked response to the click train. The criterion that we used for channel selection was based on the signal-to-noise (SNR) ratio, defined for each channel as the ratio between the RMS of the signal in the first 30 ms after click train onset and the RMS of the signal in the last 30 ms prior to click train onset. Only channels with $\text{SNR} > 3$ dB were taken into the analysis.

Following channel selection, per placement, ECoG data from multiple channels were used to decode click pair ITDs in a multivariate trial-by-trial decoding approach (Wolff et al., 2017; Aukstulewicz et al., 2019). First, we focused on decoding click pair ITDs based on the RMS in the 0-30 ms time window following click train onset. Specifically, per trial, we split the data into three sets: (1) the test trial itself, (2) the remaining trials with the same click pair ITD as the test trial, and (3) the remaining trials with a different click pair ITD than the test trial. Based on these three sets, we obtained three vectors with average RMS values concatenated across channels. We then calculated the multivariate Mahalanobis distance values between (1) the test trial vector and the average vector of trials with the same ITD, as well as (2) the test trial vector and the

average vector of trials with a different ITD. The Mahalanobis distance values were scaled by the noise covariance matrix of all channels, i.e., the covariance based on single-trial residual RMS after removing the mean RMS from each trial (Muhle-Karbe et al., 2020), separately for each ITD. The resulting Mahalanobis distance values, obtained for a given trial k relative to other “same” or “different” trials, were used to calculate the overall decoding distance metric according to the following equation:

$$decoding(k) = \frac{distance(k, different) - distance(k, same)}{distance(k, different) + distance(k, same)} \quad (4.2.3)$$

This procedure was repeated four times (corresponding to four click pairs) for each trial in a leave-one-out cross-validation approach, and the resulting decoding values were averaged across trials to obtain ITD decoding estimates for each of the four click pairs. Decoding estimates were tested for statistical significance for each click pair using a signed rank test, correcting for multiple comparisons across click pairs using Bonferroni correction.

In a further exploratory analysis, we aimed at testing whether neural activity later than the first 30 ms following click train onset can be used to decode click pair ITD. To this end, we repeated the decoding analysis in a sliding time-window approach, using a window length of 30 ms (with a time step of 5 ms). Specifically, for each time window, we extracted the RMS envelope (downsampled to 200 Hz and resulting in 7 RMS values per time window), de-measured it by removing the average across the time window (separately for each channel), and concatenated the de-measured values across channels (Wolff et al., 2020). The resulting vectors of RMS fluctuations in multiple channels were used to calculate the

Mahalanobis distance metrics, and the corresponding decoding estimates, as described above. Decoding estimate time series were tested for statistical significance for each click pair and time point using a signed rank test, correcting for multiple comparisons using a false discovery rate of 0.05 (Benjamini and Hochberg, 1995).

4.3 Results

4.3.1 Behavioral task showed profound onset dominance

Using the protocols described above, the rats were trained 5 days a week, with two sessions daily. One training session lasted 20 minutes. Usually, the rats would perform ~160 trials in one training session, but the number would vary depend on the how difficult the task was, how thirsty and how active the rats were. Thus, the number of trials in a session could vary from just below 100, to as many as over 200. The rats were initially trained with combined ITD and ILD cues for 13 to 17 training sessions to reach 80% correct responses in at least two sessions. Then, they were trained with only one ITD value. The removal of ILD cue did not affect the performance much, therefore, they were only trained 2 to 3 sessions to reach up to 80% correct rate at least twice. However, for the multiple ITD values training stage, they had to take 18 to 21 training sessions before obtaining a correct rate over 75% at least twice. We initially trained 5 rats with this protocol, four of which reached the required high performance with ITD-only stimuli after about two weeks of training. The one rat which failed to achieve the required criterion after 2 weeks of training was excluded from the cohort used for

TWF testing. For most sessions, the rats could perform ~160 trials per session (20 minutes), although the number would vary depending on how difficult the task was, as well as on how thirsty and active the rats were. The lowest number of trials per session was approximately 100, and the highest exceeded 200 trials.

Following multiple ITD values training stage, the rats were trained with “honesty” TWF stimuli. Once their performance was over 80% correct in two or more sessions, they were presented with “honesty + probe” stimuli. For the 50 Hz and 300 Hz click rates, only 2 sessions were needed for all the rats to reach the final “honesty + probe” testing stage. For the 20 Hz and 900 Hz click rates, 4 and 6 sessions respectively were required to reach the final behavioral stage.

After completing the “honesty” training, psychoacoustic testing began, and the rats were tested with “honesty + probe” stimuli. In total (combined across all 4 rats), 42 sessions, 32 sessions, 33 sessions, and 28 sessions were collected for stimulus pulse rates of 20 Hz, 50 Hz, 300 Hz, and 900 Hz, respectively. The numbers of probe trials and honesty trials, and the correct rate in honesty trials in each condition for each rat is summarized in **Table 4.3.1**. Rat # 1802 was the best performer in honesty trials for all click rates. The correct rate in honesty trials and the number of training sessions needed in the “honesty” training stage suggest that the task difficulty was similar across the four tested click rates. Note that even at the most difficult 900 Hz click rate, all rats had more than 80% correct responses in honesty trials.

Table 4.3.1: A summary of the data collected in the final “honesty + probe” testing stage

Condition	Animal	Probe trials	Honesty trials	Correct trials in honesty trials	Correct rate in honesty trials
20 Hz	1801	558	1095	879	80.27%
	1802	517	1077	984	91.36%
	1803	564	1152	983	85.33%
	1805	626	1163	946	81.34%
50 Hz	1801	458	888	759	85.47%
	1802	495	923	844	91.44%
	1803	469	898	763	84.97%
	1805	457	943	765	81.12%
300 Hz	1801	449	928	784	84.48%
	1802	525	986	881	89.35%
	1803	423	816	675	82.72%
	1805	422	814	652	80.10%
900 Hz	1801	399	796	643	80.78%
	1802	413	868	800	92.17%
	1803	388	798	657	82.33%
	1805	410	882	707	80.16%
Total		7573	15027	12722	84.66%

An analysis of the probe trials obtained during these testing sessions revealed a profound and consistent onset dominance (precedence effect) across all animals and all click rates. As shown in **Figure 4.3.1**, the weights of the first click pair were modulated by the click rate. Specifically, the weights for the first click pair were higher for higher click rates. The weights dropped dramatically for the second click pair, and the weights of third click pair were in inverse order with the click rates. Finally, for the fourth click pair, the weights reached a similar value (~ 1) for all click rates. The weightings on the last clicks increased slightly comparing to the second last clicks. As shown in **Figure 4.3.2**, based on the p values obtained in the Probit regression, the first-click weights were significantly different from zero ($p < 0.01$) for all click rates. For later clicks, the results were

more heterogeneous across click rates and rats. For the second click pair, all rats had significant weighting for 20 Hz and 50 Hz stimuli (Rat # 1803 at 50 Hz and Rat # 1805 at 20 Hz with $p < 0.05$, others with $p < 0.01$); two rats had significant weighting for 300 Hz stimuli; and no significant weighting was seen for 900 Hz stimuli. For the third click, three rats out of four had significant weights for 20 Hz stimuli ($p < 0.01$). For the sixth click, three rats showed significant weights for 50 Hz stimuli ($p < 0.05$). For the last click, one rat (#1805) showed significant weighting on for 20 Hz ($p < 0.05$) and 300 Hz ($p < 0.01$) stimuli.

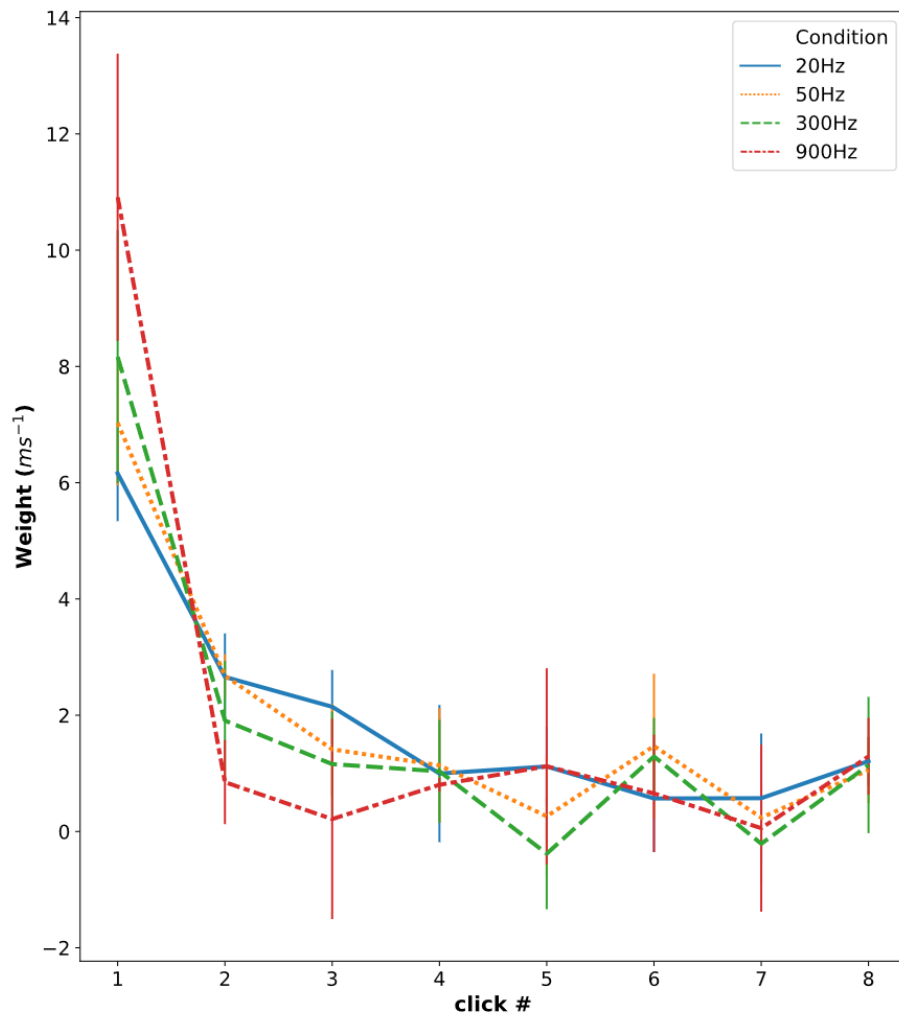


Figure 4.3.1: Temporal weighting functions for interaural time differences at different click rates in rats.

The x-axis shows the individual clicks in the 8-click train, and the y-axis shows the coefficient (“temporal weight”) based on the Probit regression. The unit of the coefficients is expressed as standard deviations of the standard normal Gaussian per ms of ITD. The best-fit regression model would predict that an increase in ITD by 1 ms of the corresponding click should result in the increment of the z-score (how many standard deviations below or above the mean) by the corresponding coefficient value. Error bars represent standard deviation across four rats at the same click rates. The weight of the first click was predominantly higher than that of the rest of the clicks. The onset weighting was highest at 900 Hz and decreased according to the decreasing click rates. The weight of the 8th (last) click was greater comparing to the 7th click.

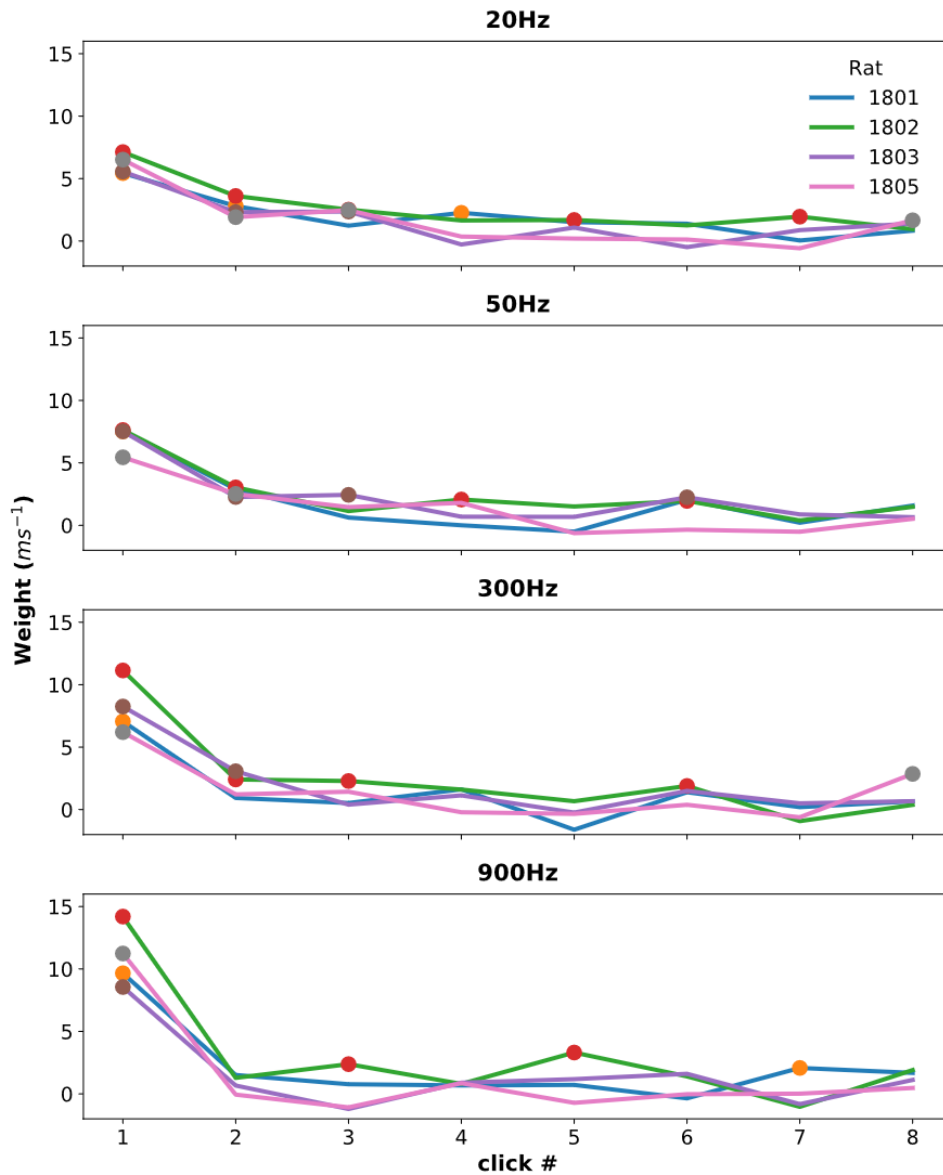


Figure 4.3.2: Temporal weighting functions for ITDs at different click rates for each individual rat.

The x-axis shows the individual click in the 8-click train, and the y-axis shows the coefficient (“temporal weight”) based on the Probit regression. Strong onset dominance was seen across all click rates of all rats. The weights of the clicks following the first click increased as click rate decreased. Rat # 1805 showed significant weight on the last click at 20 Hz and 300 Hz. Colored solid circle markers: $p < 0.05$. Noted that the p values here only indicate the significance level of the coefficient (weighting) of the corresponding click pair compared to zero for a specific rat at a specific click rate.

In summary, the behavioral results shown in **Figures 4.3.1** and **4.3.2** demonstrate that rats temporally weight ITD cues in ways that are very similar to the temporal weightings described by Stecker and colleagues for human listeners (Stecker and Hafter, 2002; Stecker et al., 2013; Stecker, 2018), as all four rats in our cohort showed a very strong and consistent onset weighting at all tested click rates.

4.3.2 Channel-wise regression shows weak precedence effect in ECoG signals from the auditory cortex

In total, I recorded 7 ECoG electrode placements from 4 trained rats, in which 4 placements were recorded from the right AC, and 3 from the left AC. At each electrode placement we recorded responses to our “sparse” TWF stimuli at two click rates: 300 Hz and 900 Hz, yielding a total of 14 electrophysiology data sets.

Although the behavioral experiments showed the expected, consistent and strong weighting of the first pulse, the ECoG results were a great deal less consistent, with highly variable responses from animal to animal and from recording site to recording site, and overall only a weak trend towards larger onset weightings for influence of click ITDs on the RMS of the neural response to each click train. While at some ECoG electrode placements we observed a strong and statistically significant weighting of the first pulse (e.g. **Figure 4.3.3 A**) in a large majority of channels, at many other electrode placements we saw a much more mixed picture without any convincing trends toward increased onset weights (e.g. **Figure 4.3.3 B**).

To provide an overview of our complete dataset of 14 electrode placements across our 4 animals, we show boxplots in **Figure 4.3.4** which give the distributions of absolute regression weights (beta values), for all those regression weights which were significantly different from zero at $p < 0.05$. There were in total 3416 beta values, 1708 each for 300 Hz and 900 Hz. Out of 3416 beta values, 419 (213 for 300 Hz, and 206 for 900 Hz) beta values (12.3%) had p value less than 0.05.

In this figure we chose to plot absolute beta values because the sign of the beta depends on whether the recorded neural population happens to have a preference for ipsilateral or contralateral leading ITDs, and the sign is therefore not relevant to the question of whether the first or second click in the stimulus has a stronger influence on the amplitude of the response. Data for stimuli with 300 or 900 Hz click rates are shown separately.

The median absolute beta values for the first, second, third, and fourth clicks for 300 Hz stimuli were 0.6162, 0.5412, 0.5093, and 0.5994, and for 900 Hz stimuli they were 0.7668, 0.5239, 0.5693, and 0.5181 at 900 Hz, respectively. There is thus a very weak trend for median absolute betas at onset and offset to be larger than those for middle part at 300 Hz, and at onset to be greater than those for the rest parts at 900 Hz, but the trend is surprisingly weak considering the robust behavioral onset weighting (compare earlier behavior figures **Figure 4.3.1** and **Figure 4.3.2**).

Note in **Figure 4.3.3** that neighboring recording sites are highly correlated. Therefore, betas from neighboring sites are not statistically independent observations, which makes judging the statistical significance of any trend in the ECoG

data very difficult. Given the small size of the trend and the high variability seen in the distributions shown in **Figure 4.3.3**, it is doubtful that it would reach statistical significance and in any event, “the effect size” is certainly so small as to be unlikely to form an adequate basis to explain the behavioral result.

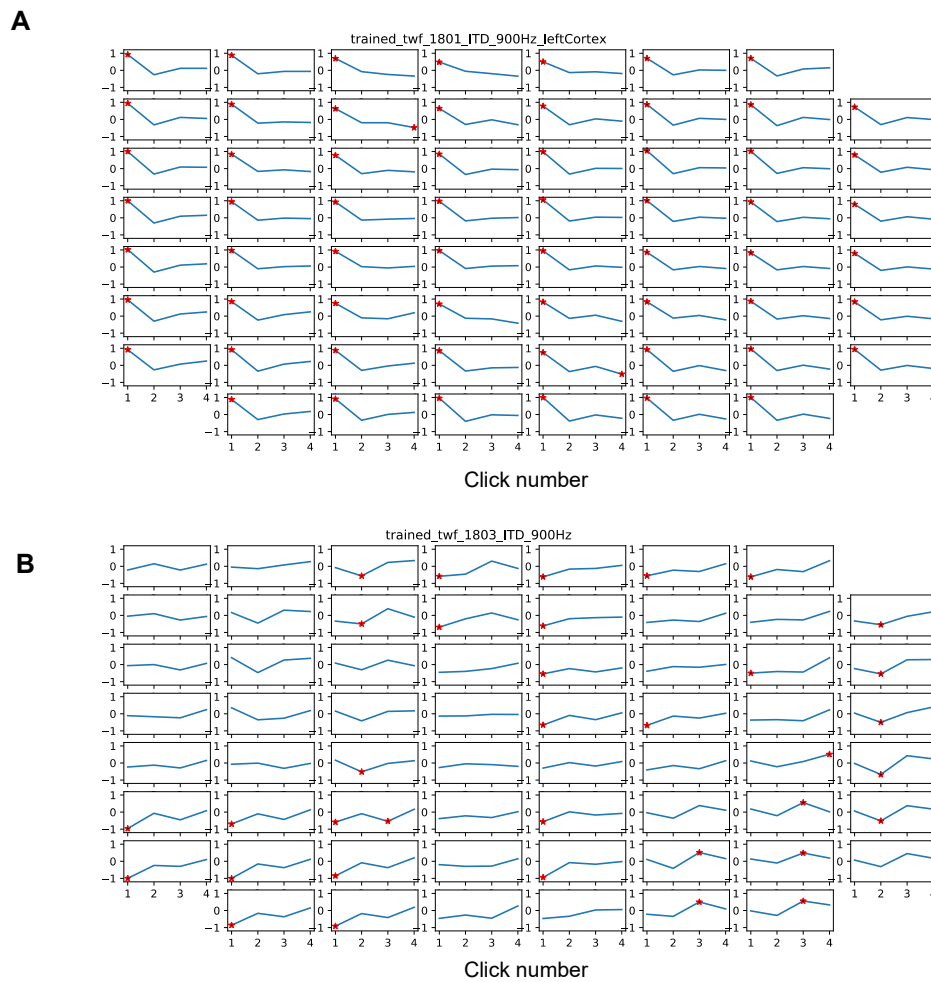


Figure 4.3.3: Examples of the weightings on each click at 61 recorded sites.

In each subplot, the x-axis shows the individual click in the 4-click train and the y-axis shows the beta value (“temporal weight” in the unit of ms^{-1}) returned from the Ordinary Least Squares regression. Each subplot represents the weightings on the channel that is in the same position of the electrode (an 8×8 array, no channels on the top right, bottom left and bottom right, see **Figure 4.2.2**). (A) Strong onset weighting shown at all recorded sites in rat # 1801 at 900 Hz. (B) Mixed weighting patterns were seen at the same click rate as in (A) but of different rat (rat # 1803). A red asterisk (*) is used to mark regression weights that are significant at $p < 0.05$.

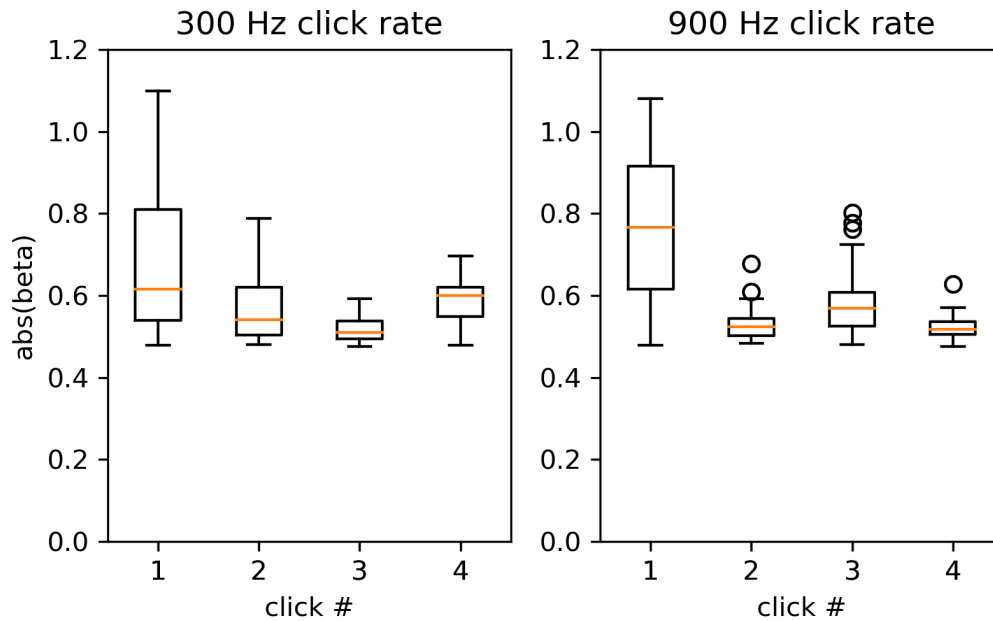


Figure 4.3.4: Boxplots for the absolute weight with p value < 0.05 of four ECoG recorded rats at 300 Hz and 900 Hz click rates.

The x-axis shows the individual click in the 4-click train and the y-axis shows the absolute beta value (“temporal weight”) obtained from the Ordinary Least Squares regression with p value < 0.05 . The median absolute weightings on the first click and last click are slightly higher than those of the middle clicks at 300 Hz. At 900 Hz, the median absolute weightings on the first click is higher than those of the other clicks.

4.3.3 Multivariate decoding shows strong precedence effect in ECoG signals from the auditory cortex

Unlike in the univariate (channel-by-channel) analysis described above, the results of the multivariate decoding analysis were surprisingly aligned with the behavioral results. When analyzing the average RMS activity observed within the first 30 ms after click train onset, and pooling RMS values over multiple channels

(**Figure 4.3.5 A**), the ITD decoding estimate of the first click was markedly higher than the other clicks. Specifically, only decoding of the first click was significantly different from zero ($p = 0.003$, $Z = 2.981$), while the decoding of the remaining clicks was not significant (all $p > 0.25$). Furthermore, the decoding of the first click was significantly higher than the decoding of all remaining clicks (all $p < 0.003$), while there were no significant differences in decoding between the remaining clicks (all $p > 0.2$). While a comparison of ITD decoding between 900 Hz and 300 Hz stimulation revealed that ITD decoding of the first click was nominally higher for 900 Hz (mean \pm SEM: 0.009 ± 0.004) than for 300 Hz stimulation (mean \pm SEM: 0.007 ± 0.003), this difference was not statistically significant ($p > 0.2$). Therefore, based on neural responses to click trains pooled from multiple ECoG channels, only the ITD of the first click pair could be decoded, showing a strong precedence effect.

In a further analysis, we investigated the decoding dynamics in a longer time window ranging between 0 and 200 ms relative to click train onset (**Figure 4.3.5 B**), beyond the initial 30 ms analyzed above. Here, rather than using average activity to decode ITD, we used activity fluctuations within a given time window. Decoding based on activity fluctuations (rather than average activity) makes this analysis especially sensitive to short-lived transients in neural activity (Wolff et al., 2020). This analysis revealed that ITD of the first click pair could only be decoded based on early neural responses, corresponding to time windows centered at 15-25 ms following click train onset ($p_{\text{FDR}} < 0.05$, corrected across time windows). Unlike in the decoding analysis based on average activity, where only the first click pair ITD could be decoded, in this analysis we also observed short-

lived but significant decoding of the remaining click pair ITDs (click pairs 2 and 3: 15-20 ms, click pair 4: 25-30 ms; all $p_{FDR} < 0.05$, corrected across time windows), suggesting that brief neural transients to single click pairs might be more sensitive to individual ITDs than overall activity. However, as in the decoding based on average activity, also in this analysis the peak ITD decoding of the first click pair was more robust than the peak decoding estimates of the remaining click pairs (all $p < 0.003$), and no differences were observed between peak decoding estimates of click pairs 2-4 (all $p > 0.3$).

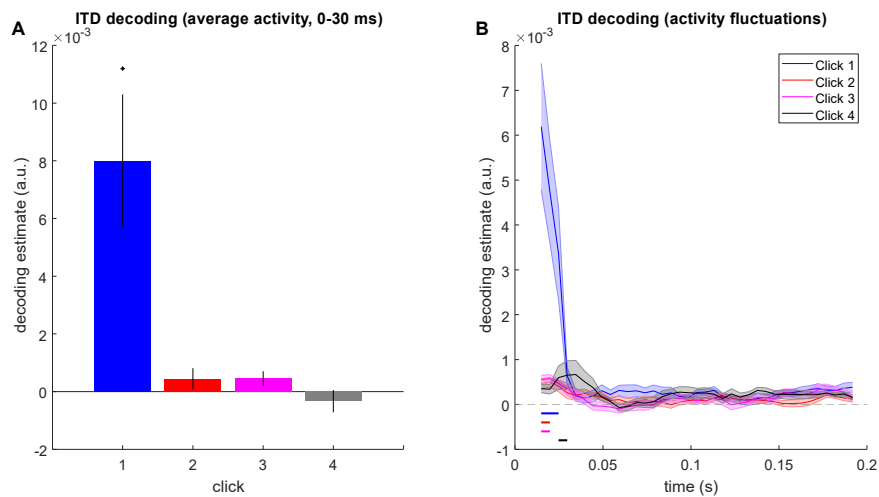


Figure 4.3.5: Neural decoding based on average RMS activity and active fluctuations.

(A) ITD decoding based on average RMS activity between 0-30 ms relative to click burst onset. Error bars denote SEMs across placements. Asterisk indicates statistical significance ($p < 0.05$, Bonferroni-corrected). (B) ITD decoding time-series based on activity fluctuations in each 30-ms-long sliding time window. Shaded areas denote SEMs across placements. Horizontal bars indicate statistical significance ($p < 0.05$, FDR-corrected).

4.4 Discussion

4.4.1 Principal findings

This study demonstrates the temporal precedence effect in binaural hearing in rats, as quantified by the rats' behavioral and neural TWFs and by neural decoding based on auditory cortical signals. To the best of our knowledge, this is the first study to measure TWFs with behavioral and electrophysiological approaches to quantify the precedence effect in a non-human species. Onset dominance of click trains with ITD cues were prevalent in rat behavioral test and in ECoG-based decoding (pooling information from multiple channels). Interestingly, onset dominance in the temporal weighting of ITDs was much less robust in the analysis of single ECoG channels using OLS regression.

Our findings support the view that the hearing system of rat processes binaural cues in a similar way to that of humans, relying heavily on the onsets when localizing sound. In agreement with the TWFs published in a human psychoacoustic study which demonstrated that the weight on the first click was lower for longer inter-click interval (ICI; 5-10 ms) than that for short ICI (2 ms) (Stecker et al., 2013), the presented behavioral and ECoG neural decoding results in rats also showed decreased onset dominance as the frequency of click trains decreased (longer ICI).

4.4.2 Possible mechanism of precedence effect

What is the underlying mechanism of the precedence effect? When a high rate click train is presented, our binaural system focus on the signal onset and extract less information from successive clicks in a train. This phenomenon is termed “binaural adaptation” and will disappear at a click rate less than 100 Hz (Buell and Hafter, 1988). A study focused on the restarting (trigger a resampling of the interaural information) of the adapted binaural system demonstrated that each click in the train was equally effective for slow click trains while only the first click of the train was effective for fast click trains (Hafter and Buell, 1990). That study also suggested that the binaural system could be restarted by a gap as short as 5 ms. It is worth noting the main trigger for a restart was not the gap *per se*, but rather the change in the stimulus (Hafter and Buell, 1990). Therefore, in the case of typical click trains, a “sample-on-demand” process may govern the processing of high-frequency interaural stimuli, whereby successively less information is utilized by the binaural system until a change is presented in the stimulus.

However, in the case of our study, the stimuli were different from ordinary click trains. The acoustic stimuli here contained different ITD information in each click pair, which led to no consistent ICI in the left or right ear. If the “restart of adaptation” theory can be applied to our stimuli, attention should be paid to the changes. How sensitive is our auditory system to the change in the stimulus? How obvious is the change in proportion to the original stimulus? If the change is greater than the detection threshold, a restart will happen. However, one thing

that the “restart of adaptation” hypothesis is not very specific about, is what exactly the brain is supposed to adapt to. Is it an averaged ICI over several trials, or a specific, or precise ICI? And in the later case, would the brain adapt to the ICI for clicks arriving at each ear, or only to the ICI of a perhaps slightly hypothetical “fused binaural image”? These questions are as yet unanswered, but are in principle amenable to investigation, and they are relevant to the current study because the jitter in the ITDs of our TWF click train stimuli might be expected to introduce enough variation in the ICI in each ear to prevent adaptation to a fixed ICI. In our behavioral study, the maximum jitter in one click pair was 0.125 ms. Thus, the jitter to ICI ratio is 11.26% at 900 Hz, 3.75% at 300 Hz, 0.63% at 50 Hz, and 0.25% at 20 Hz. Ugan and Yagcioglu (2014) calculated Weber fraction for ICIs as $\text{discrimination threshold} / \text{ICI} \times 100\%$. The mean Weber fractions they reported for ten normal hearing subjects were 5.7% at 3.3 Hz, 3.2% at 10 Hz, ~6.25% at 20 Hz, ~2% at 50 Hz, and about 0.5% at rates higher than 67 Hz (0.25% at 200 Hz). They did not test the rates higher than 200 Hz. Our jitter to ICI ratios at 20 Hz and 50 Hz are far lower than the mean Weber fraction in their report, which means hard to detect the jitter and no “restart” will be triggered. This is inconsistent with our behavioral findings that both the first and the second clicks showed significant weighting comparing to zero (i.e. a restart on the second click). For click trains delivered at the 300 Hz and 900 Hz rates, we could not directly compare our results with their study, but could only estimate the mean Weber fraction using the value at 200 Hz. At 300 Hz and 900 Hz, the jitter to ICI ratios are more than 10 folds of the mean Weber fraction, which indicates that the jitter should be easy to detect and should trigger “restart”. However, this

is not the case in our results neither. Both the behavioral results and neural decoding results of our experiments showed profound onset weightings but relatively flat weightings on the remaining clicks at 300 Hz and 900 Hz, demonstrating no “restart”. Therefore, in a dynamic ITD setting, the restart of binaural adaptation seems not appropriate to explain the precedence effect.

Similar to our study, Kelly (1974) had tested click pair stimuli in rats with small time differences, and found the lower bound and upper bound of the time differences for discrimination of paired clicks was 31 to 62 μ s and 20.0 to 32.0 ms, respectively. Based on Kelly’s observation and our recent study (Li et al., 2019), the ITD range ([- 0.125 ms, + 0.125 ms]) we used here is clearly above the lower bound of the time differences that could be detected by rats. However, this raises the following questions: if the change in the stimulus is large enough to trigger a response, why are the clicks following the first click pair virtually ignored by the brain? Solomons (1900) assumed that if only a few neurons are initially stimulated and yield a maximum response, then more neurons are activated later on, and their total response is equalized. On the other hand, the refractory period theory (Stein, 1965) does not seem to accurately explain our results. In the view of the refractory period theory, the first click ignites the firing of neurons. As a result of refraction, the second click, even though it is over the sensation threshold, cannot trigger a spike within a short period of time. However, since the refractory period of rat neurons ranges between 0.53 and 1.1 ms (Gallistel et al., 1969), our results suggest that the suppression duration is far longer than the expected refractory period, consistent with the report of Litovsky and Yin (1998).

Previous binaural signal processing model simulated the behavioral of precedence effect (Lindemann, 1986) and a computational model accounts for physiological and psychophysical responses to precedence effect for click stimuli in low-frequency inferior colliculus neurons (Xia et al., 2010) demonstrated that the mechanism of the precedence effect is related to the long-lasting inhibition of neural responses following stimulation onset (Litovsky and Yin, 1998), persisting beyond the short-lived refractory period. It is unclear how long the “long-lasting” inhibition period lasts in rats, but based on our results it is likely to be in the range of 20 ms, since the precedence effect fades at 50 Hz in our behavioral results (i.e., the weightings of the second click become significant different from zero at 50 Hz in all rats). Psychophysically, the precedence effect is strongest with ICI shorter than 10 ms (Wallach et al., 1949; Freyman et al., 1991). In the primary auditory cortex (AI) of unanesthetized rabbits, 50% recovery of the response suppression to the temporally lagging stimulus occurred at an average lag of ~20 ms (Fitzpatrick et al., 1999). Similarly, a free-field single unit recording from the AI of anesthetized cats showed that the response suppression to lagging stimuli monotonically increased as the inter-stimulus delay (ISD) decreased, and was weakest for a few hundred milliseconds, then became stronger, and completely suppressed at about 50 ms (Reale and Brugge, 2000).

4.4.3 Neural decoding as a correlate of the precedence effect in the auditory cortex of rats

Auditory cortex is involved in the precedence effect in human (Liebenthal and Pratt, 1997; Liebenthal and Pratt, 1999). In our investigation of the neural

correlates of TWFs with a characteristic, strong onset-bias in ECoG recordings from the AC, we initially used using channel-wise OLS regression. This analysis, however, produced very variable and inconsistent results, with some recording sites showing the large and expected significant temporal weights at the click train onset, but many others showing unexpected TWF patterns with the largest, or most significant, weight placed on the 2nd or 3rd click, in the middle of the 4 click train. Overall, the trend for the first click in the series to have the on average (median) largest weight was small, and we were not able to show that it has statistical significance. There is therefore a discrepancy here between the behavioral data, which show a very strong and consistent onset bias in the TWFs, and the auditory cortex LFPs, which do not. This surprising finding led to our second attempt to analyze the ECoG data by using a neural decoding method. This time, pooling signals from multiple ECoG channels, we harvested a perfect precedence effect in the AC, consistent with the results demonstrated in behavioral tests.

The two analysis approaches are conceptually and mathematically distinct, and therefore the observed discrepancies between the two sets of results might be due to several reasons. One possible reason is that the linear regression might not be sensitive enough to capture the effects on neural activity induced by precedence effect in the AC. Although both linear models (e.g., linear state-space models) and nonlinear models (e.g., radial basis function auto-regressive models) are effective in predicting ECoG dynamics (Yang et al., 2019), OLS regression – while intuitive – might not be the optimal method to uncover differences in neural activity induced by relatively short and rapidly changing stimuli (such as the

click pairs with jittered ITD used here). Another plausible explanation is that activity in an entire population of neurons is essential to encode the precedence effect. The OLS regression was applied here to analyze neural activity on a channel-by-channel basis, with a limited number of neurons contributing to responses within one channel. Crucially, the application of OLS is based on the assumption that the firing rates of neurons are independent with equal variances (Kass et al., 2005). However, nearby neurons interact with each other, and cannot be realistically considered as independent. Conversely, the multivariate decoding method selected channels with a high signal-to-noise ratio, and pooled signals from these channels, integrating activity patterns over a much larger population of neurons. In the multivariate analysis, we also scaled the responses of each channel by their noise covariance, accounting for dependencies between channels. As a result, the multivariate pattern analysis that we used for neural decoding yielded valuable insights into the neural correlates of the precedence effects in two distinct ways. First, pooling neural activity over space (channels) – which can enhance neural decoding accuracy (Grootswagers et al., 2017; Nemrodov et al., 2018) – resulted in uncovering a robust neural correlate of the precedence effect. Second, pooling neural activity over time – which highlights transient, short-lived neural activity patterns (Wolff et al., 2020) – resulted in uncovering weaker but significant decoding of the later clicks based on the initial neural transients, albeit with a robust precedence effect for the first click pair.

4.4.4 Precedence effect is encoded in the auditory cortex of rats as in other mammals

Our neural decoding results for both tested click trains (300 Hz and 900 Hz) showed a profound precedence effect in the auditory cortex of rats. Auditory cortex is critical for spatial hearing in mammals, such as Japanese Macaques (Heffner and Heffner, 1990), ferrets (King et al., 2007) and cats (Jenkins and Merzenich, 1984). Investigations on humans and cats demonstrated that an intact AC is necessary for the localization dominance of the precedence effect (Cranford and Oberholtzer, 1976; Cornelisse and Kelly, 1987). The stimuli we used here to test the precedence effect were based on manipulating the ITD. Crucially, AI is also related to the transformation of information from ITD to sound source localization (Tsytsarev, 2009). Unilateral lesions of AI result in poor performance in localizing brief sound in the contralateral sound field (Cranford et al., 1971; Jenkins and Merzenich, 1984; Kavanagh and Kelly, 1987). Interestingly, the AC of rats, unlike that of cats, may not be essential in sound localization, as lesions on the contralateral AC did not alter the sound localization of rats (Kelly, 1980). However, this does not necessarily mean that there is no ITD sensitivity in the rat AC, and indeed previous studies demonstrated ITD sensitivity in the AC of rats (Kelly and Phillips, 1991; Tsytsarev, 2009). Our ECoG data also showed the LFP responses are sensitive to ITD more often than we would expect by chance, because up to 12.3% (at a chance level of 5%) of beta values obtained from OLS regression had a p -value < 0.05 .

4.5 Conclusion

In conclusion, rats in our study demonstrated a robust precedence effect in their behavioral TWFs, just like humans do. When the ICI was less than 20 ms, rats strongly relied on the initial sound, and their ultimate behavioral response was largely dependent on the click train onset. Furthermore, while neural signals recorded from the auditory cortex showed heterogeneous weighting of click pairs, the precedence effect was demonstrated when pooling signals from multiple ECoG channels in the decoding analysis.

While these findings describe a tentative neural correlate of the precedence effect on neural activity recorded from the auditory cortex of rats, the underlying mechanisms need further investigation. Since we only used noise burst click-pair trains to evaluate the precedence effect in rats, future studies should use more complex sounds, akin to those heard in the natural environment, to further elucidate the mechanisms of the precedence effect.

5 Chapter 5 Conclusions and Future Perspectives

5.1 Conclusions

In the psychoacoustic behavioral test, we demonstrated that the rats can use envelope ITD to localize sound, and its sensitivity is as accurate as other common seen mammals. The sensitivity to ITD is governed by click rates and envelope type as evidenced by the LFP recorded from the inferior colliculus of rats. In general, the ITD sensitivity of rats decreased as the click rate increased, and dropped to near chance level at 900 Hz. At the same click rate, rats were more sensitive to rectangular windowed stimuli than Hanning windowed ones.

The precedent effect is also preserved in the rat's hearing perception. In the behavioral test, the rat depended heavily on the first click to perform the task, and the weights of the first click was positively correlated with click rates. Similarly, the ECoG neural decoding results illustrated significant onset dominance.

Hence, we confirmed that the rat is a highly suitable model for the study of mammalian ITD processing. In a rat cochlear implant model, attention should be paid to the stimulation rate, since the current popular stimulation rate in clinical use is at or above 900 Hz, but the rats showed dramatic deteriorate sensitivity to ITD at that rate range.

5.2 Future perspective

Since we already found a suitable model in binaural hearing research, in the next step, we will try to use this model to study different types of stimulation strategies in the cochlear implant rats to find out a potential solution to encode usable interaural time difference in the processor.

References

Andersen, R., Knight, P., and Merzenich, M. (1980). The thalamocortical and corticothalamic connections of AI, AII, and the anterior auditory field (AFF) in the cat: Evidence of two largely segregated systems of connections. *The Journal of Comparative Neurology* 194, 663-701. doi: 10.1002/cne.901940312

Auksztulewicz, R., Myers, N., Schnupp, J., and Nobre, A. (2019). Rhythmic Temporal Expectation Boosts Neural Activity by Increasing Neural Gain. *The Journal of Neuroscience* 39, 9806-9817. doi: 10.1523/jneurosci.0925-19.2019

Ball, T., Kern, M., Mutschler, I., Aertsen, A., and Schulze-Bonhage, A. (2009). Signal quality of simultaneously recorded invasive and non-invasive EEG. *NeuroImage* 46, 708-716. doi: 10.1016/j.neuroimage.2009.02.028

Battmer, R., Dillier, N., Lai, W., Begall, K., Leyton, E., González, J., Manrique, M., Morera, C., Müller-Deile, J. (2010). Speech perception performance as a function of stimulus pulse rate and processing strategy preference for the Cochlear™ Nucleus® CI24RE device: Relation to perceptual threshold and loudness comfort profiles. *International Journal of Audiology* 49, 657-666. doi: 10.3109/14992021003801471

Benjamini, Y., and Hochberg, Y. (1995). Controlling the False Discovery Rate: A Practical and Powerful Approach to Multiple Testing. *Journal of the Royal Statistical Society: Series B (Methodological)* 57, 289-300. doi: 10.1111/j.2517-6161.1995.tb02031.x

Bennett, E., and Litovsky, R. (2020). Sound localization in toddlers with normal hearing and with bilateral cochlear implants revealed through a novel “reaching for sound” task. *Journal of the American Academy of Audiology* 31, 195-208. doi: 10.3766/jaaa.18092

Benson, D., and Teas, D. (1976). Single unit study of binaural interaction in the auditory cortex of the chinchilla. *Brain Research* 103, 313-338. doi: 10.1016/0006-8993(76)90801-5

Bernstein, L. (2001). Auditory processing of interaural timing information: New insights. *Journal of Neuroscience Research* 66, 1035-1046. doi: 10.1002/jnr.10103

Bernstein, L., and Trahiotis, C. (2009). How sensitivity to ongoing interaural temporal disparities is affected by manipulations of temporal features of the en-

- velopes of high-frequency stimuli. *The Journal of the Acoustical Society of America* 125, 3234. doi: 10.1121/1.3101454
- Beyerl, B. (1978). Afferent projections to the central nucleus of the inferior colliculus in the rat. *Brain Research* 145, 209-223. doi: 10.1016/0006-8993(78)90858-2
- Boring, E. (1917). A chart of the psychometric function. *The American Journal of Psychology* 28, 465-470. doi: 10.2307/1413891
- Brewer, A., and Barton, B. (2016). Maps of the auditory cortex. *Annual Review of Neuroscience* 39, 385-407. doi: 10.1146/annurev-neuro-070815-014045
- Brown, A., and Stecker, G. (2010). Temporal weighting of interaural time and level differences in high-rate click trains. *The Journal of the Acoustical Society of America* 128, 332-341. doi: 10.1121/1.3436540
- Brown, A., and Stecker, G. (2011). Temporal weighting functions for interaural time and level differences. II. The effect of binaurally synchronous temporal jitter. *The Journal of the Acoustical Society of America* 129, 293-300. doi: 10.1121/1.3514422
- Brown, K., and Balkany, T. (2007). Benefits of bilateral cochlear implantation: a review. *Current Opinion in Otolaryngology & Head and Neck Surgery* 15, 315-318. doi: 10.1097/moo.0b013e3282ef3d3e
- Brugge, J., Reale, R., Hind, J., Chan, J., Musicant, A., and Poon, P. (1994). Simulation of free-field sound sources and its application to studies of cortical mechanisms of sound localization in the cat. *Hearing Research* 73, 67-84. doi: 10.1016/0378-5955(94)90284-4
- Brugge, J., Reale, R., Jenison, R., and Schnupp, J. (2001). Auditory cortical spatial receptive fields. *Audiology and Neuro-Otology* 6, 173-177. doi: 10.1159/000046827
- Brughera, A., Dunai, L., and Hartmann, W. (2013). Human interaural time difference thresholds for sine tones: The high-frequency limit. *The Journal of the Acoustical Society of America* 133, 2839-2855. doi: 10.1121/1.4795778
- Buell, T., and Hafter, E. (1988). Discrimination of interaural differences of time in the envelopes of high-frequency signals: Integration times. *The Journal of the Acoustical Society of America* 84, 2063-2066. doi: 10.1121/1.397050
- Buzsáki, G., Anastassiou, C., and Koch, C. (2012). The origin of extracellular fields and currents — EEG, ECoG, LFP and spikes. *Nature Reviews Neuroscience* 13, 407-420. doi: 10.1038/nrn3241
- Canolty, R., Edwards, E., Dalal, S., Soltani, M., Nagarajan, S., Kirsch, H., Berger, M., Barbaro, N., and Knight, R. (2006). High Gamma power is phase-locked to

- Theta oscillations in human neocortex. *Science* 313, 1626-1628. doi: 10.1126/science.1128115
- Chao (2010). Long-term asynchronous decoding of arm motion using electrocorticographic signals in monkey. *Frontiers in Neuroengineering* . doi: 10.3389/fneng.2010.00003
- Chau, J., Lin, J., Atashband, S., Irvine, R., and Westerberg, B. (2010). Systematic review of the evidence for the etiology of adult sudden sensorineural hearing loss. *The Laryngoscope* , NA-NA. doi: 10.1002/lary.20873
- Chen, Z., and Yuan, W. (2015). Central plasticity and dysfunction elicited by aural deprivation in the critical period. *Frontiers in Neural Circuits* 9. doi: 10.3389/fncir.2015.00026
- de Cheveigné, A., and Simon, J. (2008). Denoising based on spatial filtering. *Journal of Neuroscience Methods* 171, 331-339. doi: 10.1016/j.jneumeth.2008.03.015
- Choi, J., Moon, I., Kim, E., Park, H., Kim, B., Chung, W., Cho, Y., Brown, C., and Hong, S. (2017). Sound localization and speech perception in noise of pediatric cochlear implant recipients: bimodal fitting versus bilateral cochlear implants. *Ear and Hearing* 38, 426-440. doi: 10.1097/aud.0000000000000401
- Chung, Y., Hancock, K., and Delgutte, B. (2016). Neural coding of interaural time differences with bilateral cochlear implants in unanesthetized rabbits. *Journal of Neuroscience* 36, 5520-5531. doi: 10.1523/jneurosci.3795-15.2016
- Clopton, B., and Winfield, J. (1976). Effect of early exposure to patterned sound on unit activity in rat inferior colliculus. *Journal of Neurophysiology* 39, 1081-1089. doi: 10.1152/jn.1976.39.5.1081
- Cornelisse, L., and Kelly, J. (1987). The effect of cerebrovascular accident on the ability to localize sounds under conditions of the precedence effect. *Neuropsychologia* 25, 449-452. doi: 10.1016/0028-3932(87)90033-9
- Cranford, J., Ravizza, R., Diamond, I., and Whitfield, I. (1971). Unilateral ablation of the auditory cortex in the cat impairs complex sound localization. *Science* 172, 286-288. doi: 10.1126/science.172.3980.286
- Cranford, J., and Oberholtzer, M. (1976). Role of neocortex in binaural hearing in the cat. II. The 'precedence effect' in sound localization. *Brain Research* 111, 225-239. doi: 10.1016/0006-8993(76)90768-x
- Creel, D. (1980). Inappropriate use of albino animals as models in research. *Pharmacology Biochemistry and Behavior* 12, 969-977. doi: 10.1016/0091-3057(80)90461-x

- Crone, N., Korzeniewska, A., and Franaszczuk, P. (2011). Cortical gamma responses: Searching high and low. *International Journal of Psychophysiology* 79, 9-15. doi: 10.1016/j.ijpsycho.2010.10.013
- Dietz, M., Wang, L., Greenberg, D., and McAlpine, D. (2016). Sensitivity to interaural time differences conveyed in the stimulus envelope: estimating inputs of binaural neurons through the temporal analysis of spike trains. *Journal of the Association for Research in Otolaryngology* 17, 313-330. doi: 10.1007/s10162-016-0573-9
- Druga, R., and Syka, J. (1984). Ascending and descending projections to the inferior colliculus in the rat. *Physiologia Bohemoslovaca* 33, 31-42.
- Dunn, C., Noble, W., Tyler, R., Kordus, M., Gantz, B., and Ji, H. (2010). Bilateral and unilateral cochlear implant users compared on speech perception in noise. *Ear and Hearing* 31, 296-298. doi: 10.1097/aud.0b013e3181c12383
- Eapen, R., Buss, E., Adunka, M., Pillsbury, H., and Buchman, C. (2009). Hearing-in-noise benefits after bilateral simultaneous cochlear implantation continue to improve 4 years after implantation. *Otology & Neurotology* 30, 153-159. doi: 10.1097/mao.0b013e3181925025
- Ebert, C., Blanks, D., Patel, M., Coffey, C., Marshall, A., and Fitzpatrick, D. (2008). Behavioral sensitivity to interaural time differences in the rabbit. *Hearing Research* 235, 134-142. doi: 10.1016/j.heares.2007.11.003
- Edmonds, B., and Krumbholz, K. (2013). Are interaural time and level differences represented by independent or integrated codes in the human auditory cortex?. *Journal of the Association for Research in Otolaryngology* 15, 103-114. doi: 10.1007/s10162-013-0421-0
- Ehret, G. (1997). The auditory cortex. *Journal of Comparative Physiology A: Sensory, Neural, and Behavioral Physiology* 181, 547-557. doi: 10.1007/s003590050139
- Ehret, G. & Romand, R. (Ed.), (1997) *The central auditory system*. (New York: Oxford University Press).
- Emmett, S., and Francis, H. (2015). The socioeconomic impact of hearing loss in US adults. *Otology & Neurotology* 36, 545-550. doi: 10.1097/mao.0000000000000562
- Faller, C., and Merimaa, J. (2004). Source localization in complex listening situations: Selection of binaural cues based on interaural coherence. *The Journal of the Acoustical Society of America* 116, 3075-3089. doi: 10.1121/1.1791872
- Faye-Lund, H. (1985). The neocortical projection to the inferior colliculus in the albino rat. *Anatomy and Embryology* 173, 53-70. doi: 10.1007/bf00707304

- Fitzpatrick, D., Kuwada, S., Kim, D., Parham, K., and Batra, R. (1999). Responses of neurons to click-pairs as simulated echoes: Auditory nerve to auditory cortex. *The Journal of the Acoustical Society of America* 106, 3460-3472. doi: 10.1121/1.428199
- Flammino, F., and Clopton, B. (1975a). Cues for auditory localization in the rat. *Journal of the American Audiology Society* 1, 11-14.
- Flammino, F., and Clopton, B. (1975b). Neural responses in the inferior colliculus of albino rat to binaural stimuli. *The Journal of the Acoustical Society of America* 57, 692-695. doi: 10.1121/1.380494
- Freeman, W., Rogers, L., Holmes, M., and Silbergeld, D. (2000). Spatial spectral analysis of human electrocorticograms including the alpha and gamma bands. *Journal of Neuroscience Methods* 95, 111-121. doi: 10.1016/s0165-0270(99)00160-0
- Freyman, R., Clifton, R., and Litovsky, R. (1991). Dynamic processes in the precedence effect. *The Journal of the Acoustical Society of America* 90, 874-884. doi: 10.1121/1.401955
- Gallistel, C., Rolls, E., and Greene, D. (1969). Neuron function inferred from behavioral and electrophysiological estimates of refractory period. *Science* 166, 1028-1030. doi: 10.1126/science.166.3908.1028
- Goldberg, J., and Brown, P. (1969). Response of binaural neurons of dog superior olivary complex to dichotic tonal stimuli: some physiological mechanisms of sound localization.. *Journal of Neurophysiology* 32, 613-636. doi: 10.1152/jn.1969.32.4.613
- Goupell, M., Laback, B., and Majdak, P. (2009). Enhancing sensitivity to interaural time differences at high modulation rates by introducing temporal jitter. *The Journal of the Acoustical Society of America* 126, 2511-2521. doi: 10.1121/1.3206584
- Grantham, D., Ashmead, D., Ricketts, T., Labadie, R., and Haynes, D. (2007). Horizontal-plane localization of noise and speech signals by postlingually deafened adults fitted with bilateral cochlear implants. *Ear and Hearing* 28, 524-541. doi: 10.1097/aud.0b013e31806dc21a
- Greene, N., Anbuhl, K., Ferber, A., DeGuzman, M., Allen, P., and Tollin, D. (2018). Spatial hearing ability of the pigmented Guinea pig (*Cavia porcellus*): Minimum audible angle and spatial release from masking in azimuth. *Hearing Research* 365, 62-76. doi: 10.1016/j.heares.2018.04.011
- Grieco-Calub, T., and Litovsky, R. (2012). Spatial acuity in two-to-three-year-old children with normal acoustic hearing, unilateral cochlear implants and bilateral

cochlear implants. *Ear and Hearing* 33, 561-572. doi: 10.1097/aud.0b013e31824c7801

Grootswagers, T., Wardle, S., and Carlson, T. (2017). Decoding Dynamic Brain Patterns from Evoked Responses: A Tutorial on Multivariate Pattern Analysis Applied to Time Series Neuroimaging Data. *Journal of Cognitive Neuroscience* 29, 677-697. doi: 10.1162/jocn_a_01068

Groppe, D., Bickel, S., Keller, C., Jain, S., Hwang, S., Harden, C., and Mehta, A. (2013). Dominant frequencies of resting human brain activity as measured by the electrocorticogram. *NeuroImage* 79, 223-233. doi: 10.1016/j.neuroimage.2013.04.044

Grothe, B., Pecka, M., and McAlpine, D. (2010). Mechanisms of sound localization in mammals. *Physiological Reviews* 90, 983-1012. doi: 10.1152/physrev.00026.2009

Haftner, E., and Buell, T. (1990). Restarting the adapted binaural system. *The Journal of the Acoustical Society of America* 88, 806-812. doi: 10.1121/1.399730

Hämäläinen, M., Hari, R., Ilmoniemi, R., Knuutila, J., and Lounasmaa, O. (1993). Magnetoencephalography—theory, instrumentation, and applications to noninvasive studies of the working human brain. *Reviews of Modern Physics* 65, 413-497. doi: 10.1103/revmodphys.65.413

Hancock, K., Noel, V., Ryugo, D., and Delgutte, B. (2010). Neural coding of interaural time differences with bilateral cochlear implants: effects of congenital deafness. *Journal of Neuroscience* 30, 14068-14079. doi: 10.1523/jneurosci.3213-10.2010

Hartmann, W., and Macaulay, E. (2014). Anatomical limits on interaural time differences: an ecological perspective. *Frontiers in Neuroscience* 8, 34. doi: 10.3389/fnins.2014.00034

Heffner, H., and Heffner, R. (1985). Sound localization in wild Norway rats (*Rattus norvegicus*). *Hearing Research* 19, 151-155. doi: 10.1016/0378-5955(85)90119-4

Heffner, H., and Heffner, R. (1990). Effect of bilateral auditory cortex lesions on sound localization in Japanese macaques. *Journal of Neurophysiology* 64, 915-931. doi: 10.1152/jn.1990.64.3.915

Heffner, H. E. and Heffner, R. S. (2003) Audition. In: *Handbook of Research Methods in Experimental Psychology*, Blackwell Publishing Ltd.

Heffner, H., Heffner, R., Contos, C., and Ott, T. (1994). Audiogram of the hooded Norway rat. *Hearing Research* 73, 244-247.

- Henning, G. (1974). Detectability of interaural delay in high-frequency complex waveforms. *The Journal of the Acoustical Society of America* 55, 84-90. doi: 10.1121/1.1928135
- Herreras, O. (2016). Local field potentials: myths and misunderstandings. *Frontiers in Neural Circuits* 10. doi: 10.3389/fncir.2016.00101
- Hoeffding, V., and Harrison, J. (1979). Auditory discrimination: role of time and intensity in the precedence effect. *Journal of the Experimental Analysis of Behavior* 32, 157-166. doi: 10.1901/jeab.1979.32-157
- van Hoesel, R., Jones, G., and Litovsky, R. (2009). Interaural time-delay sensitivity in bilateral cochlear implant users: Effects of pulse rate, modulation rate, and place of stimulation. *Journal of the Association for Research in Otolaryngology* 10, 557-567. doi: 10.1007/s10162-009-0175-x
- van Hoesel, R. (2004). Exploring the benefits of bilateral cochlear implants. *Audiology and Neuro-Otology* 9, 234-246. doi: 10.1159/000078393
- van Hoesel, R., and Tyler, R. (2003). Speech perception, localization, and lateralization with bilateral cochlear implants. *The Journal of the Acoustical Society of America* 113, 1617-1630. doi: 10.1121/1.1539520
- Hoffman, M., Quittner, A., and Cejas, I. (2014). Comparisons of social competence in young children with and without hearing loss: A dynamic systems framework. *Journal of Deaf Studies and Deaf Education* 20, 115-124. doi: 10.1093/deafed/enu040
- Insanally, M., Trumpis, M., Wang, C., Chiang, C., Woods, V., Palopoli-Trojani, K., Bossi, S., Froemke, R., and Viventi, J. (2016). A low-cost, multiplexed μ ECoG system for high-density recordings in freely moving rodents. *Journal of Neural Engineering* 13, 026030. doi: 10.1088/1741-2560/13/2/026030
- Irvine, D., Park, V., and Mattingley, J. (1995). Responses of neurons in the inferior colliculus of the rat to interaural time and intensity differences in transient stimuli: Implications for the latency hypothesis. *Hearing Research* 85, 127-141. doi: 10.1016/0378-5955(95)00040-b
- Itskov, P., Vinnik, E., Honey, C., Schnupp, J., and Diamond, M. (2012). Sound sensitivity of neurons in rat hippocampus during performance of a sound-guided task. *Journal of Neurophysiology* 107, 1822-1834. doi: 10.1152/jn.00404.2011
- Jackson, L., Heffner, R., and Heffner, H. (1999). Free-field audiogram of the Japanese macaque (*Macaca fuscata*). *The Journal of the Acoustical Society of America* 106, 3017-3023. doi: 10.1121/1.428121

- Jenkins, W., and Masterton, R. (1982). Sound localization: Effects of unilateral lesions in central auditory system. *Journal of Neurophysiology* 47, 987-1016. doi: 10.1152/jn.1982.47.6.987
- Jenkins, W., and Merzenich, M. (1984). Role of cat primary auditory cortex for sound-localization behavior. *Journal of Neurophysiology* 52, 819-847. doi: 10.1152/jn.1984.52.5.819
- Jones, E., Oliphant, T., and Peterson, P. (2001) SciPy: open source scientific tools for Python.
- Joris, P., Schreiner, C., and Rees, A. (2004). Neural processing of amplitude-modulated sounds. *Physiological Reviews* 84, 541-577. doi: 10.1152/physrev.00029.2003
- Joris, P., and Yin, T. (1995). Envelope coding in the lateral superior olive. I. Sensitivity to interaural time differences. *Journal of Neurophysiology* 73, 1043-1062. doi: 10.1152/jn.1995.73.3.1043
- Kajikawa, Y., and Schroeder, C. (2015). Generation of field potentials and modulation of their dynamics through volume integration of cortical activity. *Journal of Neurophysiology* 113, 339-351. doi: 10.1152/jn.00914.2013
- Kan, A., and Litovsky, R. (2018). Lateralization of interaural time and level differences measured with cochlear implant sound processors. *The Journal of the Acoustical Society of America* 144, 1711-1711. doi: 10.1121/1.5067592
- Kan, A., and Litovsky, R. (2015). Binaural hearing with electrical stimulation. *Hearing Research* 322, 127-137. doi: 10.1016/j.heares.2014.08.005
- Kass, R., Ventura, V., and Brown, E. (2005). Statistical Issues in the Analysis of Neuronal Data. *Journal of Neurophysiology* 94, 8-25. doi: 10.1152/jn.00648.2004
- Kavanagh, G., and Kelly, J. (1986). Midline and lateral field sound localization in the albino rat (*Rattus norvegicus*). *Behavioral Neuroscience* 100, 200-205. doi: 10.1037/0735-7044.100.2.200
- Kavanagh, G., and Kelly, J. (1987). Contribution of auditory cortex to sound localization by the ferret (*Mustela putorius*). *Journal of Neurophysiology* 57, 1746-1766. doi: 10.1152/jn.1987.57.6.1746
- Keating, P., Nodal, F., Gananandan, K., Schulz, A., and King, A. (2013). Behavioral sensitivity to broadband binaural localization cues in the ferret. *Journal of the Association for Research in Otolaryngology* 14, 561-572. doi: 10.1007/s10162-013-0390-3

- Keithley, E., Ryan, A., and Feldman, M. (1992). Cochlear degeneration in aged rats of four strains. *Hearing Research* 59, 171-178. doi: 10.1016/0378-5955(92)90113-2
- Kelly, J. (1974). Localization of paired sound sources in the rat: small time differences. *The Journal of the Acoustical Society of America* 55, 1277-1284. doi: 10.1121/1.1914697
- Kelly, J. (1980). Effects of auditory cortical lesions on sound localization by the rat. *Journal of Neurophysiology* 44, 1161-1174. doi: 10.1152/jn.1980.44.6.1161
- Kelly, J., Buckthrought, A., and Kidd, S. (1998). Monaural and binaural response properties of single neurons in the rat's dorsal nucleus of the lateral lemniscus. *Hearing Research* 122, 25-40. doi: 10.1016/s0378-5955(98)00082-3
- Kelly, J., Glenn, S., and Beaver, C. (1991). Sound frequency and binaural response properties of single neurons in rat inferior colliculus. *Hearing Research* 56, 273-280. doi: 10.1016/0378-5955(91)90177-b
- Kelly, J., and Masterton, B. (1977). Auditory sensitivity of the albino rat. *Journal of Comparative and Physiological Psychology* 91, 930-936. doi: 10.1037/h0077356
- Kelly, J., and Phillips, D. (1991). Coding of interaural time differences of transients in auditory cortex of *Rattus norvegicus*: Implications for the evolution of mammalian sound localization. *Hearing Research* 55, 39-44. doi: 10.1016/0378-5955(91)90089-r
- Khodagholy, D., Gelineas, J., Thesen, T., Doyle, W., Devinsky, O., Malliaras, G., and Buzsáki, G. (2014). NeuroGrid: recording action potentials from the surface of the brain. *Nature Neuroscience* 18, 310-315. doi: 10.1038/nn.3905
- Kidd, S., and Kelly, J. (1996). Contribution of the dorsal nucleus of the lateral lemniscus to binaural responses in the inferior colliculus of the rat: interaural time delays. *The Journal of Neuroscience* 16, 7390-7397. doi: 10.1523/jneurosci.16-22-07390.1996
- King, A., Bajo, V., Bizley, J., Campbell, R., Nodal, F., Schulz, A., and Schnupp, J. (2007). Physiological and behavioral studies of spatial coding in the auditory cortex. *Hearing Research* 229, 106-115. doi: 10.1016/j.heares.2007.01.001
- Klein-Hennig, M., Dietz, M., Hohmann, V., and Ewert, S. (2011). The influence of different segments of the ongoing envelope on sensitivity to interaural time delays. *The Journal of the Acoustical Society of America* 129, 3856-3872. doi: 10.1121/1.3585847

- Klumpp, R., and Eady, H. (1956). Some measurements of interaural time difference thresholds. *The Journal of the Acoustical Society of America* 28, 859-860. doi: 10.1121/1.1908493
- Koka, K., Jones, H., Thornton, J., Lupo, J., and Tollin, D. (2011). Sound pressure transformations by the head and pinnae of the adult Chinchilla (*Chinchilla lanigera*). *Hearing Research* 272, 135-147. doi: 10.1016/j.heares.2010.10.007
- Koka, K., Read, H., and Tollin, D. (2008). The acoustical cues to sound location in the rat: measurements of directional transfer functions. *The Journal of the Acoustical Society of America* 123, 4297-4309. doi: 10.1121/1.2916587
- Korver, A., Smith, R., Camp, G., Schleiss, M., Bitner-Glindzicz, M., Lustig, L., Usami, S., and Boudewyns, A. (2017). Congenital hearing loss. *Nature Reviews Disease Primers* 3. doi: 10.1038/nrdp.2016.94
- Laback, B., Egger, K., and Majdak, P. (2015). Perception and coding of interaural time differences with bilateral cochlear implants. *Hearing Research* 322, 138-150. doi: 10.1016/j.heares.2014.10.004
- Laback, B., and Majdak, P. (2008). Binaural jitter improves interaural time-difference sensitivity of cochlear implantees at high pulse rates. *Proceedings of the National Academy of Sciences* 105, 814-817. doi: 10.1073/pnas.0709199105
- Laback, B., Majdak, P., and Baumgartner, W. (2007). Lateralization discrimination of interaural time delays in four-pulse sequences in electric and acoustic hearing. *The Journal of the Acoustical Society of America* 121, 2182-2191. doi: 10.1121/1.2642280
- Laszig, R., Aschendorff, A., Stecker, M., Müller-Deile, J., Maune, S., Dillier, N., Weber, B., Hey, M., Begall, K. (2004). Benefits of bilateral electrical stimulation with the nucleus cochlear implant in adults: 6-month postoperative results. *Otology & Neurotology* 25, 958-968.
- Li, K., Chan, C., Rajendran, V., Meng, Q., Roskoth-Kuhl, N., and Schnupp, J. (2019). Microsecond sensitivity to envelope interaural time differences in rats. *The Journal of the Acoustical Society of America* 145, EL341-EL347. doi: 10.1121/1.5099164
- Liebenthal, E., and Pratt, H. (1997). Evidence for primary auditory cortex involvement in the echo suppression precedence effect: a 3CLT study. *Journal of Basic and Clinical Physiology and Pharmacology* 8. doi: 10.1515/jbcpp.1997.8.3.181
- Liebenthal, E., and Pratt, H. (1999). Human auditory cortex electrophysiological correlates of the precedence effect: Binaural echo lateralization suppression. *The*

Journal of the Acoustical Society of America 106, 291-303. doi: 10.1121/1.427057

Lindemann, W. (1986). Extension of a binaural cross-correlation model by contralateral inhibition. II. The law of the first wave front. *The Journal of the Acoustical Society of America* 80, 1623-1630. doi: 10.1121/1.394326

Lingner, A., Wiegrebe, L., and Grothe, B. (2012). Sound localization in noise by gerbils and humans. *Journal of the Association for Research in Otolaryngology* 13, 237-248. doi: 10.1007/s10162-011-0301-4

Litovsky, R. (1997). Developmental changes in the precedence effect: Estimates of minimum audible angle. *The Journal of the Acoustical Society of America* 102, 1739-1745. doi: 10.1121/1.420106

Litovsky, R., Colburn, H., Yost, W., and Guzman, S. (1999). The precedence effect. *The Journal of the Acoustical Society of America* 106, 1633-1654. doi: 10.1121/1.427914

Litovsky, R., Jones, G., Agrawal, S., and van Hoesel, R. (2010). Effect of age at onset of deafness on binaural sensitivity in electric hearing in humans. *The Journal of the Acoustical Society of America* 127, 400-414. doi: 10.1121/1.3257546

Litovsky, R., Parkinson, A., and Arcaroli, J. (2009). Spatial hearing and speech intelligibility in bilateral cochlear implant users. *Ear and Hearing* 30, 419-431. doi: 10.1097/aud.0b013e3181a165be

Litovsky, R., and Yin, T. (1998). Physiological studies of the precedence effect in the inferior colliculus of the cat. II. Neural Mechanisms. *Journal of Neurophysiology* 80, 1302-1316. doi: 10.1152/jn.1998.80.3.1302

Liu, Y., Coon, W., de Pestors, A., Brunner, P., and Schalk, G. (2015). The effects of spatial filtering and artifacts on electrocorticographic signals. *Journal of Neural Engineering* 12, 056008. doi: 10.1088/1741-2560/12/5/056008

Lovett, R., Kitterick, P., Hewitt, C., and Summerfield, A. (2010). Bilateral or unilateral cochlear implantation for deaf children: an observational study. *Archives of Disease in Childhood* 95, 107-112. doi: 10.1136/adc.2009.160325

Masri, S., Zhang, L., Luo, H., Pace, E., Zhang, J., and Bao, S. (2018). Blast exposure disrupts the tonotopic frequency map in the primary auditory cortex. *Neuroscience* 379, 428-434. doi: 10.1016/j.neuroscience.2018.03.041

Masterton, B., Thompson, G., Bechtold, J., and RoBards, M. (1975). Neuroanatomical basis of binaural phase-difference analysis for sound localization: A comparative study. *Journal of Comparative and Physiological Psychology* 89, 379-386. doi: 10.1037/h0077034

- Mickey, B., and Middlebrooks, J. (2005). Sensitivity of auditory cortical neurons to the locations of leading and lagging sounds. *Journal of Neurophysiology* 94, 979-989. doi: 10.1152/jn.00580.2004
- Middlebrooks, J., Makous, J., and Green, D. (1989). Directional sensitivity of sound-pressure levels in the human ear canal. *The Journal of the Acoustical Society of America* 86, 89-108. doi: 10.1121/1.398224
- Mills, A. (1958). On the minimum audible angle. *The Journal of the Acoustical Society of America* 30, 237-246. doi: 10.1121/1.1909553
- Moore, D. (1991). *Anatomy and Physiology of Binaural Hearing*. *Audiology* 30, 125-134. doi: 10.3109/00206099109072878
- Mudry, A., and Mills, M. (2013). The early history of the cochlear implant: a retrospective. *JAMA Otolaryngology–Head & Neck Surgery* 139, 446-453. doi: 10.1001/jamaoto.2013.293
- Muhle-Karbe, P., Myers, N., and Stokes, M. (2020). A hierarchy of functional states in working memory. . doi: 10.1101/2020.04.16.044511
- Müller, U., and Barr-Gillespie, P. (2015). New treatment options for hearing loss. *Nature Reviews Drug Discovery* 14, 346-365. doi: 10.1038/nrd4533
- Møller, A., and Rees, A. (1986). Dynamic properties of the responses of single neurons in the inferior colliculus of the rat. *Hearing Research* 24, 203-215. doi: 10.1016/0378-5955(86)90019-5
- Nelken, I., Chechik, G., Mscic-Flogel, T., King, A., and Schnupp, J. (2005). Encoding stimulus information by spike numbers and mean response time in primary auditory cortex. *Journal of Computational Neuroscience* 19, 199-221. doi: 10.1007/s10827-005-1739-3
- Nemrodov, D., Niemeier, M., Patel, A., and Nestor, A. (2018). The Neural Dynamics of Facial Identity Processing: Insights from EEG-Based Pattern Analysis and Image Reconstruction. *eneuro* 5, ENEURO.0358-17.2018. doi: 10.1523/eneuro.0358-17.2018
- Nicholas, J., and Geers, A. (2007). Will they catch up? The role of age at cochlear implantation in the spoken language development of children with severe to profound hearing loss. *Journal of Speech, Language, and Hearing Research* 50, 1048-1062. doi: 10.1044/1092-4388(2007/073)
- Patterson, R. (2015) . In: D.Jaeger & R.Jung (Ed.), "Pulse-resonance sounds", Springer.
- Pesaran, B., Vinck, M., Einevoll, G., Sirota, A., Fries, P., Siegel, M., Truccolo, W., Schroeder, C., and Srinivasan, R. (2018). Investigating large-scale brain dy-

- namics using field potential recordings: analysis and interpretation. *Nature Neuroscience* 21, 903-919. doi: 10.1038/s41593-018-0171-8
- Poon, P., and Chen, X. (1992). Postnatal exposure to tones alters the tuning characteristics of inferior collicular neurons in the rat. *Brain Research* 585, 391-394. doi: 10.1016/0006-8993(92)91243-8
- Prusky, G., Harker, K., Douglas, R., and Wishaw, I. (2002). Variation in visual acuity within pigmented, and between pigmented and albino rat strains. *Behavioural Brain Research* 136, 339-348. doi: 10.1016/s0166-4328(02)00126-2
- Rauch, A., Rosskothén-Kuhl, N., and Illing, R. (2016). Counter-regulation of the AP-1 monomers pATF2 and Fos: Molecular readjustment of brainstem neurons in hearing and deaf adult rats after electrical intracochlear stimulation. *Neuroscience* 313, 184-198. doi: 10.1016/j.neuroscience.2015.11.025
- Rayleigh, L. (1907). XII. On our perception of sound direction. *The London, Edinburgh, and Dublin Philosophical Magazine and Journal of Science* 13, 214-232. doi: 10.1080/14786440709463595
- Reale, R., and Brugge, J. (2000). Directional sensitivity of neurons in the primary auditory (AI) cortex of the cat to successive sounds ordered in time and space. *Journal of Neurophysiology* 84, 435-450. doi: 10.1152/jn.2000.84.1.435
- Rosskothén-Kuhl, N., Buck, A., Li, K., and Schnupp, J. (2019). Microsecond interaural time difference discrimination restored by cochlear implants after neonatal deafness. . doi: 10.1101/498105
- Rosskothén-Kuhl, N., and Illing, R. (2010). Nonlinear development of the populations of neurons expressing c-Fos under sustained electrical intracochlear stimulation in the rat auditory brainstem. *Brain Research* 1347, 33-41. doi: 10.1016/j.brainres.2010.05.089
- Rutkowski, R., Miasnikov, A., and Weinberger, N. (2003). Characterisation of multiple physiological fields within the anatomical core of rat auditory cortex. *Hearing Research* 181, 116-130. doi: 10.1016/s0378-5955(03)00182-5
- Saldaña, E., Feliciano, M., and Mugnaini, E. (1996). Distribution of descending projections from primary auditory neocortex to inferior colliculus mimics the topography of intracollicular projections. *The Journal of Comparative Neurology* 371, 15-40. doi: 10.1002/(sici)1096-9861(19960715)371:1<15::aid-cne2>3.0.co;2-o
- Sally, S., and Kelly, J. (1988). Organization of auditory cortex in the albino rat: sound frequency. *Journal of Neurophysiology* 59, 1627-1638. doi: 10.1152/jn.1988.59.5.1627

- Sanes, D., and Woolley, S. (2011). A behavioral framework to guide research on central auditory development and plasticity. *Neuron* 72, 912-929. doi: 10.1016/j.neuron.2011.12.005
- Schalk, G., and Leuthardt, E. (2011). Brain-computer interfaces using electrocorticographic signals. *IEEE Reviews in Biomedical Engineering* 4, 140-154. doi: 10.1109/rbme.2011.2172408
- Schnupp, J., Nelken, I., and King, A., (2012) Auditory neuroscience: Making sense of sound. (Cambridge: MIT Press Ltd).
- Schnupp, J., Dawe, K., and Pollack, G. (2005). The detection of multisensory stimuli in an orthogonal sensory space. *Experimental Brain Research* 162, 181-190. doi: 10.1007/s00221-004-2136-2
- Schnupp, J., Garcia-Lazaro, J., and Lesica, N. (2015). Periodotopy in the gerbil inferior colliculus: local clustering rather than a gradient map. *Frontiers in Neural Circuits* 9. doi: 10.3389/fncir.2015.00037
- Schoen, F., Mueller, J., Helms, J., and Nopp, P. (2005). Sound localization and sensitivity to interaural cues in bilateral users of the Med-El Combi 40/40+ cochlear implant system. *Otology & Neurotology* 26, 429-437. doi: 10.1097/01.mao.0000169772.16045.86
- Schreiner, C., and Langner, G. (1988). Periodicity coding in the inferior colliculus of the cat. II. Topographical organization. *Journal of Neurophysiology* 60, 1823-1840. doi: 10.1152/jn.1988.60.6.1823
- Seabold, S., and Perktold, J. (2010) Statsmodels: Econometric and statistical modeling with python. In: *Proceedings of the 9th Python in Science Conference*.
- Seeber, B., and Fastl, H. (2008). Localization cues with bilateral cochlear implants. *The Journal of the Acoustical Society of America* 123, 1030-1042. doi: 10.1121/1.2821965
- Seidl, A., and Grothe, B. (2005). Development of sound localization mechanisms in the Mongolian gerbil is shaped by early acoustic experience. *Journal of Neurophysiology* 94, 1028-1036. doi: 10.1152/jn.01143.2004
- Shackleton, T., Skottun, B., Arnott, R., and Palmer, A. (2003). Interaural time difference discrimination thresholds for single neurons in the inferior colliculus of guinea pigs. *The Journal of Neuroscience* 23, 716-724. doi: 10.1523/jneurosci.23-02-00716.2003
- Shannon, R., Cruz, R., and Galvin, J. (2011). Effect of stimulation rate on cochlear implant users' phoneme, word and sentence recognition in quiet and in noise. *Audiology and Neurotology* 16, 113-123. doi: 10.1159/000315115

- Solomons, L. (1900). A new explanation of Weber's Law. *Psychological Review* 7, 234-240. doi: 10.1037/h0065919
- Stakhovskaya, O., Sridhar, D., Bonham, B., and Leake, P. (2007). Frequency Map for the Human Cochlear Spiral Ganglion: Implications for Cochlear Implants. *Journal of the Association for Research in Otolaryngology* 8, 220-233. doi: 10.1007/s10162-007-0076-9
- Stecker, G. (2014). Temporal weighting functions for interaural time and level differences. IV. Effects of carrier frequency. *The Journal of the Acoustical Society of America* 136, 3221-3232. doi: 10.1121/1.4900827
- Stecker, G. (2018). Temporal weighting functions for interaural time and level differences. V. Modulated noise carriers. *The Journal of the Acoustical Society of America* 143, 686-695. doi: 10.1121/1.5022785
- Stecker, G., and Hafter, E. (2002). Temporal weighting in sound localization. *The Journal of the Acoustical Society of America* 112, 1046-1057. doi: 10.1121/1.1497366
- Stecker, G., Ostreicher, J., and Brown, A. (2013). Temporal weighting functions for interaural time and level differences. III. Temporal weighting for lateral position judgments. *The Journal of the Acoustical Society of America* 134, 1242-1252. doi: 10.1121/1.4812857
- Stein, R. (1965). A Theoretical Analysis of Neuronal Variability. *Biophysical Journal* 5, 173-194. doi: 10.1016/s0006-3495(65)86709-1
- Stevens, S. S. (2002) Signal detection theory. In: Pashler, H. (Ed.), *Stevens' handbook of experimental psychology*, John Wiley & Sons.
- Takamori, M., Sachs-Hombach, K., Cole, J., Cole, J., Leiter, J. C., Jr., D. B., Scudder, C., Kanai, R., Wu, D.-A., Colby, C. L., Funahashi, S., Mueller, D., Quirk, G. J., Ono, T., Phillips, A. G., Sasaki, Y., Watanabe, T., Nishimaru, H., Sandercock, T. G., Simner, J., Frank, C., Zahm, D. S., Heimer, L., Pearson, K., Dubuc, R., Rossignol, S., Busse, R., Macefield, V. G., Tanabe, H., Manabe, T. and Bogduk, N. (2009) L. In: *Encyclopedia of Neuroscience*, Springer.
- Thakkar, T., Kan, A., Jones, H., and Litovsky, R. (2018). Mixed stimulation rates to improve sensitivity of interaural timing differences in bilateral cochlear implant listeners. *The Journal of the Acoustical Society of America* 143, 1428-1440. doi: 10.1121/1.5026618
- The National Institute for Health and Care Excellence (2019). Cochlear implants for children and adults with severe to profound deafness. 2019-03-07. www.nice.org.uk/guidance/ta566.

- Tolnai, S., Beutelmann, R., and Klump, G. (2017). Exploring binaural hearing in gerbils (*Meriones unguiculatus*) using virtual headphones. *PloS one* 12, e0175142. doi: 10.1371/journal.pone.0175142
- Tolnai, S., Beutelmann, R., and Klump, G. (2018). Interaction of interaural cues and their contribution to the lateralisation of Mongolian gerbils (*Meriones unguiculatus*). *Journal of Comparative Physiology A* 204, 435-448. doi: 10.1007/s00359-018-1253-5
- Treutwein, B. (1995). Adaptive psychophysical procedures. *Vision Research* 35, 2503-2522. doi: 10.1016/0042-6989(95)00016-x
- Tsytsarev, V. (2009). Optical imaging of interaural time difference representation in rat auditory cortex. *Frontiers in Neuroengineering* 2. doi: 10.3389/neuro.16.002.2009
- Turton, L., and Smith, P. (2012). Prevalence & characteristics of severe and profound hearing loss in adults in a UK National Health Service clinic. *International Journal of Audiology* 52, 92-97. doi: 10.3109/14992027.2012.735376
- Tyler, R., Dunn, C., Witt, S., and Preece, J. (2003). Update on bilateral cochlear implantation. *Current opinion in otolaryngology & head and neck surgery* 11, 388-393.
- Ungan, P., and Yagcioglu, S. (2014). Significant variations in Weber fraction for changes in inter-onset interval of a click train over the range of intervals between 5 and 300 ms. *Frontiers in Psychology* 5. doi: 10.3389/fpsyg.2014.01453
- U.S. Food & Drug Administration (2020). Other products and devices to improve Hearing. 2020-02-14. <https://www.fda.gov/medical-devices/hearing-aids/other-products-and-devices-improve-hearing>.
- Vollmer, M., Beitel, R., Schreiner, C., and Leake, P. (2017). Passive stimulation and behavioral training differentially transform temporal processing in the inferior colliculus and primary auditory cortex. *Journal of Neurophysiology* 117, 47-64. doi: 10.1152/jn.00392.2016
- Wakeford, O., and Robinson, D. (1974). Lateralization of tonal stimuli by the cat. *The Journal of the Acoustical Society of America* 55, 649-652. doi: 10.1121/1.1914577
- Wallach, H., Newman, E., and Rosenzweig, M. (1949). A precedence effect in sound localization. *The Journal of the Acoustical Society of America* 21, 468-468. doi: 10.1121/1.1917119
- Wesolek, C., Koay, G., Heffner, R., and Heffner, H. (2010). Laboratory rats (*Rattus norvegicus*) do not use binaural phase differences to localize sound. *Hearing Research* 265, 54-62. doi: 10.1016/j.heares.2010.02.011

- World Health Organization (2020). Deafness prevention. 2020-02-14. <https://www.who.int/news-room/fact-sheets/detail/deafness-and-hearing-loss>.
- Winer, J. A. (1992) The functional architecture of the medial geniculate body and the primary auditory cortex. In: *The Mammalian Auditory Pathway: Neuroanatomy*, Springer New York.
- Woldorff, M., Tempelmann, C., Fell, J., Tegeler, C., Gaschler-Markefski, B., Hinrichs, H., Heinze, H., and Scheich, H. (1999). Lateralized auditory spatial perception and the contralaterality of cortical processing as studied with functional magnetic resonance imaging and magnetoencephalography. *Human Brain Mapping* 7, 49-66. doi: 10.1002/(sici)1097-0193(1999)7:1<49::aid-hbm5>3.0.co;2-j
- Wolff, M., Jochim, J., Akyürek, E., and Stokes, M. (2017). Dynamic hidden states underlying working-memory-guided behavior. *Nature Neuroscience* 20, 864-871. doi: 10.1038/nn.4546
- Wolff, M., Kandemir, G., Stokes, M., and Akyürek, E. (2020). Unimodal and Bimodal Access to Sensory Working Memories by Auditory and Visual Impulses. *The Journal of Neuroscience* 40, 671-681. doi: 10.1523/jneurosci.1194-19.2019
- Woods, V., Wang, C., Bossi, S., Insanally, M., Trumpis, M., Froemke, R., and Viventi, J. (2015) A low-cost, 61-channel μ ECoG array for use in rodents. In: *2015 7th International IEEE/EMBS Conference on Neural Engineering (NER)*.
- Xia, J., Brughera, A., Colburn, H., and Shinn-Cunningham, B. (2010). Physiological and psychophysical modeling of the precedence effect. *Journal of the Association for Research in Otolaryngology* 11, 495-513. doi: 10.1007/s10162-010-0212-9
- Yang, X., and Grantham, D. (1997). Echo suppression and discrimination suppression aspects of the precedence effect. *Perception & Psychophysics* 59, 1108-1117. doi: 10.3758/bf03205525
- Yang, Y., Sani, O., Chang, E., and Shanechi, M. (2019). Dynamic network modeling and dimensionality reduction for human ECoG activity. *Journal of Neural Engineering* 16, 056014. doi: 10.1088/1741-2552/ab2214
- Yao, J., Bremen, P., and Middlebrooks, J. (2013). Rat primary auditory cortex is tuned exclusively to the contralateral hemifield. *Journal of Neurophysiology* 110, 2140-2151. doi: 10.1152/jn.00219.2013
- Zwislocki, J., and Feldman, R. (1956). Just noticeable differences in dichotic phase. *The Journal of the Acoustical Society of America* 28, 860-864. doi: 10.1121/1.1908495